Novel Directional Protection Scheme for the FREEDM Smart Grid System

by

Nitish Sharma

A Thesis Presented in Partial Fulfillment
of the Requirements for the Degree
Master of Science

Approved July 2015 by the
Graduate Supervisory Committee:

George Karady, Chair
Keith Holbert
Raja Ayyanar

ARIZONA STATE UNIVERSITY

August 2015

ABSTRACT

This research primarily deals with the design and validation of the protection system for a large scale meshed distribution system. The large scale system simulation (LSSS) is a system level PSCAD model which is used to validate component models for different time-scale platforms, to provide a virtual testing platform for the Future Renewable Electric Energy Delivery and Management (FREEDM) system. It is also used to validate the cases of power system protection, renewable energy integration and storage, and load profiles. The protection of the FREEDM system against any abnormal condition is one of the important tasks. The addition of distributed generation and power electronic based solid state transformer adds to the complexity of the protection. The FREEDM loop system has a fault current limiter and in addition, the Solid State Transformer (SST) limits the fault current at 2.0 per unit. Former students at ASU have developed the protection scheme using fiber-optic cable. However, during the NSF-FREEDM site visit, the National Science Foundation (NSF) team regarded the system incompatible for the long distances. Hence, a new protection scheme with a wireless scheme is presented in this thesis. The use of wireless communication is extended to protect the large scale meshed distributed generation from any fault. The trip signal generated by the pilot protection system is used to trigger the FID (fault isolation device) which is an electronic circuit breaker operation (switched off/opening the FIDs). The trip signal must be received and accepted by the SST, and it must block the SST operation immediately. A comprehensive protection system for the large scale meshed distribution system has been developed in PSCAD with the ability to quickly detect the faults. The

validation of the protection system is performed by building a hardware model using commercial relays at the ASU power laboratory.

ACKNOWLEDGEMENTS

I would like to thank my advisor and chair Dr. George Karady for his advice and continued support throughout my work, for his patience, motivation, enthusiasm, and immense knowledge. His guidance helped me in all the times of research and writing of the thesis. I attribute the level of Master's degree to his encouragement and effort and without him the thesis would not have been completed. One simply could not wish for a better friendlier supervisor. Thanks for giving me the opportunity to be a part of the FREEDM research.

Besides my advisor, I would like to thank Dr. Raja Ayyanar and Dr. Keith Holbert for being part of my thesis committee. I would like to thank Darshit Shah and Bhanu from MST, Abhay Negi from NCSU for their help in the simulation of LSSS loop.

I would like to thank my parents who have supported me throughout the entire process, both by keeping me harmonious and helping me putting pieces together. The most special thanks go to Nidhi Gaur, who has given me her unconditional support through all this long process.

TABLE OF CONTENTS

CHAPTER Page

CHAPTER Page

LIST OF TABLES

LIST OF FIGURES

NOMENCLATURE

FREEDM	Future Renewable Electric Energy Delivery and Management
SST	Solid State Transformer
AC	Alternating Current
DC	Direct Current
DRER	Distributed Renewable Energy Resource
DESD	Distributed Energy Storage Devices
SST	Solid State Transformer
LSSS	Large Scale System Simulation
DG	Distributed Generation
CB	Circuit Breaker
CT	Current Transformer
PT	Potential Transformer
FID	Fault Isolation Device
DGI	Distributed Grid Intelligence
FCL	Fault Current Limiter
SLG	Single Line to Ground
ABC-G	Three Phase to ground
ABC-LLL	Three Phase Short Circuit
IEM	Intelligent Energy Management
IFM	Intelligent Fault Management

CHAPTER 1: INTRODUCTION TO THE FREEDM SYSTEM

1.1 Background

Energy provides the power to progress. Energy is required to turn the natural resources into useful goods. A growing proportion of energy is being met all the over the world by electricity. This trend will further be stimulated because of increasing availability of clean power. This pattern applies mainly to developing countries because their industrial progress will be based on modern technologies that use electricity power intensively. Electric power is the backbone of the industrial world of today. Further, comfort, convenience and safety of large population all over the world depend on the electric power. In fact, it is no exaggeration to say that average wage level and standard of living in any country are dependent to a large extent on the amount of power used per capita in its industry.

The fossil-fuelled power plants are the primary sources of the energy today. The lack of efficiency in this old conventional system is unforgivable. These generate power only; the heat generated is blown away in the cooling towers or disappears into the water body. Transmission line energy losses also contribute to the inefficiency. The prominent use of fossil fuels for power generation in U.S has increased the carbon-dioxide emissions that have become a concern for the government [1]. To prevent the excessive exhaustion of natural resources by power companies and without having a reduction in power generation, the federal government passed a strict law to include the renewable sources in total power generation.

Renewable energy generation like solar, wind has been increasing at a tremendous pace over the past few years. Various factors for this growth are abundant availability,

clean. Other factors propelling the growth of renewable energy generation are policy related, such as the Federal Production Tax Credit (PTC) and Renewable Energy Portfolio Standards (RPS) by various states. The PTC created under the Energy Policy Act (EPA) allows an Income tax credit of nearly 2 cents/kilowatt-hour of electricity produced, (adjusted manually for inflation) from renewable sources [2]. RPS binds the states to meet a portion of their energy needs through renewable sources. Renewable energy integration has become an important area of research these days.

1.2 FREEDM System

FREEDM (Future Renewable Electric Energy Delivery and Management) is an initiative by the National Science Foundation (NSF) for the enhancement of the renewable energy generation, penetration and integration of the renewable energy into power system grid [3].

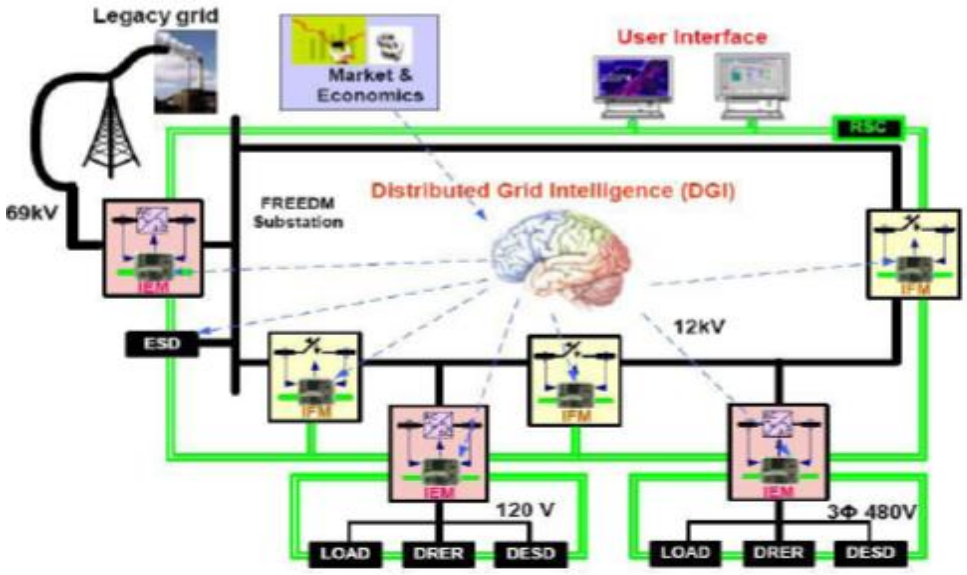

Figure 1.1: FREEDM System [3]

FREEDM system has a capability of operating in faulted conditions and reacting to the needs of the system as per demand. The integration of the renewable energy can be used to supply the demand as well as can be stored in DESD (distributed energy storage devices). The FREEDM system has advanced power electronic technologies with information sharing technology to develop a modern smart grid. The DRER (distributed renewable energy resources) take care of the renewable energy integration, and DESD (distributed energy storage devices) is used to store energy when supply is sufficient but demand is low. The DRER, DESD, and loads are managed with DGI (distributed grid intelligence) which is the brain of the FREEDM system [4]. The system also has novel power electronic device FID (fault isolation device) which has asymmetrical current breaking capacity and can clear faults in microseconds. The SSTs (Solid State Transformer) are one of the main features of this system. They have replaced conventional 60 Hz power transformer with a new power electronic power processing package. The SST is a cascaded rectifier, dual active bridge converter, and inverter. It has an input of 7.2 kV and output of 120 V AC (single phase), 208 V AC (three phase) and 400 V DC.

The FREEDM loop is shown in Figure 1.2. SST is a 3 level device which has AC-DC/ DC-DC/ DC-AC stage, and it can allow the bi-directional flow of power. The substation SST is rated at 6 MVA, 230 V/12.47 kV, and it supply power to the FREEDM loop. The distribution SST is rated at 12.47 kV/ 120 V, the DRER, and DESD can be directly connected to the DC link of the distribution SST. The protection scheme will detect a fault in the loop that in turn activates the trip signal to FIDs. All the coordination

between FIDs and SST are done with the help of DGI through RSC (Reliable and Secured Communication Network) [5] [6].

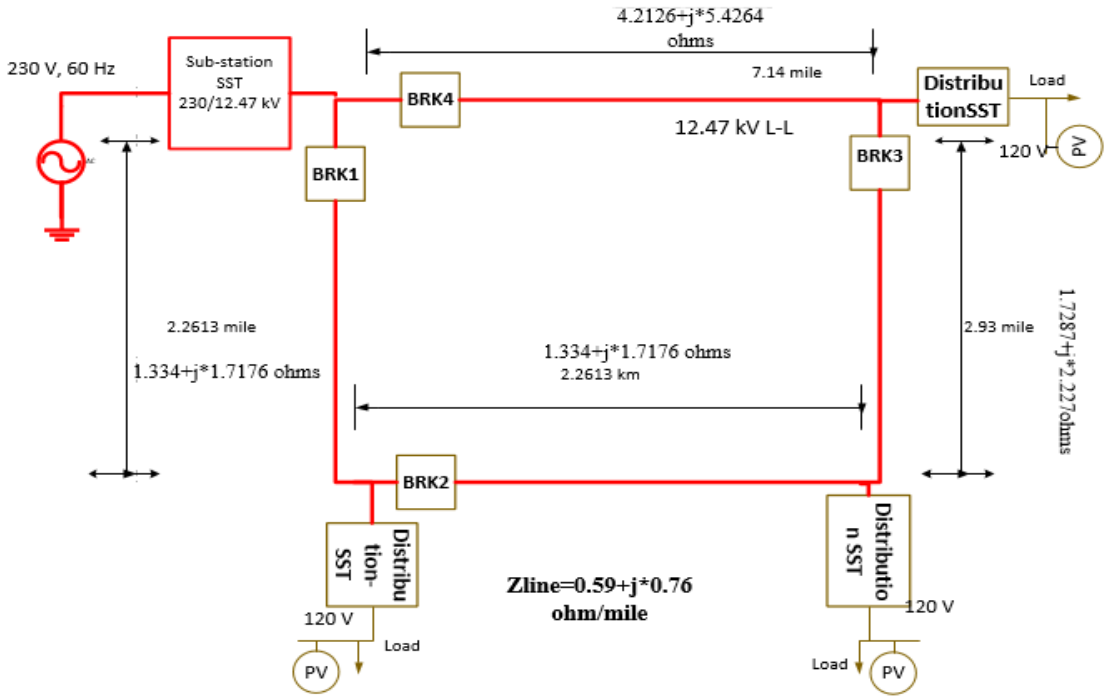

Figure 1.2: FREEDM Loop [5]

The FCL (Fault Current Limiter) will limit the fault current in the circuit. Also, the SST has an inherent capability of limiting the fault current at 2.0 per unit. The protection scheme has to detect successfully a fault in the system and eventually FIDs will isolate the faulted section of the main loop.

1.3 Objectives of the Research

The bi-directional flow of power in the FREEDM system limits the use of traditional protection scheme for the system protection. Moreover, mesh systems have higher short circuit currents and a significant dip in voltage and frequency. Thus, these systems are more sensitive to fault and power oscillations. The conventional overcurrent methodology will not work in FREEDM system. Hence, this must be modified for the

loop system without sacrificing speed and selectivity of the scheme. ASU students have previously developed a pilot differential protection for the loop system. It was able to detect faults in a cycle, but it suffered from the problem of time delay and communication [7]. The Ethernet cable was used to transfer the current signal from relays to the central processor and then to faulted breaker of the section. This whole process introduced a significant time delay in the trip signal making it unreliable for the long distance.

A protection method for the looped system without communication from multiple sources is introduced in [7]. The directional relays with time-inverse overcurrent characteristics were used to detect the fault in the system. This scheme could be used as a reliable backup protection during the failure of communication. In this case, DGI would not be able to communicate with the FIDs as there is no communication system is involved. Hence, the implementation of this scheme would take away the smart grid factor from the system.

A new scheme is developed with directional relays where fiber-optic communication is shown in [7]. This system eliminated the use of a central controller for decision making and hence it was fast enough to detect the faults. Although, the scheme was quick enough to detect the faults in the system, it suffered from the reliability issues. The fiber-optic cable cannot be used for the long distance communication and also it is less appealing in terms of aesthetics.

A solution to the above problems is suggested in this thesis as a part of FREEDM research work.

- A protection system with wireless communication scheme has been developed in this thesis. The directional overcurrent based relays are used to detect and

sectionalize the faulty section from the healthy system. The wireless communication has comparable speed and selectivity. A hardware prototype is developed at ASU power lab using commercial SEL-351 and SEL-3031 radio links.

- The reconfiguration of the system after the successful switching off the faulty section is presented. The reconfiguration effort requires the update of the system architecture with reclosing and automatic sectionalizing link type switches.
- Directional Pilot Protection is incorporated in the LSSS system (Large Scale System Simulation Sub thrust) which is a computer simulation of the IEEE-34 developed distribution network model. This is an accurate and exact representation of the protection system by a computer program, which uses commercial digital relays.
- The proper operation of the protection system installed in the LSSS system is tested for all possible faults. This testing has validated the correct functioning of the proposed protection system.

1.4 Organization of the Thesis

Chapter 2 presents the literature review of the existed protection schemes like over current protection, pilot protection system. A brief overview of the wireless system for the power system protection has been presented. Chapter 3 presents the development of directional relay in PSCAD. The use of negative sequence and positive sequence based directional element for fault detection is discussed. The PSCAD model of the recloser

system for the distribution system is demonstrated. Chapter 4 presents the wireless communication scheme for the pilot protection. A hardware prototype using commercial digital relays is shown. Chapter 5 gives a detailed explanation of the LSSS system in the FREEDM system. Chapter 6 explains the developed protection scheme for the LSSS protection. A detailed procedure for protection against all possible type of faults is shown. The results of the protection scheme for the faults in each zone of LSSS system are presented. Chapter 7 presents conclusions and future work.

Appendix A presents an overview on negative and positive sequence directional relay. Appendix B presents line data of the LSSS mesh distribution system. Appendix C shows the FORTRAN code of positive sequence directional element for detecting symmetrical faults. Appendix D gives the FORTRAN code used for decision making in PSCAD.

CHAPTER 2: LITERATURE REVIEW

2.1 Protective Relays

Protective relays are the devices that detect abnormal conditions in electrical circuits by continuously measuring the electrical quantities that are different under normal and fault conditions. The basic electrical quantities that may change during fault conditions are voltage, current, phase angle (direction) and frequency. Having detected the fault, the relay operates to complete the trip circuit that results in the opening of the circuit breaker and therefore in the disconnection of the faulty circuit [8].

A well designed and efficient protective relaying should have:

1. Speed
2. Selectivity
3. Sensitivity
4. Reliability

2.2 Overcurrent Protection [8]

These relays operate when the applied current rises above a specified value (pick-up current)

Instantaneous overcurrent protection

The operation takes place after a negligibly small interval of time from the incidence of current that causes action.

Definite time over current protection

The time of operation is entirely independent of the magnitude of the current which causes operation.

Inverse time overcurrent protection

The time of operation is dependent on the magnitude of the pickup current. High fault current operate the relay faster than the lower value of fault current.

Inverse definite minimum time over current protection

The time of operation is approximately inversely proportional to the smaller values of current causing operation and tends to definite minimum time as the value increases without limit.

A set of typical time-current characteristic curves for the relay is shown in Figure 2.1.

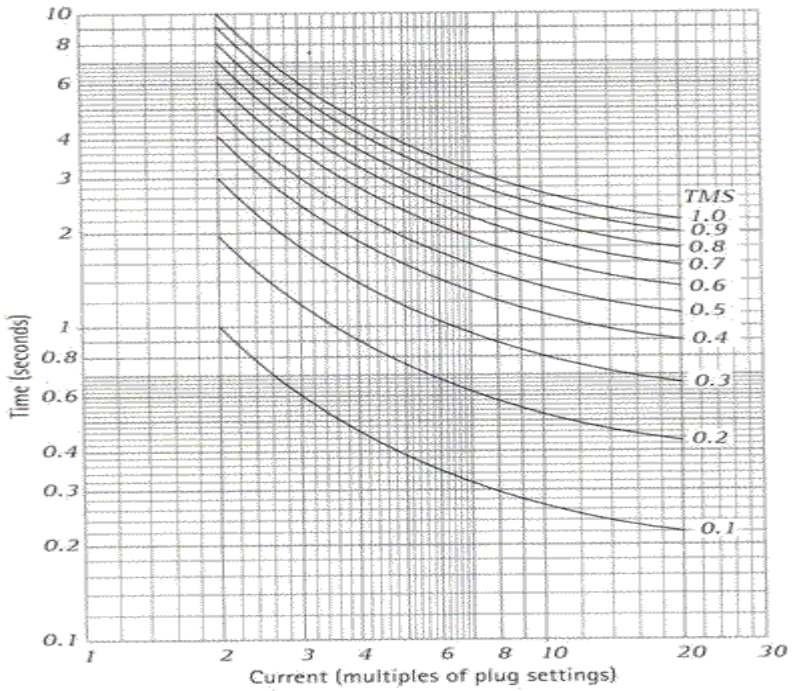

Figure 2.1: Inverse Definite Minimum Time (IDMT) Characteristics [8]

The curve displays the relation between the operating current in terms of current setting multiplier along the x-axis and operating time in seconds along the y-axis. A current setting multiplier indicates the number of times the relay current is in excess of the current setting. The current setting multiplier is also referred to as plug setting multiplier (PSM) [8]. Thus

$$PSM = \frac{\text{primary current}}{\text{primary setting current}} = \frac{\text{Primary current}}{\text{Relay current setting X C.T ratio}} \quad (2.1)$$

Usually, the rated current of the relay is equal to the rated secondary current of CT.

2.3 Differential Overcurrent Protection

A differential protection operates when the phasor difference of two or more similar electrical quantities exceeds a predetermined amount. Most differential relays are of the current differential type. Figure 2.2 shows the arrangement of an over-current relay connected to work on the current difference principle.

Suppose that current *I* flow through the primary circuit to an external fault. If the two circuit transformers have the same ratio and are connected as shown in Figure 2.2, no current will flow through the relay, and it will remain inoperative [8].

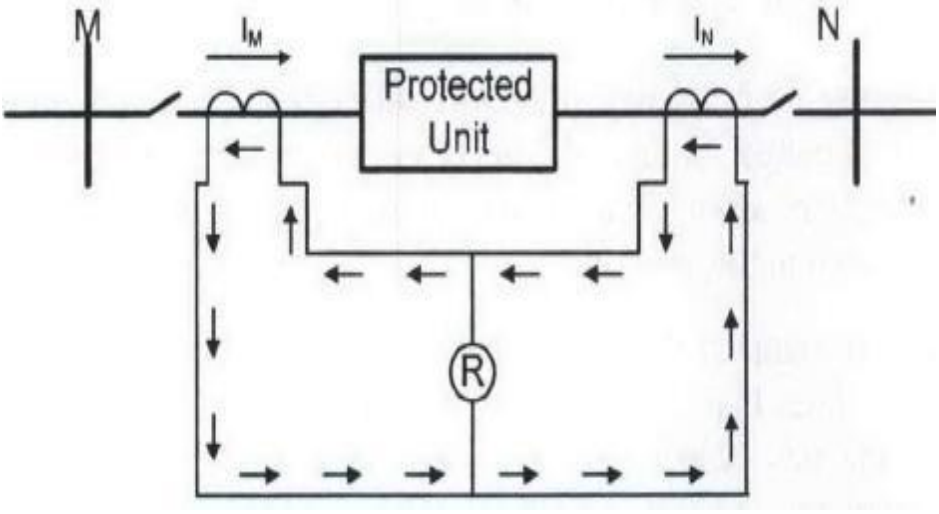

Figure 2.2: Operation of Differential Relay without Internal Fault [8]

If now an internal fault occurs as in Figure 2.3 and if current flows to the fault from both sides, the current flowing through the relay will be I_1+I_2. It may be noted that the fault current need not necessarily flow to the fault from both sides to cause current

flow in the relay. A flow on the one side only, or even some current flowing out of the one side while a large current enters the other side will cause a differential current.

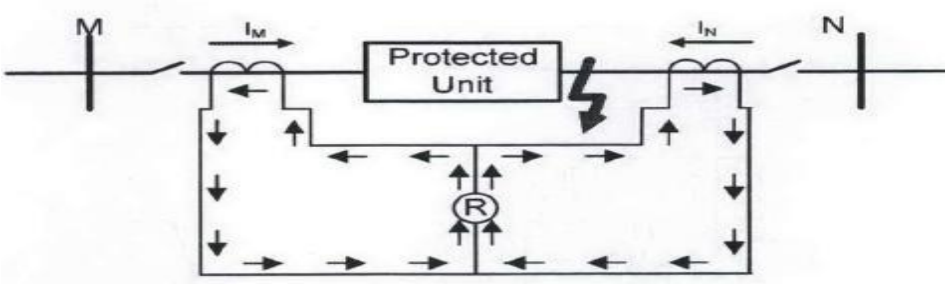

Figure 2.3: Operation of Differential Relay with Internal Fault [8]

In other words the differential relay current will be proportional to the phasor difference between the currents entering and leaving the protected circuit, and if the differential current exceeds the pick up value of the relay, the relay will operate.

This type of differential relay is likely to function inaccurately with heavy through (i.e. external) faults since the supposedly identical current transformers may not have identical secondary currents due to constructional errors or under severe through fault conditions. C.T's may saturate and cause unequal secondary currents, and the difference of the secondary currents may approach the pick-up value of the relay. This disadvantage is overcome in the percentage differential relay.

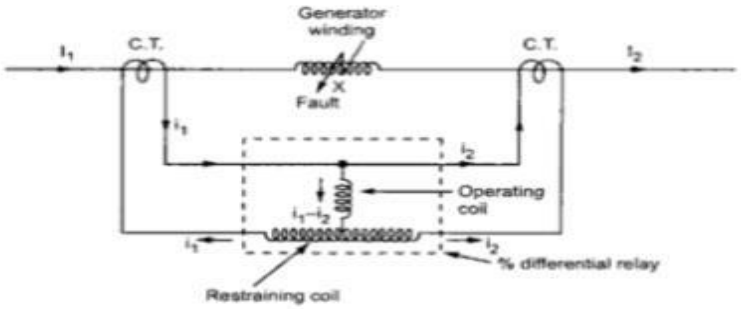

Figure 2.4: Percentage Differential Relay [8]

The differential current in the operating coil is I_1-I_2, while the current in the restraining coil R is $(I_1+I_2)/2$, since the operating coil is connected to the midpoint of the restraining coil, in other words if the number of turns on the restraining coil are N, the total ampere-turns are $I_1N/2 + I_2N/2$, which is the same as if $(I_1+I_2)/2$ were to flow through the whole coil. The operating characteristic of this type of relay is shown in Figure 2.5 which shows that except at small currents, the ratio of the differential operating current to the average restraining current is a fixed percentage.

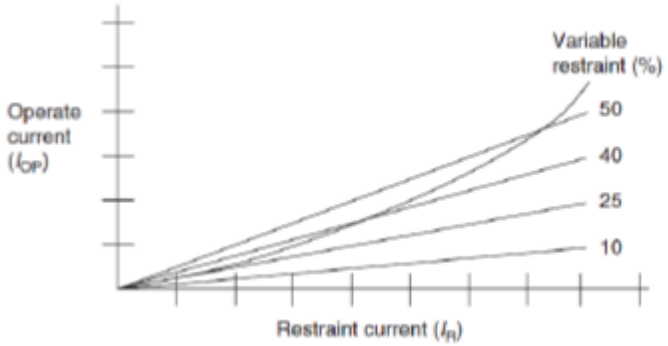

Figure 2.5: Characteristic of Percentage Differential Relay [8]

2.4 Directional Relay

To achieve operation for the fault flowing in a particular direction, it is necessary to add a directional element in the relay. Such a relay that responds to fault flow in a given direction is called a directional relay. In directional relays, voltage is taken as the reference quantity. Let *I* be the relay current. In Figure 2.6 the relay current is shown leading the relay voltage by an angle ɵ. V and *I* produce flux $Ø_v$ and $Ø_i$, $Ø_v$ lagging V by an angle $Ø_v$ and $Ø_i$ being in phase with *I*.

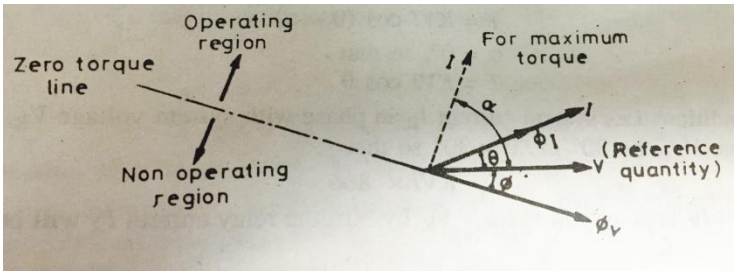

Figure 2.6: Directional Element Phasor Diagram [8]

Torque, therefore, $T = Ø_i * Ø_v * \sin(Θ+Ø)$ (2.2)

Where $Ø_v \propto V$ and $Ø_i \propto V$ so that torque equation for the directional element of the relay is

$$T = KVI \sin(Θ+Ø) \quad (2.3)$$

Maximum torque occurs when sin (Θ+Ø) is a maximum i.e. when Θ+Ø=90°, while zero torque occurs when Θ+Ø=0° or 180° this being satisfied when the relay current phasor lies along the chain dotted line that is at right angles to the maximum torque threshold. The directional elements will, therefore, operate provided that the current phasor lie within 90° of the maximum torque line if the current phasor is displaced by more than 90° the elements will restrain.

2.5 Negative Sequence directional Element [9]

The Negative-Sequence Directional Element is used, the most commonly thought of element is one that looks at the negative-sequence voltage on, and negative-sequence current through, a transmission line and compares the relative phase angles of the two quantities. A forward fault is declared when the negative-sequence current leads the negative-sequence voltage by 180 degrees minus the characteristic angle of the transmission line. This component can be described by the following equation [9]:

$$T32Q = |V_2| * |I_2| * \cos(\angle V_2 - \angle I_2 - \alpha) \quad (2.4)$$

Where V_2 and I_2 are negative sequence voltage and current respectively

α is the line angle in degrees

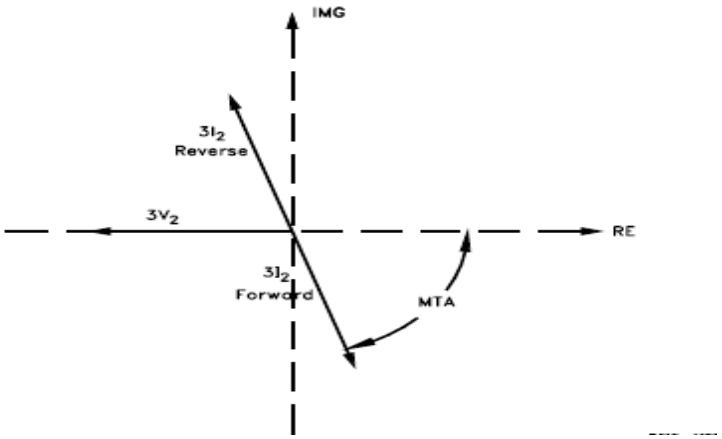

Figure 2.7: Negative sequence Directional Characteristics [9]

For the line to ground fault in a system in the above section, the A-phase current would lag the A-phase voltage by the line angle of the line. To calculate the negative-sequence current for this fault, we use the same equation as we used for the negative-sequence voltage substituting current for voltage.

2.6 Positive Sequence Directional Element [10]

The use of positive sequence directional element is prevalent during three phase faults also known as symmetrical faults. Figure 2.8 shows the transmission line for the analysis of positive sequence directional element for fault detection. The positive sequence network for a forward fault F1 and reverse fault F2 is shown in Figure 2.9. The ZM1, ZL1, ZN1 are the positive sequence impedances of the source M, the line, and the source N, and ΔZ1 is a fault-type-related impedance.

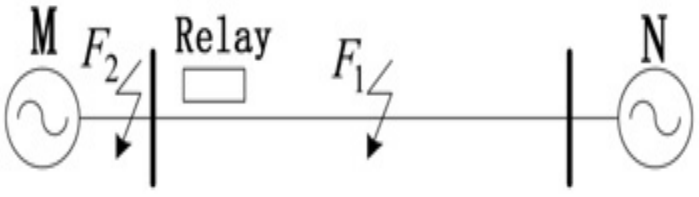

Figure 2.8: Transmission Line Subjected to Fault [10]

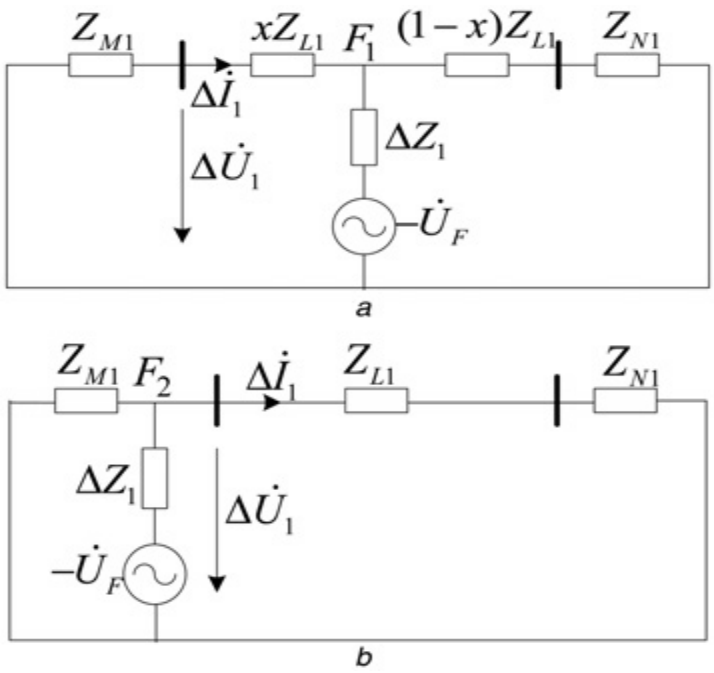

Figure 2.9: Positive Sequence Component Network [10]

The directional element detects the presence of symmetrical faults by comparing the phase angle difference between the positive sequence current and voltage to a defined range as given in [10]. The directional protection principle based on the PSFC networks has some unique features such as [10]:

(1) It can be applied to any fault

(2) It is independent of load conditions

(3) The phase relationship between voltage and current at the relay point is determined only by the positive sequence impedance between the relay location and the system neutral.

A unique pilot wire differential protection scheme for distribution systems is discussed in [11]. The traditional approach to pilot wire relaying is shown in this paper. The differential scheme is utilizing the pilot wires where information is transferred with

the help of communication link. The use of current differential protection using pilot wires has a promising future because of sensitivity and robustness of this method. The system can be classified into a different type of protection system based on the medium of communication used for information sharing.

A protection system which could be used to detect square wave fault current, as mentioned in [12]. This method is useful when fault current causes current transformer saturation. Also, the presence of fault current limiter and solid state transformer will limit the current at 2.0 pu in FREEDM system. The GPS synchronized protection system is used to detect the fault. The system is divided into various sections. Each section has a multi-terminal differential protection system, which adds up the GPS- synchronized current in the section. If the section current is non-zero, then the fault is in the section. The differential protection can be applied to an entire system by using an advanced communication link for data processing.

The design and implementation of a very fast pilot protection scheme for the next generation distribution system are described in [13]. The time stamped signals are converted to digital format and transmitted to a processing unit via a communication link. The processing unit compares the measurement. Based on these measurements, a decision has been made. The protection is based on a pilot protection algorithm with overcurrent protection. This system is found to be faster compared to the conventional differential protection system. The average trip signal delay time is determined to be five milliseconds. However, this system suffers from the problem of time synchronization. If due to any error or delay in one of the synchronization channel, the feasibility of this type of system would be limited.

The designs and limitations of using directional element models have been discussed in [14]. Various laboratory and field tests are presented to examine the limits of sensitivity and other conditions like loss of voltage, loss of power. The designs of directional element continue to evolve with changing power scenario. A comparison of electromechanical relays and modern digital relays is presented in detail. The sensitivity analysis is one of the most important factors to understand the behavior of relay. Although automatic settings of the modern relays are helpful, the proper application of these configurations is necessary to maintain reliability and flexibility. A comprehensive study of the system is crucial to apply the loss of power and loss of voltage settings. The positive sequence impedance directional element could be used during loss of power conditions.

The protection of the closed-loop system is proposed in [15]. The flexibility of the closed loop system has been increased by use of intelligent electronic devices. The closed loop system has significantly improved the availability of power and quality of power. The coordination of relays in closed loop system is essential to maintain reliability and quality of power. In radial system faults can be divided based on overcurrent scheme and having coordination time between adjacent relays. The same method cannot be used for loop system. The use of directional element along with overcurrent relay is standard practice for loop system.

The directional current protection utilizes both a voltage transformer (connected in parallel to the circuit) and a current transformer that are both wired to the digital relay on one side such that the relay can act as a wattmeter [16]. This will allow the voltage and current to multiply so the phase difference between the two values can be extracted.

Should the current be lagging the voltage by up to 180 degrees, the switch will close causing the coil to be energized and trip the circuit. Whereas if the current was leading the voltage by up to 180 degrees, the relay will not close the switch and the breaker will not trip as a result. The phase in which the current leads or lags the voltage will be dependent on whether the fault is located to the left of the transformer or the right of the transformer. This is useful in shutting off the side of the circuit that is faulty to not impede the operation of the entire circuit. The distance protection also uses both voltage and a current transformer to react to circuit fault faster than an overcurrent protection relay [17]. This is because the relay takes the voltage to the current ratio. This is so when the current rapidly increases; there will also be a rapid decrease in the voltage. If the current increases by a factor of 2 while the voltage decreases by a factor of 3. This means that the impedance relay will detect a change in the circuit by a magnitude of 6. This is much larger than simply the change in current by a factor of 2 so the relay will be much more responsive in detecting faults. This impedance relay has a "reach" characteristic that identifies how far down the line the relay detects faults. They are usually set to 80%, 100% and 120% down the transmission line for different zones. Each reach characteristic covers an individual zone. For the closest zone, the time delay is smaller than the zone that is further away. This will prevent multiple relays from turning off for a single fault. This feature will also clearly show the part of the circuit where the fault is located.

The selectivity is of paramount importance i.e. non-faulted part of the power system should not be affected by faults outside its zone of protection [18]. The distance protection is not recommended for short lines without communication. The use of communication channel makes directional overcurrent protection attractive for short

lines. It has fast tripping speed as compared to distance protection. The use of digital channels for pilot relaying due to higher data transfer rate, reliability is on the rise. A discussion on the requirements of communication channel for joint pilot schemes is discussed in [19]. The issues related to channel asymmetry and channel switching has been addressed. The widespread use of point-to-point connections for pilot relaying seems to be logical instead of replacing a dedicated relay channel. The fiber-optic gives fast and error-free point-to-point connection, but channel interruption due to fiber cut is a grave concern of utilities. The use of wireless communication is appealing in terms of reliability and security. These days wireless network are almost comparable to fiber-optic in terms of speed and reliability.

CHAPTER 3: PILOT DIRECTIONAL PROTECTION AND RECLOSER IN PSCAD

The pilot differential scheme is based on the principle of overcurrent differential protection. The relay measure the current and voltage signals, based on these a calculated quantity is communicated to the adjacent relay. The comparison of the calculated signals and decision making for trip generation takes place in the relay or a centralized processor. Figure 3.1 shows the basic pilot scheme.

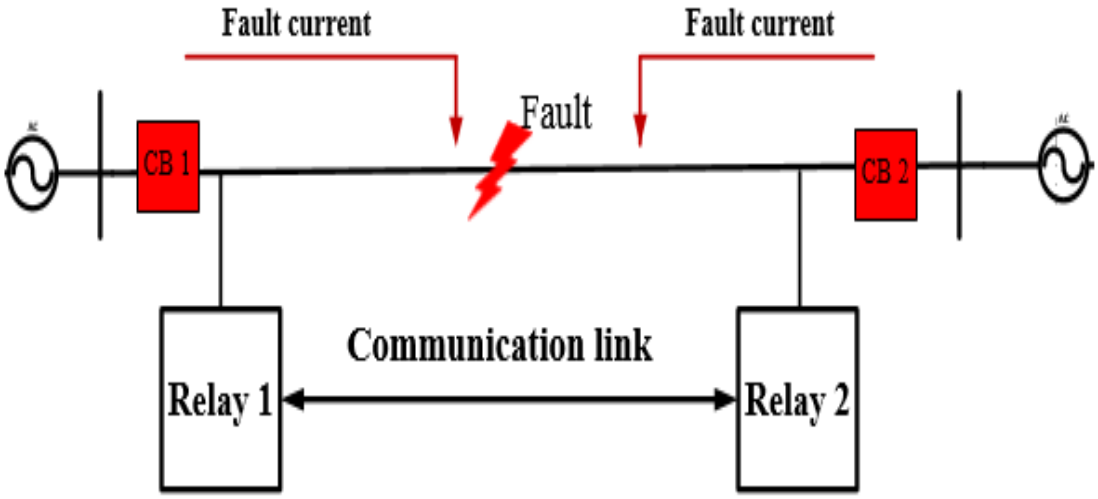

Figure 3.1: Pilot Protection Scheme [7]

3.1 Negative Sequence Directional Element [20]

The negative sequence directional element calculates the negative sequence impedance to determine the fault location. The calculated scalar quantity Z_2 is compared with two threshold values to determine whether the fault is in forward or reverse direction to a relay [20].

$$Z_2 = \frac{Re[V_2.(I_2.1\angle\theta)^*]}{{I_2}^2} \quad (3.1)$$

$$V_2 = Negative\ sequence\ voltage$$
$$I_2 = Negative\ Sequence\ current$$
$$Z_2 = Negative\ Sequence\ Impedance$$

$$if\ Z_2 < Z_{2F}, fault\ is\ in\ forward\ direction$$
$$if\ Z_2 > Z_{2R}, fault\ is\ in\ reverse\ direction$$
$$if\ Z_{2F} < Z_2 < Z_{2R}, there\ is\ no\ fault$$

$$Z_{2F} = Forward\ threshold\ impedance$$
$$Z_{2R} = Reverse\ threshold\ impedance$$

The negative sequence quantities do not exist in the system during the normal operation. The calculated negative sequence impedance lies within the forward threshold and reverse threshold values. However, during a fault, sequential components come into play and Z_2 could be used to determine the fault location. If the calculated Z_2 is less than forward threshold impedance, then the fault is in a forward direction to a relay. If the calculated Z_2 is greater than reverse threshold impedance, then the fault is in a reverse direction to a relay. During a symmetrical fault, negative sequence components are negligible in the system, and the directional element fails to detect the fault. Hence, to overcome this, the relay uses positive sequence components during symmetrical faults to identify the directionality of the fault current. The previous value of voltage and current, phase and magnitude are compared with the present value of voltage and current magnitude and phase in the circuit. Any inconsistency in the two values indicates the presence of a fault [7].

3.1.1 Application of Directionality in PSCAD

The current and voltage sequence components are obtained from the fundamental phase quantities and are given as inputs to the 'Negative sequence directional element 32 Q (E32Q)' available in PSCAD. The negative sequence directional element does not work during the normal operation but, it generates +1 or -1 during a fault depending on the direction of fault. It uses negative sequences impedance as the deciding factor to determine the fault location.

For a line to ground fault, it uses the voltage of un-faulted phases for the relay to be operational. Similarly, for a line-line fault, it uses the voltage of the un-faulted phases to be operational. However, for a symmetrical fault, the sequence components are less dominant, and it fails to detect the direction of the fault. This hurdle is overcome when digital relays are used [7] [20].

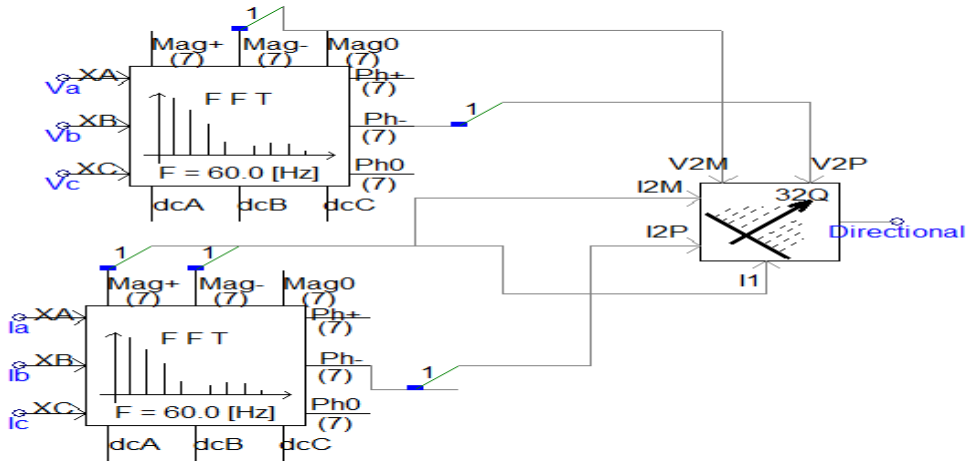

Figure 3.2: Implementing Directional Element in PSCAD

Figure 3.2 shows the PSCAD diagram for obtaining the direction of the fault. It works in a similar way as explained in the previous section. During the normal operation, its output remains zero. If the calculated Z_2 is less than forward threshold impedanceZ_{2F},

the directional element generates +1, and if the calculated impedance is greater than the reverse threshold impedanceZ_{2R}, it generates an output of -1.

3.1.2 Test Case

A simple radial circuit as shown in Figure 3.3 is simulated in PSCAD. The purpose of this simulation is to demonstrate the capability of negative sequence directional element for fault detection. This is a simple system and in the later stages the same approach will be used to protect large mesh distribution system.

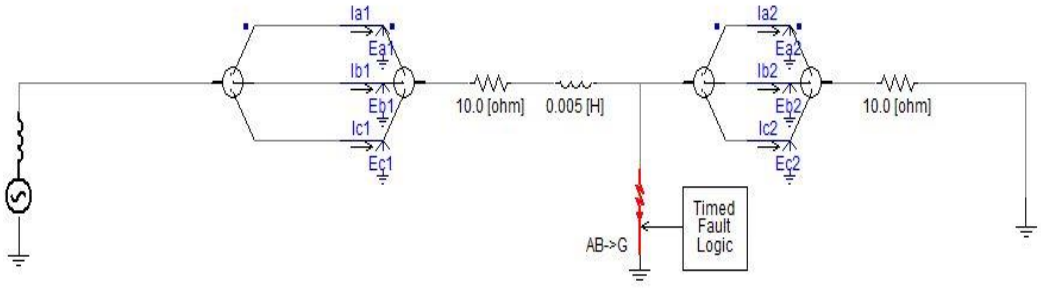

Figure 3.3: Radial System in PSCAD

A simple radial system is simulated in PSCAD, and it is subjected to a line to ground faults, double L-L, and double line to ground. The values of forward and reverse threshold values are found using following method given in [20].

The Voltage input is 230 kV and peak current in the system is 22A. An LL-G ground is simulated in figure 3.3. Z2F is normally 0.5 times of line impedance, and Z2R is 0.1+Z2F. The line impedance is chosen to be 10 ohms. Therefore, Z2F is set at 5 Ω and Z2R is set at 5.1 Ω. Based on above settings the following results are obtained for the different cases.

Case1: When fault is behind Relay 1

The L-G faults, LL-G, and LL faults are applied in the reverse direction of the Relay 1. In this case, only reverse impedance element of Relay 1 should go high.

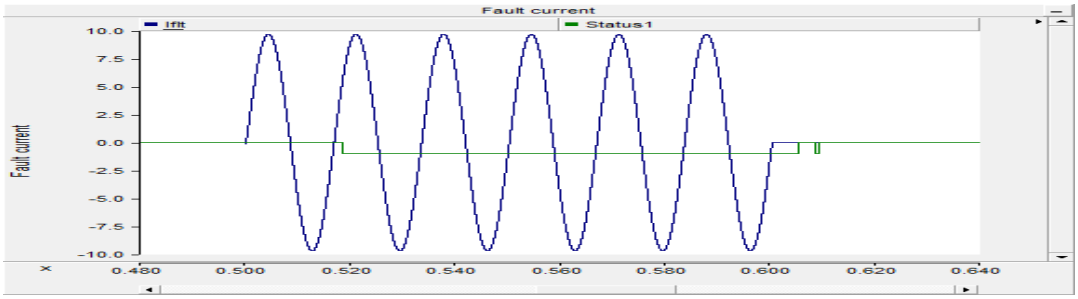

Figure 3.4: Waveform of Fault Current and Status of Impedance Element of Relay 1

Figure 3.4 shows the directional element value -1 indicating that a reverse fault has been simulated in the system. The trip signal delay is found to be one cycle.

Case 2: When fault is between Relay 1 and Relay 2 but near to Relay 1

An L-G fault is simulated between the Relay 1 and Relay 2 but near to Relay 1. In this case forward impedance element of Relay 1 and reverse impedance of Relay 2 should go high.

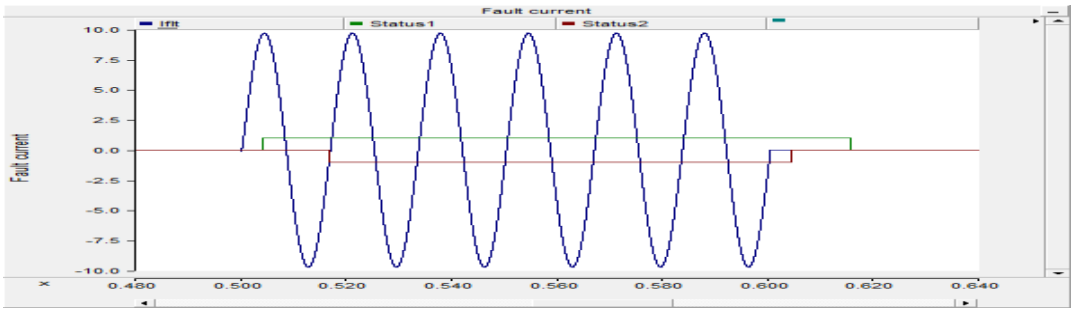

Figure 3.5: Waveform of Fault Current and Status of Impedance Element of Relay 1 and Relay 2

From Figure 3.5 the impedance element of Relay 1 is +1 and impedance element of Relay 2 is -1 that shows the fault has been simulated between Relay 1 and Relay 2.

The Relay 1 trip signal delay is found to be half cycle while for Relay 2 it is one cycle.

Case 3: An L-G fault is simulated between the Relay 1 and Relay 2 but near to Relay 2. In this case forward impedance element of Relay 1 and reverse impedance of Relay 2 should go high.

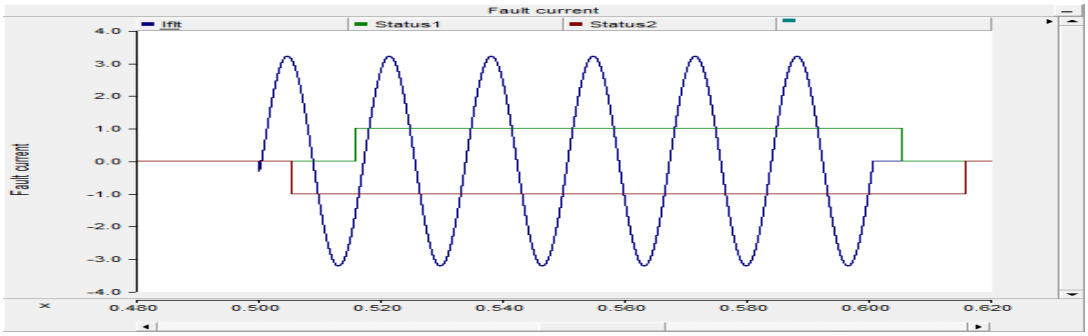

Figure 3.6: Waveform of Fault Current and Status of Impedance Element of Relay 1 and Relay 2

From Figure 3.6 the impedance element of Relay 1 is +1 and impedance element of Relay 2 is -1 this shows the fault is in between Relay 1 and Relay 2.

Case 4: Fault in forward direction of Relay 2

In this case forward impedance element of Relay 2 should go high.

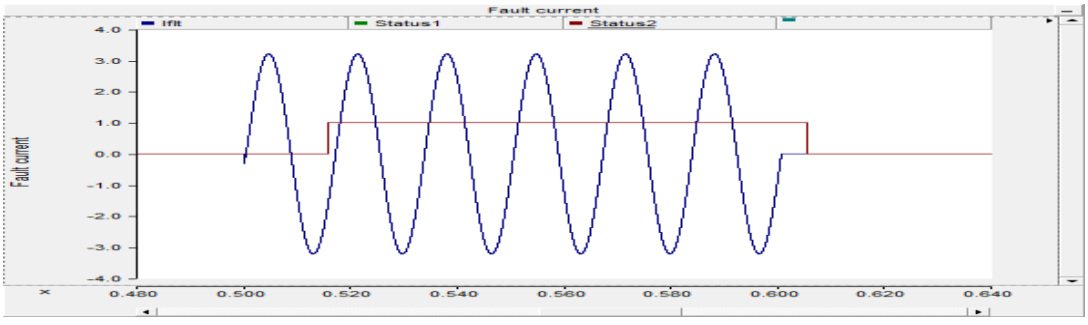

Figure 3.7: Waveform of fault current and status of impedance element of Relay 1 and Relay 2

From Figure 3.7 the impedance element of Relay 1 is +1 and impedance element of Relay 2 is +1 which shows the fault is forward direction of Relay 1 and Relay 2. The Relay 2 takes approx. one cycle for breaker opening signal.

Table 3.1:
Trip Signal Delay for Various Fault Angles for Unsymmetrical Faults

Fault Incident Angle (degrees)	**Trip Time (ms)**
10	18.23
20	19.41
40	18.32
60	18.14
90	18.75
120	18.81
150	18.65
180	17.75
200	18.65
220	18.19
240	17.70
260	17.75
300	17.90
320	18.05
335	18.10
350	18.35
360	18.45

Table 3.1 shows the trip signal delay for various fault angles. It can be seen that trip signal delay is higher at the peak of the current waveform. The use of directional negative sequence element is successfully implemented for a simple radial system. The element is successful in detecting LG, LL and LL-G faults as negative sequence voltage and current are dominant in these faults. But for a 3-phase-to-ground fault, the sequence components are less dominant, and it fails to detect the direction of the fault. A method to detect symmetrical faults in PSCAD is explained in next section.

3.2 Positive Sequence Directional Element

A positive sequence based directional element is used to detect the symmetrical fault in the circuit. During the unsymmetrical fault in the system, the presence of negative sequence elements could be used to determine the directionality of fault current. However, in case of symmetrical faults negative sequence elements are almost zero as the system remains balanced even after the fault. Hence, negative sequence elements cannot be used for detecting the fault.

A new scheme is to be developed which along with negative sequence element can be used to determine the directionality of fault. The present voltage and current waveforms are being compared with the previous history of the corresponding waveforms a few cycles before. This change in voltage and current is used to determine the directionality of fault in the system.

3.2.1 Principle of Operation

Normal positive sequence voltage and current at 60Hz frequency is taken as reference phasor to represent the healthy condition in the system. The same waveform is delayed by one cycles after the occurrence of the disturbance, to represent the healthy state of the circuit prior to a fault. After the fault in the system, the normal waveforms will represent a fault in the circuit, and these will be compared with delayed waveforms to calculate the change in voltage, current magnitude, and phase angle [21] [22].

Positive sequence element calculates the change in voltage and current phase angle. This change is used to determine the fault direction.

$$\Delta V_1 = V_{1f} - V_{1prefault} \quad (3.2)$$

$$\Delta I_1 = I_{1f} - I_{1prefault}$$

$$\emptyset = \angle \Delta V1 - \angle \Delta I1$$

ΔV_1= change in positive sequence voltage after and before the fault

ΔI_1= change in positive sequence current after and before the fault

For $\emptyset$>0: Reverse fault

$\emptyset$<0: Forward fault

3.2.2 Application of directionality in PSCAD

The currents and voltages sequence components are obtained from the fundamental phase quantities. These positive sequence voltage and current signals are delayed by one cycle as shown in Figure 3.8 and being continuously compared with the present components of positive sequence voltage and current.

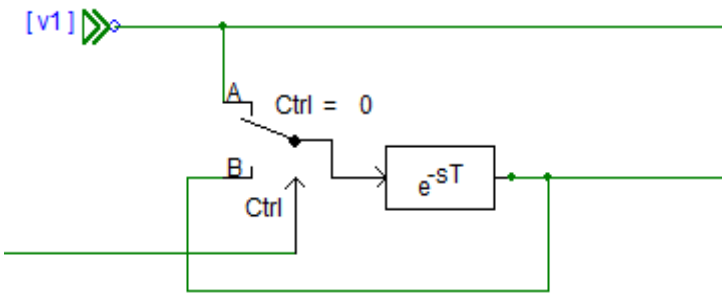

Figure 3.8: Positive Sequence Signal and Delayed Signal in PSCAD

The measurement process commences only when the control signal goes high. When there is no fault in the circuit, the change in voltage and current is zero but under the influence of fault the change becomes non-zero. A control signal is based on the overcurrent element in the circuit as shown in Figure 3.9. With a fault in the circuit,

overcurrent element goes high. Thus, it enables the calculation of the difference in voltage and current phase angle.

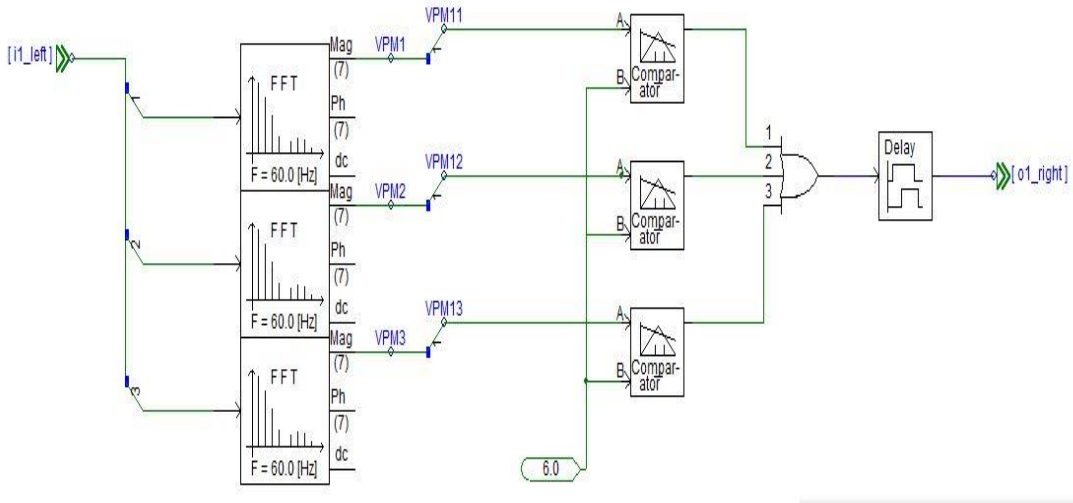

Figure 3.9: Control Signal to Commence Measurement

The directional element is reset when the control signal goes low. This system preserves the directional signal beyond the time delay when the fault is not cleared, and control signal remains high for more than one cycle.

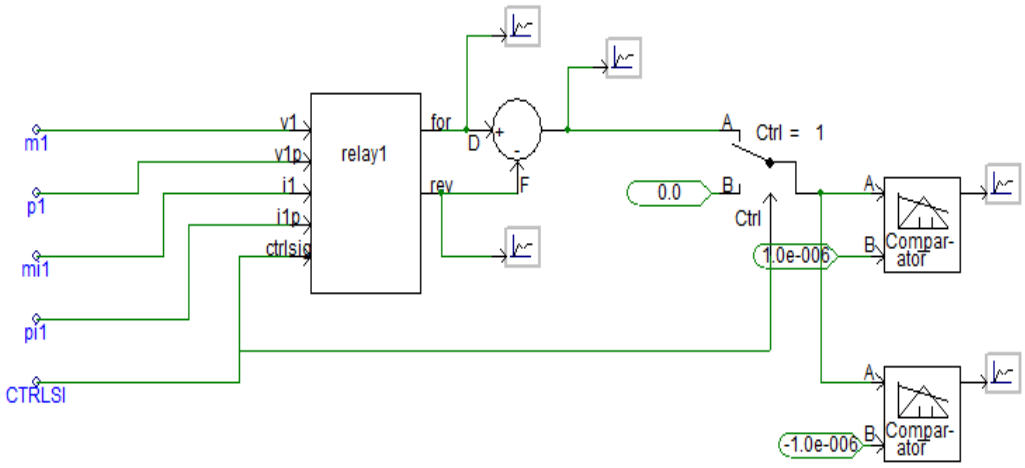

Figure 3.10: Positive Directional Element in PSCAD

The initial voltage and current phasors are passed to the relay1 block in PSCAD as in Figure 3.10. The input signal is delayed by one cycle to preserve the initial value under fault conditions. The fault and pre-fault signal is passed to voltage angle block (angle1) to calculate the voltage phase difference. Similarly, current fault and pre-fault value is given to current angle block (current angle). The difference in voltage angle and the current angle is used to calculate the fault direction as shown in Figure 3.11.

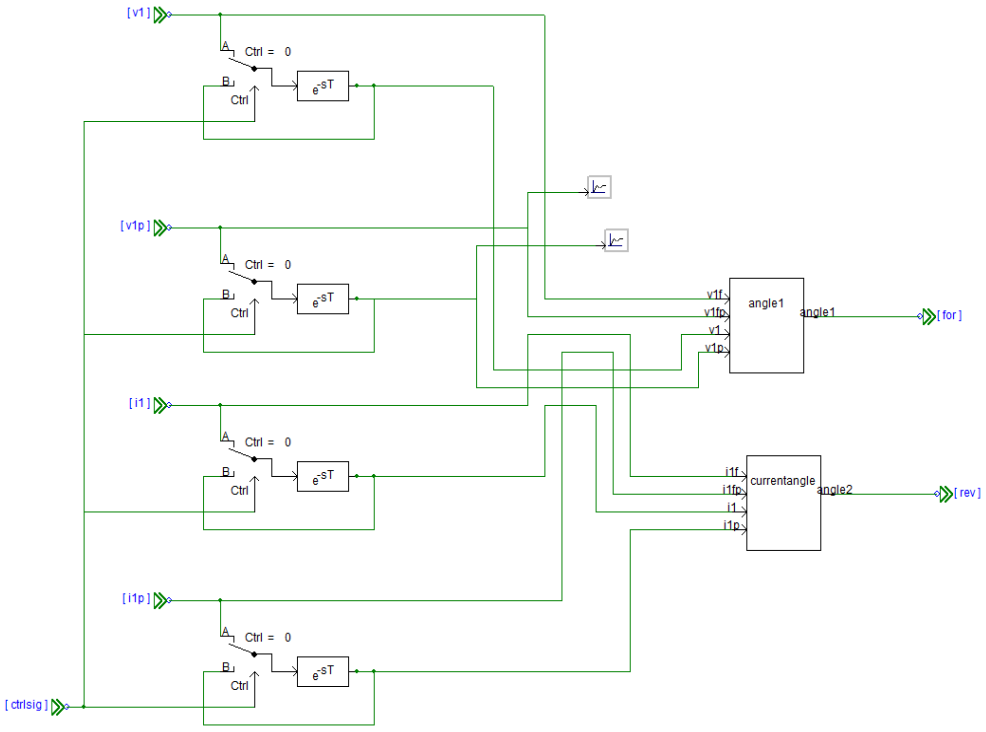

Figure 3.11: Voltage and Current Phase Angle Block in PSCAD

3.2.3 Test Case

For the circuit in Figure 3.3, a symmetrical fault is simulated at 0.5s for the duration of 0.3s

1.) When fault is behind Relay 1 and Relay 2

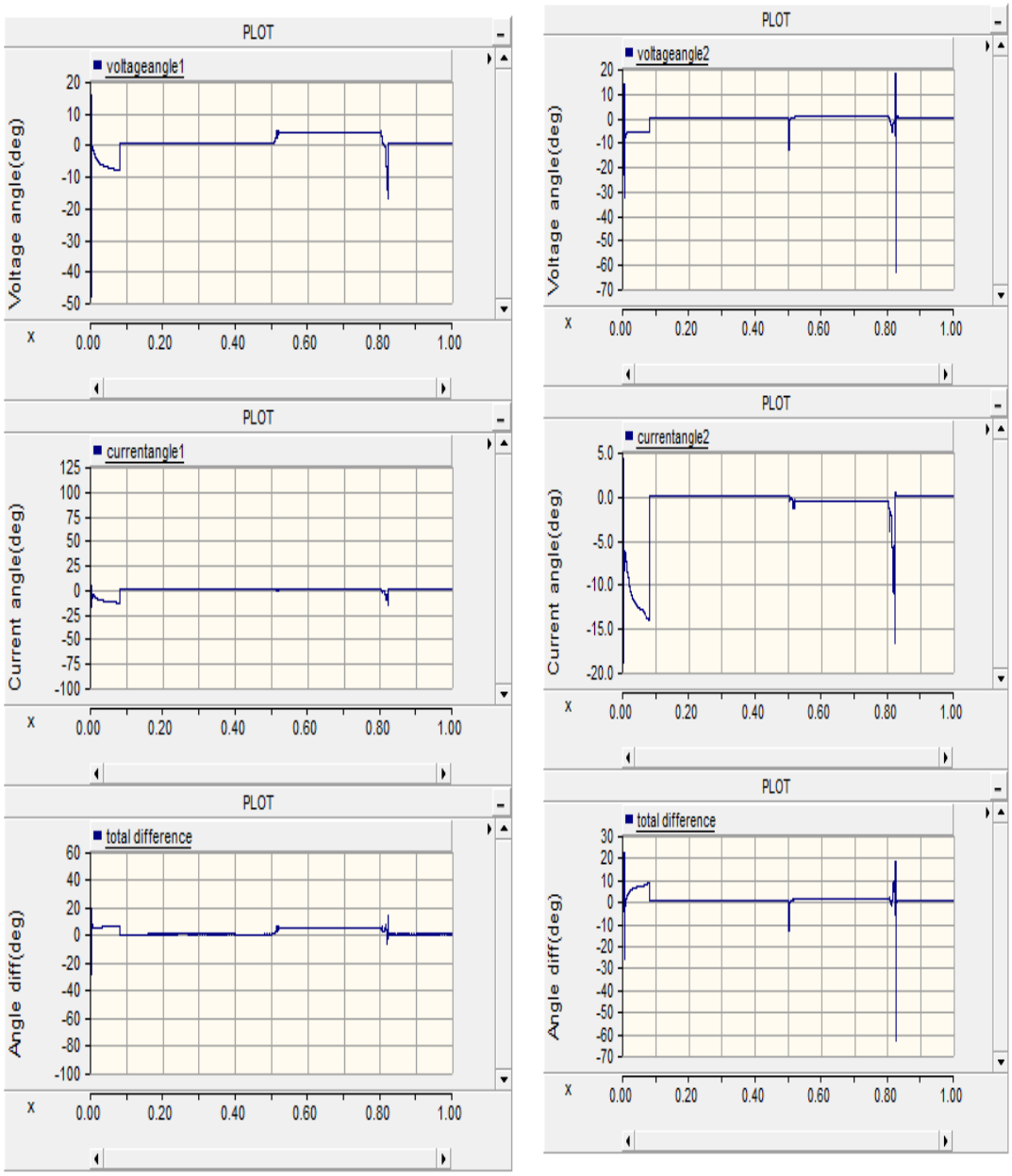

Figure 3.12: Plot of Voltage Angle, Current Angle and Total Difference in Phase Angle for Relay 1 and Relay 2

As shown in Figure 3.12, for a fault behind Relay 1, the overall difference in angle for both Relay 1 and Relay 2 is positive indicating a reverse fault.

2.) When fault is between Relay 1 and Relay 2

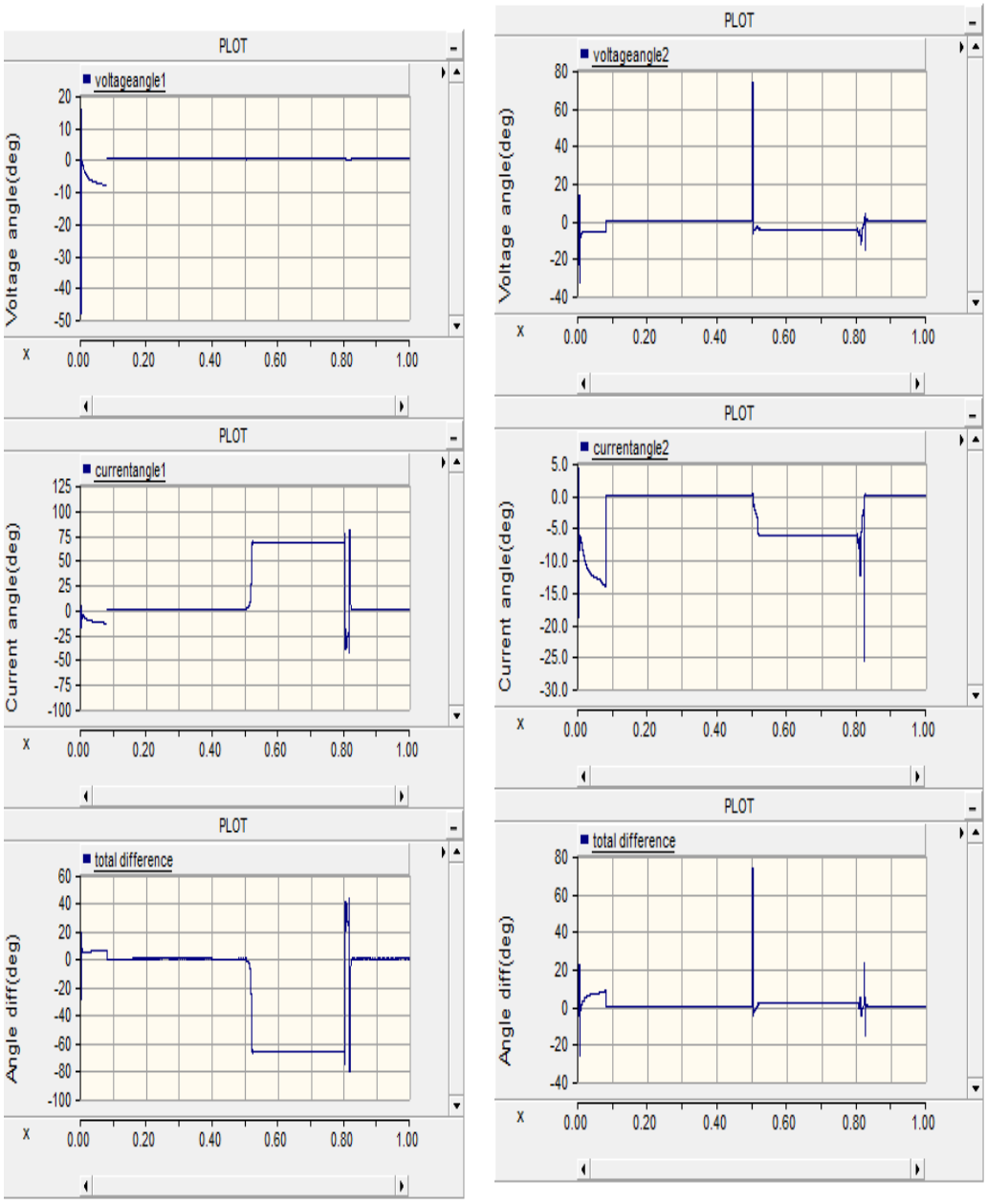

Figure 3.13: Plot of Voltage Angle, Current Angle and Total Difference in Phase Angle for Relay 1 and Relay 2

For the fault between Relay 1 and Relay 2, the overall difference in angle for Relay 1 is negative indicating forward fault while for Relay 2 it is positive indicating a reverse fault. Hence, this confirms that the fault is between Relay 1 and Relay 2.

3.3 Recloser model in PSCAD

Around 80 % of faults in the distribution system are temporary. Hence, the purpose of a recloser is to energize a faulted circuit multiple times after a time delay to prevent unnecessary loss of service during a temporary fault. Four single line-to-ground fault scenarios are tested, each resulting in different reclosing sequences [23].

3.3.1 System Description

A test distribution circuit in Figure 3.14 is used for testing the PSCAD model. The equivalent source is rated at 6 MVA, 12.47KV, 60Hz. Temporary and permanent single line to ground fault will be studied as these are the most common type of faults in the system. The maximum load current of the relay is 100 A rms.

This is a relatively small and simple distribution circuit, allowing one to limit the number of variables. The radial topology and absence of distributed generation allow for a simple analysis. Temporary and permanent single line-to-ground faults will be studied as this type of fault is most commonly encountered in a distribution system.

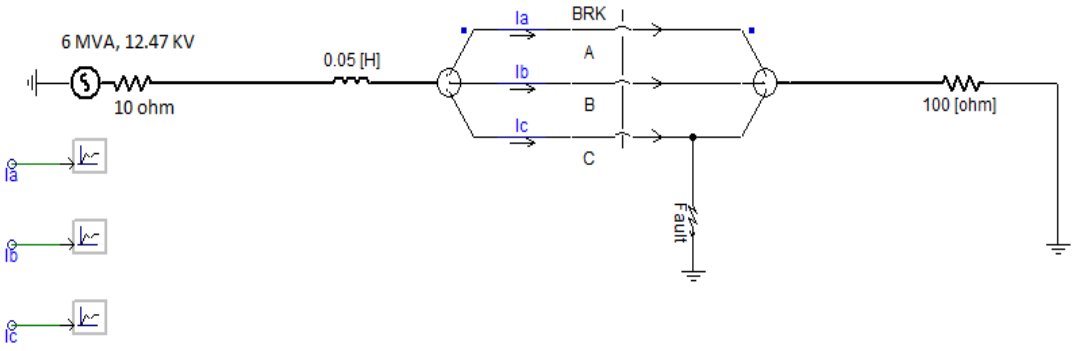

Figure 3.14: Radial Distribution Model in PSCAD

3.3.2 PSCAD Model

The objective of this model is to develop a PSCAD component that will emulate the reclosing function of the SEL-351S relay. An SEL-351S is an instantaneous overcurrent based recloser relay. The model is shown in Figure 3.15.

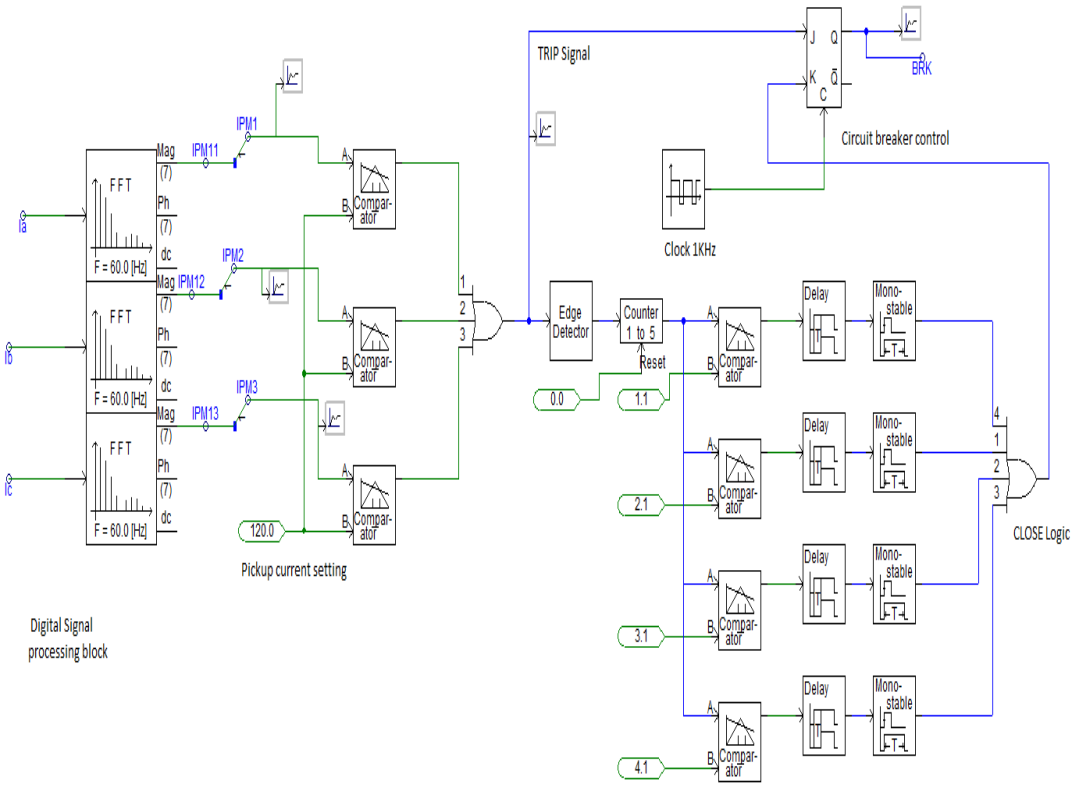

Figure 3.15: Recloser Logic in PSCAD

The first component developed is the FFT, which will take time-domain current signals from the distribution circuit model. This block is shown on the left side of Figure 3.15 with inputs from the sinusoidal three-phase current waveform. The FFT block can determine the harmonic magnitude and phase of the input signal as a function of time. The input signals are first sampled before they are decomposed into harmonic constituents.

The FFT block signals are passed to comparator block where the value of current is compared with pickup setting of the relay. The output from these block of all three phases is input to an OR gate. The OR gate will be at binary high if any of comparator is at binary high. This could signify any situation either fault in the circuit or unbalance operation of the power system. The output of OR signal is a trip signal to the circuit breaker.

Next step is to calculate the number of reclosing shots. The output of OR block is given to edge detector block. The edge detector compares its present input to its input from the previous time step. The output is dependent on whether the present input is higher than, the same as, or lower than the previous input.

The reclosing shots are calculated with the help of COUNTER block in PSCAD. The counter component will alter its state to the next 'higher' state when it receives a positive value at its input. When it receives a negative value, it will change its state to the next 'lower' state. This means increasing or decreasing its output by one. SEL-351S has four shot inbuilt recloser model. The higher value of the counter block is four to calculate four reclosing states, and the lower value is zero.

The output of the counter block is passed to the comparator blocks. The output of the first comparator will go high after first shot, the output of the second comparator will go high after second shot, and so on.

The output of the comparator block is given to MONOSTABLE and DELAY block to introduce a delay in every reclosing state once trip single has been generated. The output from these pair of blocks are input to an OR gate. The output of this OR gate

is CLOSE signal to circuit breaker. The desired reclosing operation can be obtained by implementing the states in Table 3.2

Table 3.2 Reclosing Logic for Circuit Breaker

TRIP	CLOSE	Breaker Status
0	0	0
0	1	0
1	0	1
1	1	Not allowed

3.3.3 Results

The relay is based on overcurrent protection. Four shot recloser action of SEL-351S is emulated. The pickup current of the relay is set at 120 A. A single line to ground fault is simulated in phase C. The recloser model is configured to operate in four modes. The closing of the breaker after the fault is termed as a shot. The Closing shot occurs after every five cycles (0.08s)

Mode1: With one fast operation. After a fault, the breaker opens instantaneously and after five cycles (0.08seconds) it is reclosed. Since the fault is not cleared, it open again for three cycles (0.03 seconds) and closed after the fault is cleared.

Mode2: With two fast operations

Mode3: With three fast operations

Mode4: With four fast operation and recloser is put into lockout mode (Permanent fault on the system)

Case 1: A temporary single line to ground fault is applied to phase C at one second. The fault is cleared in 0.1 sec and circuit is reclosed after one shot of fast operation (0.08s) in fast mode operation as shown in Figure 3.16.

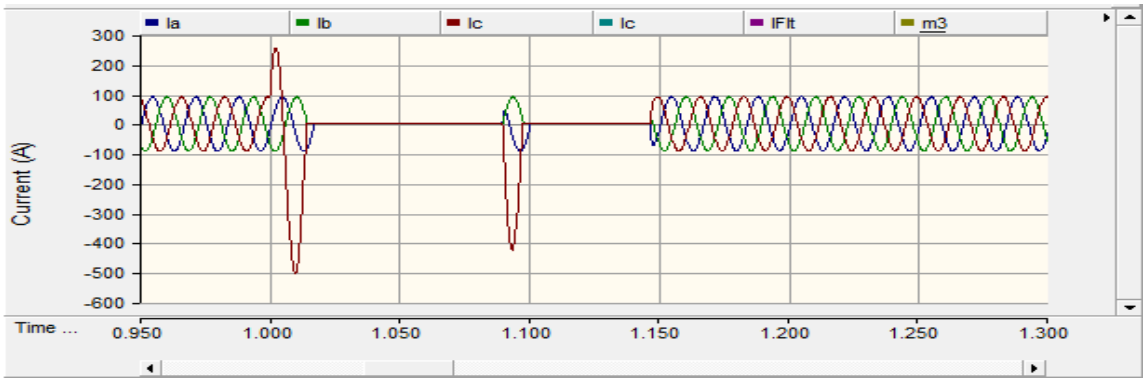

Figure 3.16: Recloser Operation in Mode 1

Case 2: A temporary single line to ground fault is applied to phase C at one second. The fault is cleared in 0.2 sec and circuit is reclosed after two shot (0.8s each) of fast operation in fast mode operation as shown in Figure 3.17.

Figure 3.17: Recloser Operation in Mode 2

Case 3: A temporary single line to ground fault is applied to phase C at one second. The fault is cleared in 0.3 sec and circuit is reclosed after two shot of fast operation (0.08s) in fast mode operation and one shot of slow operation (0.1s) as shown in Figure 3.18.

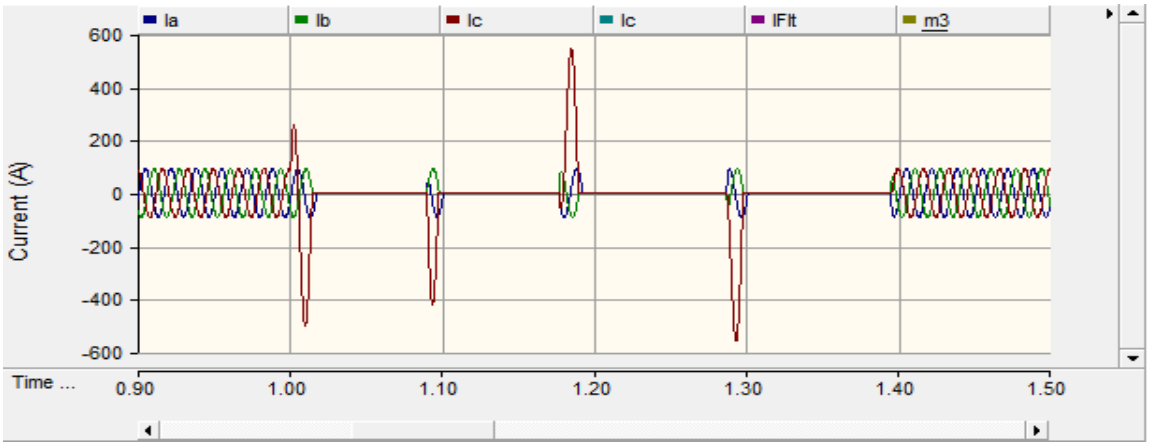

Figure 3.18: Recloser Operation in Mode 3

Case 4: A permanent single line to ground fault is applied to phase C at one second. The fault is not cleared even after two shot of operation in fast mode operation (0.08s each) and two shot of slow operation (0.1s each). The relay is put into lockout mode, and the breaker is permanently opened as shown in Figure 3.19.

Figure 3.19: Recloser Operation in Mode 4

This recloser system will be extended to large mesh distributed system for LSSS. An addition of recloser system in LSSS system would enhance the availability of supply in the system.

3.4 Summary of Results

A protection scheme for detecting unsymmetrical and symmetrical faults has been discussed in this chapter. The primary goal for pilot protection is to operate efficiently for a fault on the protected line and securely for faults outside the protected line. The negative sequence directional element is used to detect the unsymmetrical faults. The positive sequence based directional element is used to detect symmetrical faults. The operation of recloser system in PSCAD is discussed. This model will be integrated to large distribution mesh system in later stages.

CHAPTER 4: WIRELESS COMMUNICATION FOR PILOT PROTECTION

4.1 Introduction

With the increase in distributed generation and bidirectional power processing capability of modern power electronic distribution system, the directional over current scheme without implementation of pilot protection systems may not be reliable enough. Pilot wire relaying sends the voltage and current signals over a communication link that can be used for differential protection. The most common link was copper wires that were replaced by fiber-optic and Ethernet cable. But the use of this link could increase the significant amount of delay in the system and also sometimes they are expensive. The modern challenge is a method to provide digital communication for pilot protection that is reliable and affordable [24].

Digital radio could be a reliable and affordable solution for pilot protection at the distribution level. The IEEE 61850 GOOSE profile is a standard for relay to relay messaging protocols as shown in Figure 4.1. The commercial digital radios that are specially designed for the power protection system not only provide protection information but can be used for metering, control, and monitoring [25].

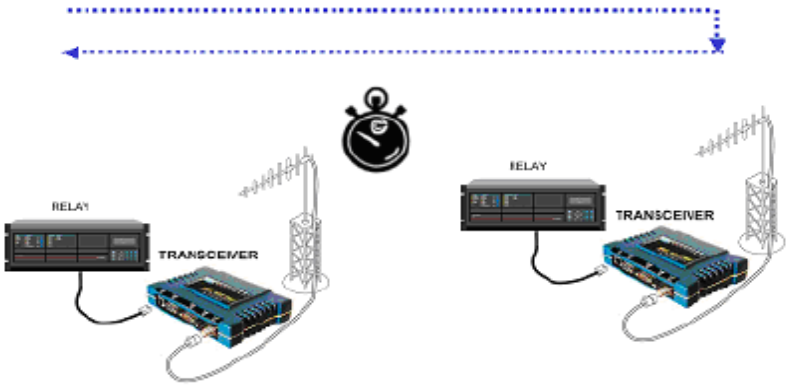

Figure 4.1: Digital Radio Pilot Protection Test Set-Up [25]

A well designed and efficient protective relaying should have:

1. Speed 2.Selectivity 3. Sensitivity 4. Reliability 5. Simplicity 6. Economy

Primary factors that need to consider before using a communication link are reliability, security, and latency. A low-bandwidth radio link as the communication link is reviewed in this chapter for the FREEDM system.

4.2 Pilot Protection with Digital Radio

Former ASU students have developed a pilot protection using fiber optic cable for the communication. However, in the industry review meeting NSF criticized the use of fiber optic channel regarded it as incompatible over long distances. Our group came up with the idea of using radio communication for the pilot protection scheme. In this report, the feasibility of wireless communication is studied.

A typical pilot protection system is shown in Figure 4.2. A multisource radial system is connected to a transmission line [25]. The circuit breaker should trip when there is a fault on a line. No tripping is generated when there is a fault outside the protected region. The two relays are communicating each other using a communication method that could be wireless or Fiber-optic.

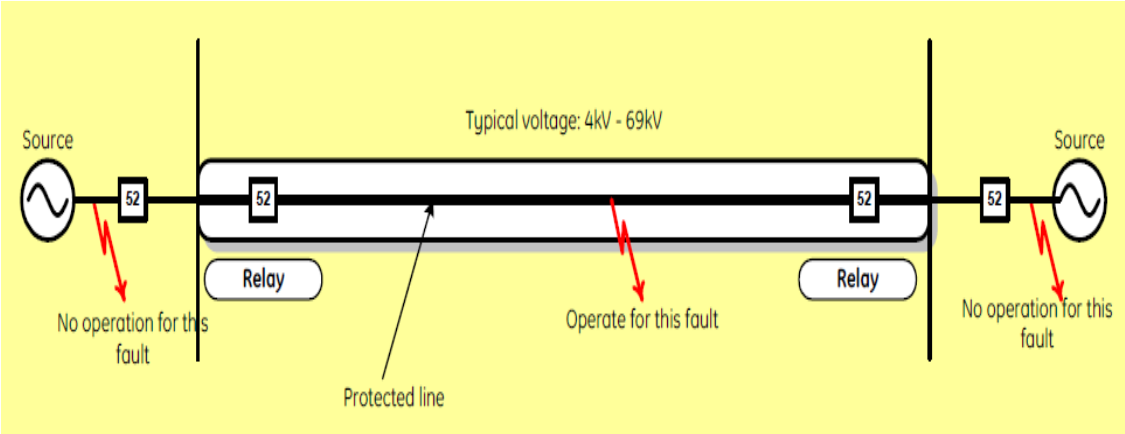

Figure 4.2: Pilot Protection System [25]

The majority of distribution systems are radial system, which allows the application of time coordinated overcurrent protective devices. The FREEDM system is a large meshed distribution system. To avoid any delays in the protection scheme, instantaneous overcurrent relays are used. Hence, an efficient scheme based on voltage and current sequence components is used along with overcurrent protection.

4.3 SEL-3031 Serial Radio Transceiver [26]

The SEL-3031 is a 900 MHz, license free, spread-spectrum radio. The SEL-3031 has the capability of providing DNP3 SCADA information, MIRRORED BITS® control for reclosing coordination and engineering access to the SEL-651R Recloser Control [26].

The most important features of this product are [26]:

1. Dual Radio operating modes: This supports point-to-point radio operation for distribution protection
2. Low latency: This is the most important factor for considering any communication method for pilot protection. Latency is termed as the time delay in sending information over a communication link.

For our research, commercial available SEL-3031 radio links are used to establish communication between two relays. The radio link prevents the need for multiple sets of radio or expensive dedicated fiber transmitting over the long distances. The SEL-3031 radio link can simultaneously communicate with up to three independent ports and protocols via point-to-point radio operation. The SEL Mirrored bit technology is used to set up communication between the two radio links [26].

4.4 Installation of SEL3031 radio

While setting up the radio link in the laboratory, various factors were studied to ensure reliable communication. The important factors for digital radio are the distance between transmitter and receiver, obstructions in the line of sight between antennas, and the natural environment beneath the path [25].

The line of sight limits the operation of the radio. The line of sight between the two antennas is shaped liked, and ellipse called Fresnel zone as shown in Figure 4.3. Obstructions in the Fresnel zone may cause multipath interference due to reflective or refractive signals that mat arrive at the receiver out of phase with the desired signals.

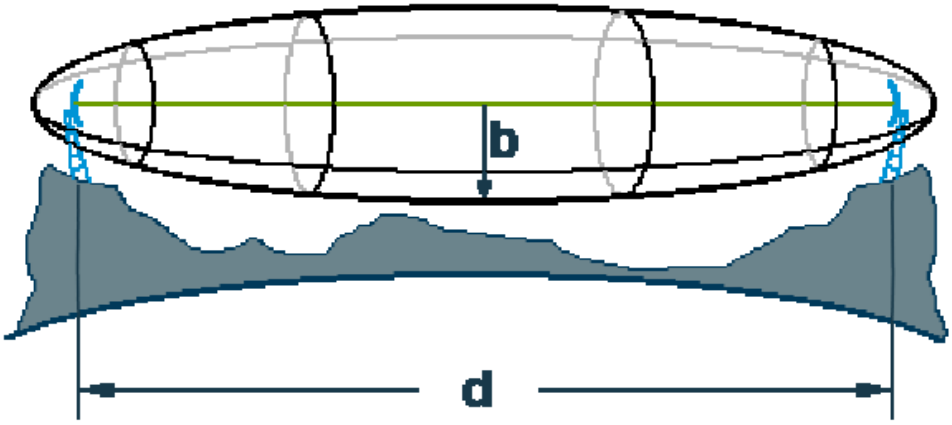

Fig 4.3: Fresnel Zone [25]

The formula used to calculate the widest distance of the Fresnel zone is as follow [25]:

$$b=17.32\sqrt{d}/4f \quad (4.1)$$

Where: b= radius of the Fresnel zone in meters

d=distance between transmitter and receiver in kilometers

f=frequency transmitted in GHz

Figure 4.4 shows the maximum Fresnel zone diameter and path loss for some typical path distances

900 MHz		
Distance Between Antennas	Fresnel Zone Diameter	Freespace Loss (dB)
300 m (1000 ft)	5 m (16 ft)	81
1.6 km (1 mi)	11.6 m (38 ft)	96
8 km (5 mi)	26 m (85 ft)	110
16 km (10 mi)	36.6 m (120 ft)	116
24 km (15 mi)	44.8 m (147 ft)	119
32 km (20 mi)	51.8 m (170 ft)	122
40 km (25 mi)	60 m (190 ft)	124

Fig 4.4: Fresnel Zone Diameter [26]

In our case, the path quality is evaluated in the following ways.

Evaluating path quality [25]: The distance between two radio links in our laboratory is around 3 feet. Hence, path quality is visually inspected. This ensures the signal strength, reliability and speed of operation. The antenna gain, feedline loss, transmitted power and receiver sensitivity is also studied.

Antenna selection [25]: The single most important item affecting radio performance is the antenna system. High quality, high gain antennas should be used. For our laboratory purpose, SEL recommended the use of Yagi antenna (directional antenna). Directional antennas confine the transmission and reception of signals to a relatively narrow lobe, allowing greater communication range, and reducing the chances of interference to and from other users outside the pattern. The antennas are aimed at each other to obtain reliability. The end of the antenna should face the associated station. The maximum allowed gain of this antenna is around 14 dBi that is sufficient for the laboratory operation.

Fade margin [25]**:** This determines the allowable signal loss between the transmitter and receiver. The fade margin is a function of antenna gain, transmitter power, receiver sensitivity, and system losses. The longer the path, the more likely deep fades will occur, requiring a greater fade margin.

$$\text{Free space loss} = 92.4+20\log(f)+20\log(d)\ \text{dB} \quad (4.2)$$

Where f= frequency in GHz

d=distance in Km

4.5 Protection Method

The directional element of a relay consists of a forward element (F32Q) and reverse element (R32Q). The forward element goes high for the fault beyond the relay, and the reverse element stays idle whereas, for the fault behind the relay, the reverse element goes high while the forward element remains inactive.

To determine the direction of a fault, the F32Q element of the relay is continuously compared with the R32Q element of the next relay over the wireless communication. This method could be implemented when there is a bidirectional flow of power. When both F32Q and R32Q are high, it confirms that the fault location is in between the relays. F32Q is forward of relay 1 and R32Q is reverse element of relay 2 as shown in Figure 4.5.

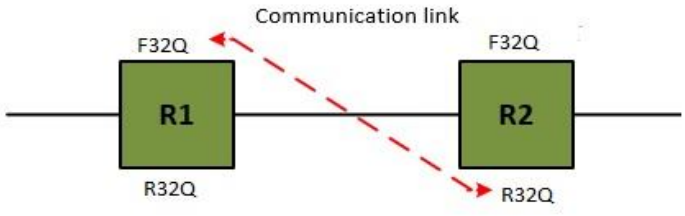

Figure 4.5: Relays Communicating Over a Link

4.6 Hardware Implementation

Commercial Schweitzer relay SEL-351S and radio link SEL-3031 is used to implement the pilot directional algorithm. Figure 4.6 shows the single line diagram of a three phase test bed used for hardware implementation [27].

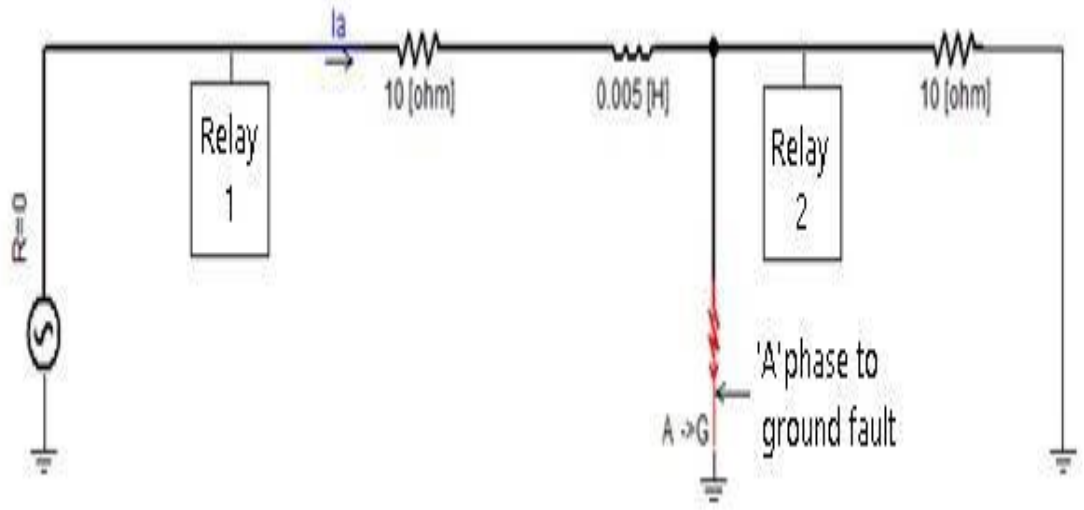

Figure 4.6: Single Line Diagram of the Hardware Test Bed

The current transformer used for relay one is installed with a ratio of 100/10. Relay one must be programmed with the CT ratio of 10. The values the relay displays and records are ten times the CT secondary current to represent the CT primary current value. Likewise, relay two is programmed in the same manner with its CT.

Table 4.1 tabulates the results of an 'A' phase ground fault. Due to the I^2R losses, CT inaccuracies, resistor imperfections, and various other factors it's expected the actual values are slightly lower than simulated values.

Table 4.1: Comparison of Various Data between Simulated, Calculated and Actual

Data	**Calculated**	**Simulated**	**Actual**
V_{input}		120 V	120 V
Z_{normal}		20.1∠5.4 Ω	20.1∠5.4 Ω
Z_{fault}		15.1∠5.4 Ω	15.1∠5.4 Ω
I_{normal}	6 A pk	5.9 A pk	5.5 A pk
I_{fault}	7.9 A pk	8.0 A pk	7.5 A pk

A 10-ohm resistor and five mH inductor connected in series are used to represent the line impedance of a feeder with a load of 10 ohm resistor. A three phase 208 V, 60Hz is used as the power supply. An SLG fault is applied using '*fault switch'* as shown in Figure 4.7 with a fault resistor of 10 ohms. The current transformer used for relay one is installed with a ratio of 100/10 while relay two installed with 100:5 CTs. The 1:1 isolation transformers are used as voltage inputs to both the relays. The SEL-3031 serial radio transceiver is used as a communication device with wireless communication as the medium between the relays. The current in the test bed during normal operation is 6 A but, when a fault is created by turning ON the switch, current in phase A jumps to 7.5 A.

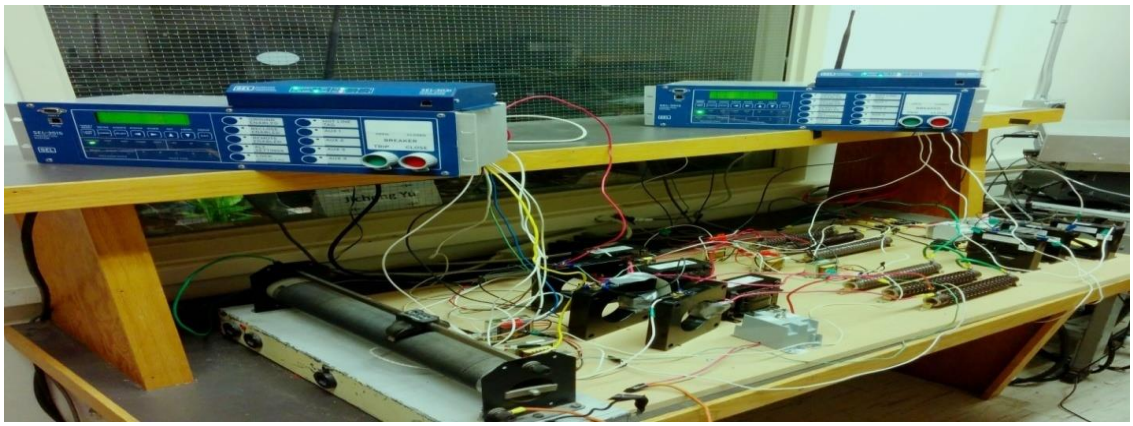

Figure 4.7: Hardware Setup at ASU Power System Lab

E32 and E50 SEL element work together to generate a directional overcurrent trip signal. Figure 4.8 shows relay one setting for a directional overcurrent trip. The relay can see both a forward or reverse fault. The relay must be programmed to ignore the no trip direction and output a trip in the proper trip direction.

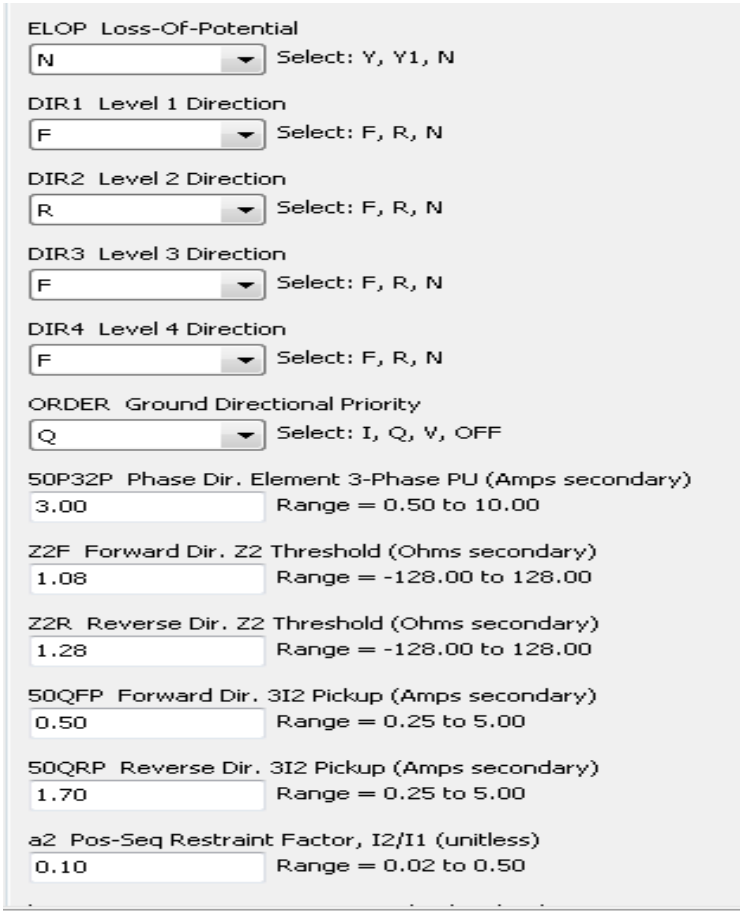

Figure 4.8: SEL AcSELerator Settings for Directional Protection

Relay one was tested with a fault and responded correctly depending on the directional setting (F or R) programmed. Table 4.2 shows the results of relay one testing for E50 and E32 used for directional overcurrent.

Table 4.2: Trip Signal for Directional Protection

Relay	Fault Direction	Relay	Fault Direction
R1	Forward	R2	Forward
R2	Forward	R3	Reverse
Trip signal	No trip	Trip signal	Trip generated

Relays calculate the negative sequence impedance to determine the direction of fault current.

4.7 Mirrored Bit Communication [29]

The mirrored bit communication is the protocol used for communication between the relays. Since the test bed used is a radial system, the fault current direction is from only one end. The forward element of R1 (F32Q) is compared with the reverse element (R32Q) of R2 to determine the fault current direction. The F32Q element of R1 is transmitted as a mirrored bit to R2, and the R32Q of R2 is transmitted to R1. When both of them are high, the fault is located at the end of R2, and the relay is programmed to trip when it receives a high signal from R1. Figure 4.9 depicts the communication method using mirrored bits [7] [29].

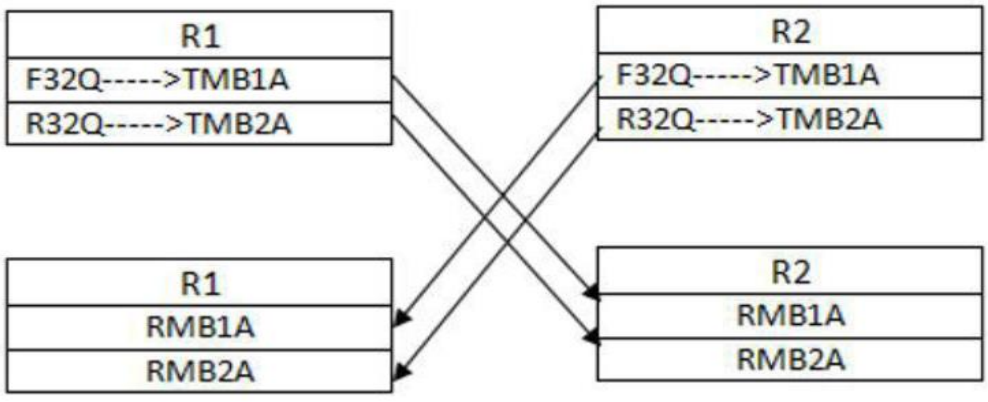

Figure 4.9: Mirrored Bit Communication in SEL Relays [29]

SEL AcSELerator analytic assistant software is used to view the trip signal generated by the system parameters as shown in Figure 4.10 [28].

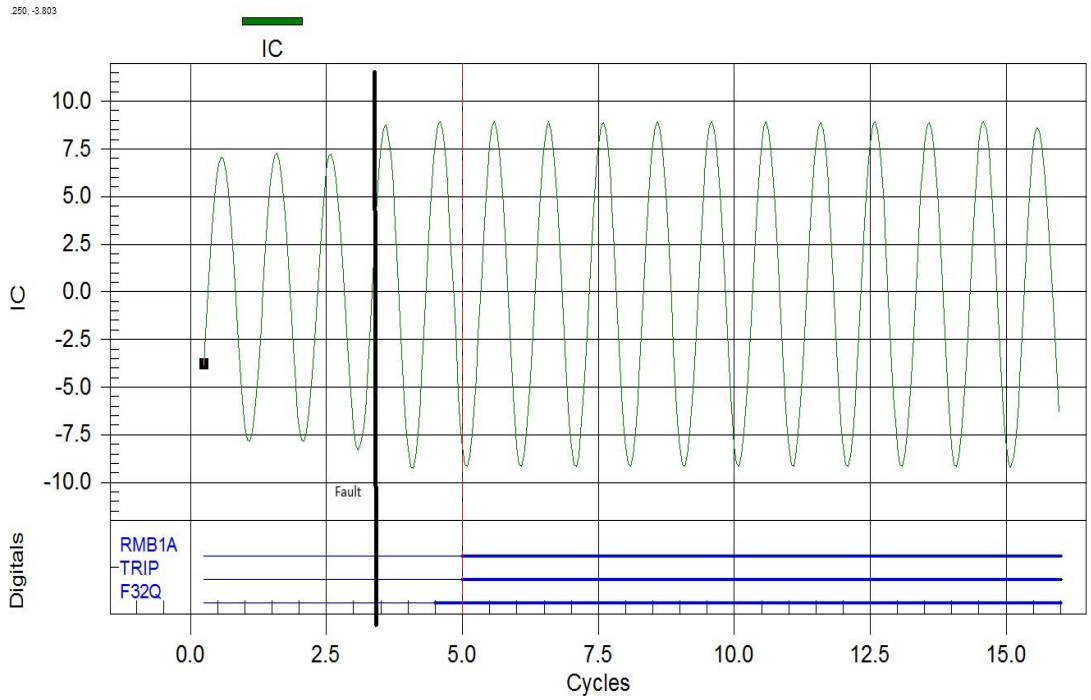

Figure 4.10: Trip Signal from AcSELerator Quickset Software [28]

In Figure 4.10, after the occurrence of a fault at 3.5 cycles, as shown by the thick black line, the F32Q bit of relay one goes high at 4.5 cycles while the trip signal is generated at five cycles. The time delay between the occurrence of fault and trip signal is 1.5 cycles. The relay can be made more sensitive depending on the value of pick up negative sequence current.

4.8 Summary of Results

A pilot directional protection scheme using wireless communication has been developed that quickly and accurately detects the direction of the faults. A hardware test bed using commercial SEL-3031 radio link and SEL-351S is used to validate the pilot directional algorithm.

CHAPTER 5: LSSS SYSTEM

5.1 Introduction

The LSSS system is a large-scale distribution system model for simulation of dynamic behavior that requires multiple nodes or wide geographic spacing to demonstrate, to show the following attributes [30]:

- Economic allocation of storage and renewable resources over a 24-hour duration (IEM functionalities)
- Fault protection and restoration
- Dynamic component interactions and mitigations
- IPM functionalities

To validate component models for different time-scale platforms, to provide standard virtual testing and demonstration platforms for the FREEDM center, and to validate use cases that include load profiles, renewable energy profiles, faults, and topologies.

The LSSS provides a platform on which system-level controls can be tested and refined.

- DGI – provides a scalable platform to demonstrate DGI functionality
- SST – provides a platform to analyze the interaction of multiple SSTs, start-up, and initialization transients
- DESD – provides a platform to investigate the interaction of various DESD with SST, study stability cascaded inverters – especially PV and SST.
- Simulation and modeling are critical aspect of the FREEDM System which requires adequate models of all the FREEDM System components/systems for

(HIL) testing, evaluation, and LSSS demonstrations. Identifying FREEDM Systems-appropriate load, DRER, DESD, and controller models is a core task of this effort that supports IEM, IFM and IPM "use cases". This project will tie directly to the LSSS test bed (for large-scale system complexity, such as emergent behavior) and to the HIL test bed (for component and small system complexity, such as pairwise SST interactions), to manage the voltage variations in the FREEDM system at the primary (high voltage) level while maintaining the efficiency of the system under varying operating conditions [31].

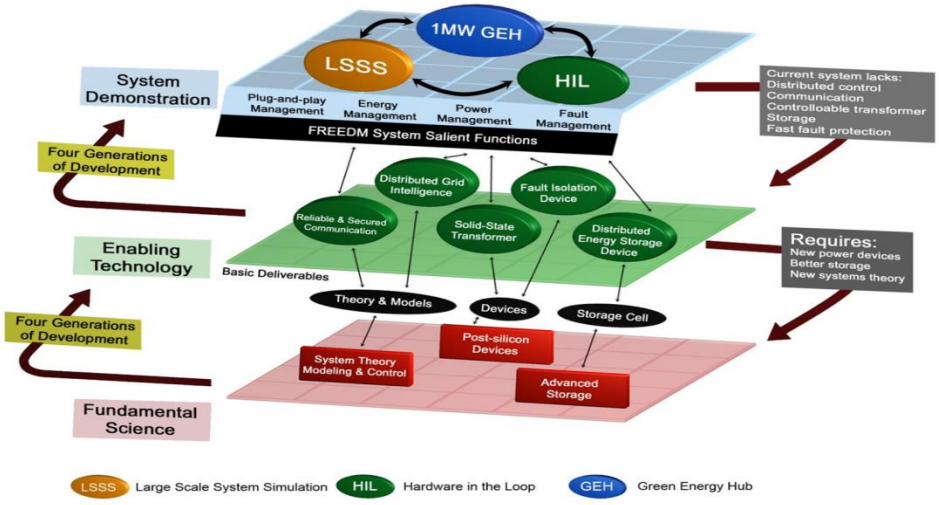

Figure 5.1: FREEDM Three Level Diagram [30]

- FID - Develop a comprehensive computer model of the hardware of the pilot protection and incorporate the model in the large-scale test bed. Develop communication with the FID electronic circuit breakers and the SST modules.

Assure that the pilot protection generated fault signal triggers the switch off/opening the FID's and initiate the blocking of the SST [32].

In particular, while radial distribution systems are common in real-world distribution but the FREEDM architecture includes meshed systems. The LSSS system is an extension of the IEEE-34 bus system in mesh form with SST as loads. Within the LSSS, the actual DGI/RSC operates as software in the loop mechanism with both systems written in the simulation. An existing PSCAD socket interface links the control signals and system readings to the DGI/RSC and, therefore, there is no difference between application to radial and meshed topologies

5.2 Solid State Transformer (SST)

The main component of LSSS system is SST. SST has three power stages, i.e., Rectifier, Dual Active Bridge, and Inverter [33]

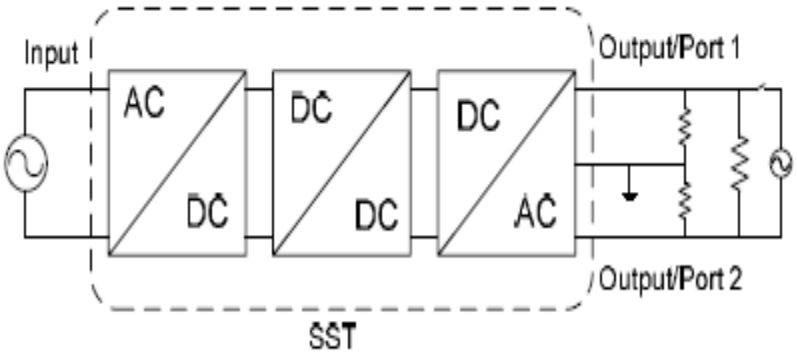

-

Figure: 5.2: SST Block Diagram [33]

The AC/DC rectifier stage converts the single phase 7.2 kV AC voltage to DC output while controlling the reactive power at the input side. The Rectifier Stage Parameters [33]:

- Inductor = 0.2H

- Output capacitor = 300uF (High voltage DC capacitor)
- Start Up resistor = 10 ohms

Whereas the rectifier regulates the high voltage DC voltage and controls the input current to be sinusoidal from the HVAC side, the low voltage DC link is controlled by the DAB converter. The dual active bridge is modeled in accordance with the equation:

$$P = \frac{n*Vhdc*Vldc}{2*fsw*L} \quad (5.1)$$

The Dual active bridge parameters:

- Output capacitor = 100uF (Low voltage DC capacitor)

The DC/AC inverter converts the 400V DC to 240/120V AC. Whereas the DC link voltage is regulated by the DAB converter while the PWM AC inverter controls the magnitude of the output side AC voltage.

The Inverter parameters:

- Output capacitor = 500uF

The SST is rated at 200KVA

SST Start-up and protection [33] [34]:

Distribution/Load SST:

The load SST start-up sequence comprises of charging the HVDC bus through the diode rectifier and then ramping up to the desired value in a controlled way.

- The load SST has an internal protection based on the grid voltage and HVDC link voltage.

- SST trips if the voltage of the HVDC (3800V) capacitor is below 0.80pu (3000V) or above 1.20pu (4500V). HVDC cap is designed for 1.2 times the rated voltage (4.56kV). Delay of 1 cycle is provided for dc bus voltage tripping
- Under voltage tripping of the load SST based on the input voltage is implemented for cases where HVDC link voltage is within bounds. The SST trips if the input voltage goes below 0.8pu. A delay of 5 cycles (80 ms) is used for riding the system through temporary faults.

Substation SST [34]:

- On occurrence of a fault, this SST is capable of limiting the fault current (output current) to 2 pu and shut off after certain designated period (long enough for the protection system to detect fault)
- As the output voltage of the SST falls during a fault, the internal logic of SST will trip the breakers once the voltage drops below 0.8pu The upper limit on output voltage for tripping SST is 1.2pu There is a delay of five cycles in the tripping logic to prevent SST from tripping in case of temporary faults.

Load SST:

- On occurrence of a fault, this SST is capable of limiting the fault current (input current) to 2 pu and shut off after certain designated period (long enough for the protection system to detect fault)
- As the input voltage of the SST falls during a fault, the internal logic of SST will trip the breakers once the voltage drops below 0.8pu. The upper limit on output voltage for tripping SST is 1.2pu. There is a delay of five cycles involved in the tripping logic to prevent SST from tripping in case of temporary faults.

- Tripping logic based on the voltage of the high voltage dc link is also included. The lower limit and upper limit for tripping are 3000V (0.789 p.u) and 4500V (1.184 p.u) respectively.

5.3 Pilot Protection Scheme – Trip Signal

The protection mentioned above is internal to the SST, which takes some time to trip the SST. The pilot protection, before the internal protection turns off the SST's, detects the fault and sends a trip signal to SST. The pilot protection scheme should be quick enough to detect the fault in the FREEDM loop. Once the fault has been detected, the SSTs should accept the trip signal to disconnect itself from the main loop. The FIDs should readily accept the trip signal to isolate the system from the fault.

Figure 5.3 shows the LSSS system in PSCAD. This is a large mesh distribution system with SSTs as loads. The rectangular blocks are the SSTs. This is an extension of an IEEE-34 system.

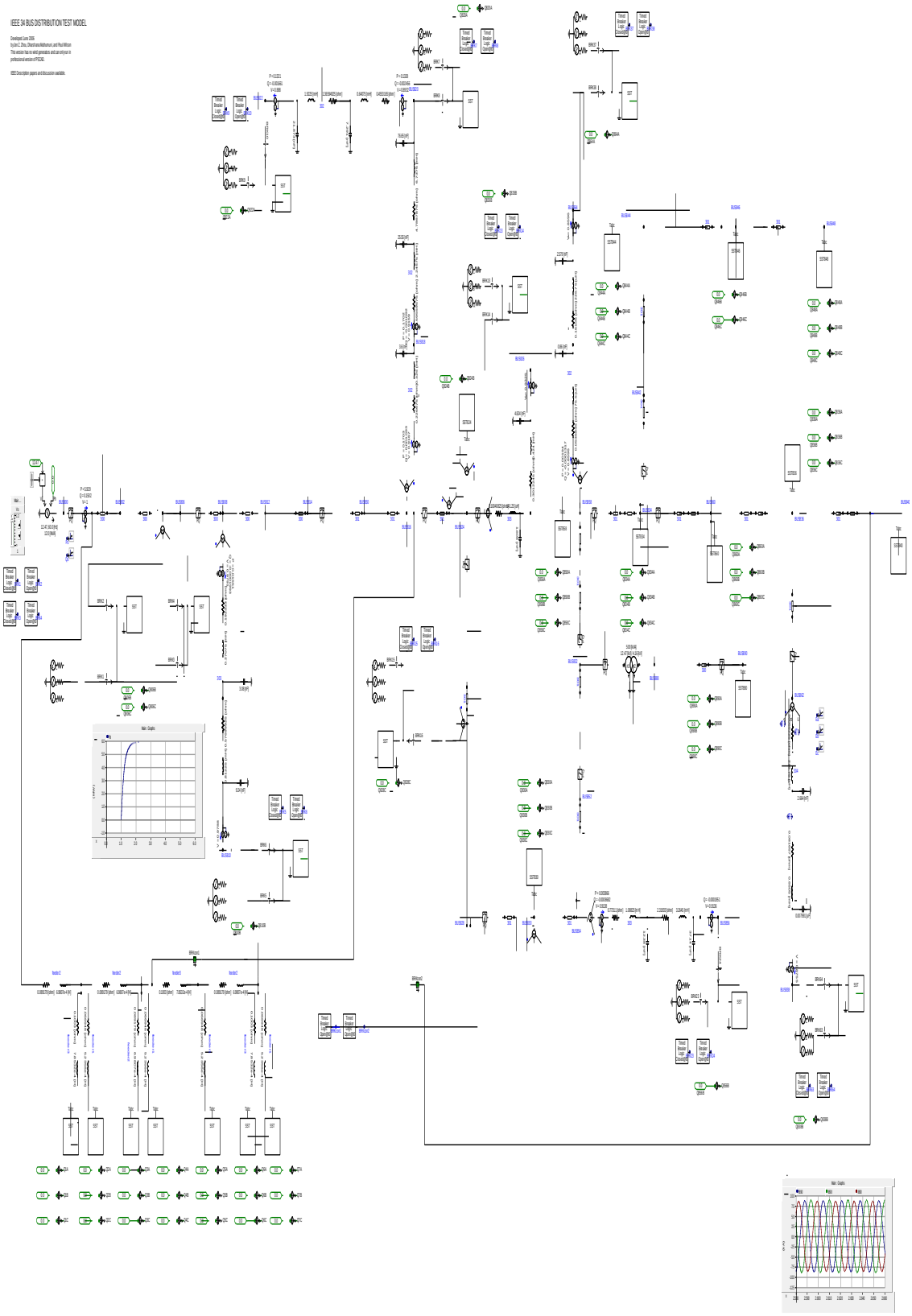

Figure 5.3: LSSS Mesh System in PSCAD

Total number of 21 SSTs are added to this system that includes both single and three phase. The loads connected to various nodes are shown in Table 5.1.

Table 5.1: Load Data at Various Nodes for the LSSS system

Node	kWa	kWb	kWc
806	0	30	25
810	0	16	0
820	34	0	0
822	135	0	0
824	0	5	0
826	0	40	0
828	0	0	4
830	17	10	25
856	0	4	0
858	7	2	6
864	2	0	0
834	4	15	13
860	36	40	130
836	30	10	42
840	27	31	9
838	0	28	0
844	144	135	135
846	0	25	20
848	20	43	20
890	150	150	150
866_1	75	75	75
866_2	75	75	75
868_1	75	75	75
868_2	75	75	75
870	75	75	75
872_1	75	75	75
872_2	75	75	75

The SSTs are connected to the distribution mesh system after one second of simulation. This is done to study the distribution mesh system behaviors and dynamic

stability of the system without SSTs. After the connection of SSTs at one second, the flow of real power is shown in Figure 5.4.

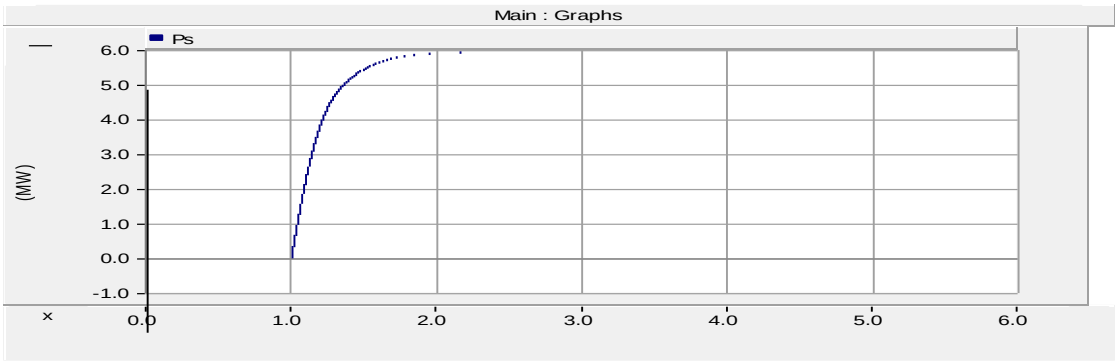

Figure 5.4: Real Power Flow in the LSSS System

The line data of the system is given in Appendix A. The presence of single phase and three phase SSTs make the protection system complicated. Also, SSTs limits the fault current at 2.0 p.u. For the first stage of operation, the SSTs are operating at unity p.f load. The SSTs can function as a distributed generator in the system. However, for this thesis SSTs are only acting as unity p.f load.

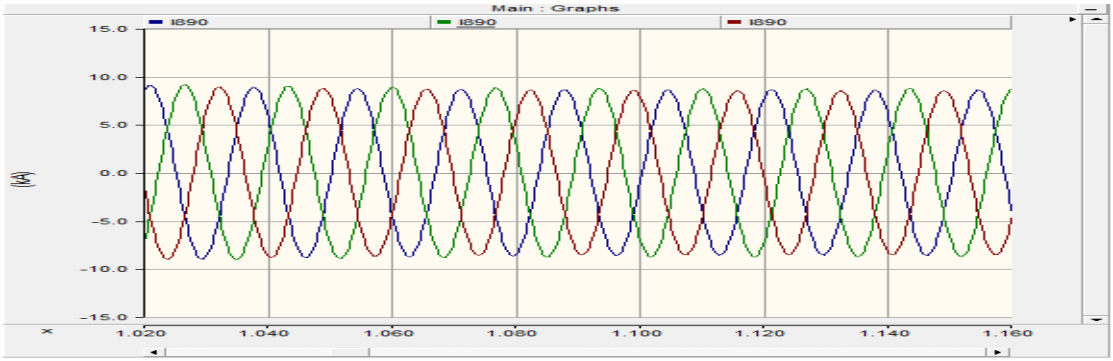

Figure 5.5: Current Waveform at SST Output

Figure 5.5 shows the stable operation in a large meshed/looped grid-tied distribution system during normal conditions. The functionality of this loop will be extended to islanded operation including autonomous energy management of energy storage and distributed generation.

CHAPTER 6: PROTECTION OF THE LSSS SYSTEM

6.1 Introduction

The ultimate customer of the FREEDM system is utilities. Utilities will not adopt the SST and FID until they can be assured that [34]

- The SSTs and FIDs will not interact poorly
- System stability will be maintained
- System reliability and resiliency will be improved (benefit > cost)

The LSSS is a demonstration platform that will provide the evidence of SST and FID operation in a distribution system. The protection of LSSS system is an important task to ensure the reliability of the system. This chapter will discuss the protection methodology used for the LSSS system in detail.

The LSSS mesh system is shown in Figure 6.1. It has an IEEE-34 bus system that is used to form a mesh system. The mesh system has been divided into six protection zones for implementing the pilot protection scheme. The zones are separated by zonal boundary protective elements that are comprised of both positive and negative directional element, overcurrent relay, and circuit breaker. The directional element is composed of negative and positive sequence elements to detect the direction of the fault. The various protection zones are shown, and each zone has two breakers. The current and voltage measurement module measures are current and the voltage at each of the circuit breakers.

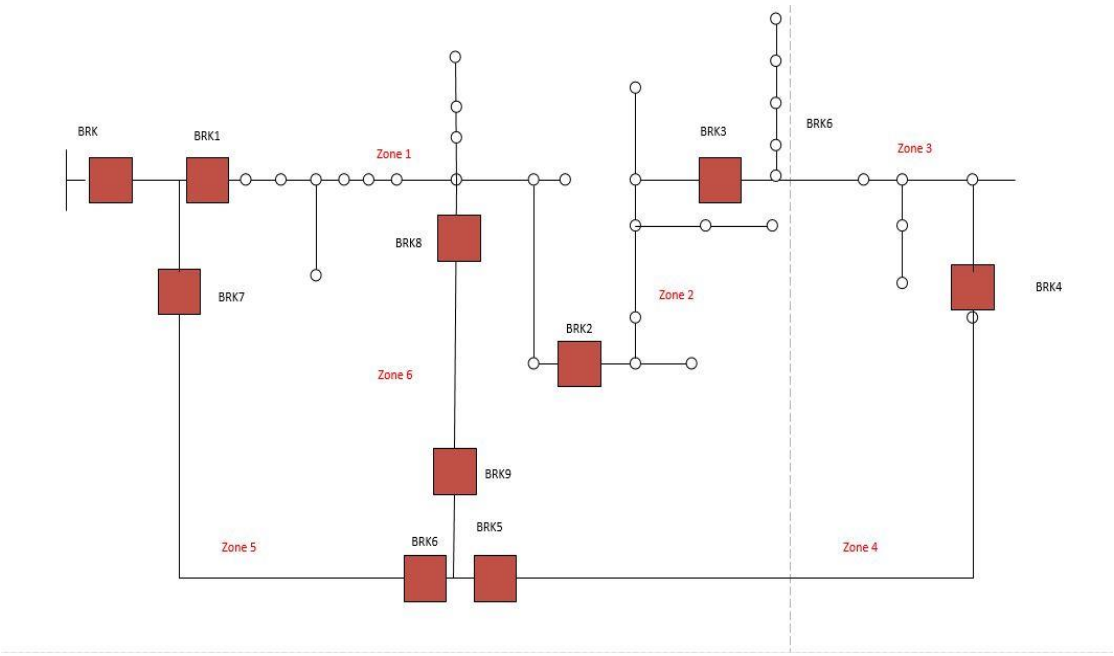

Figure 6.1: LSSS Model

The LSSS system has been divided into various zones of the protection in PSCAD as shown in Figure 6.2 and 6.3. The red color circles indicate the zone circuit breaker of the respective zones.

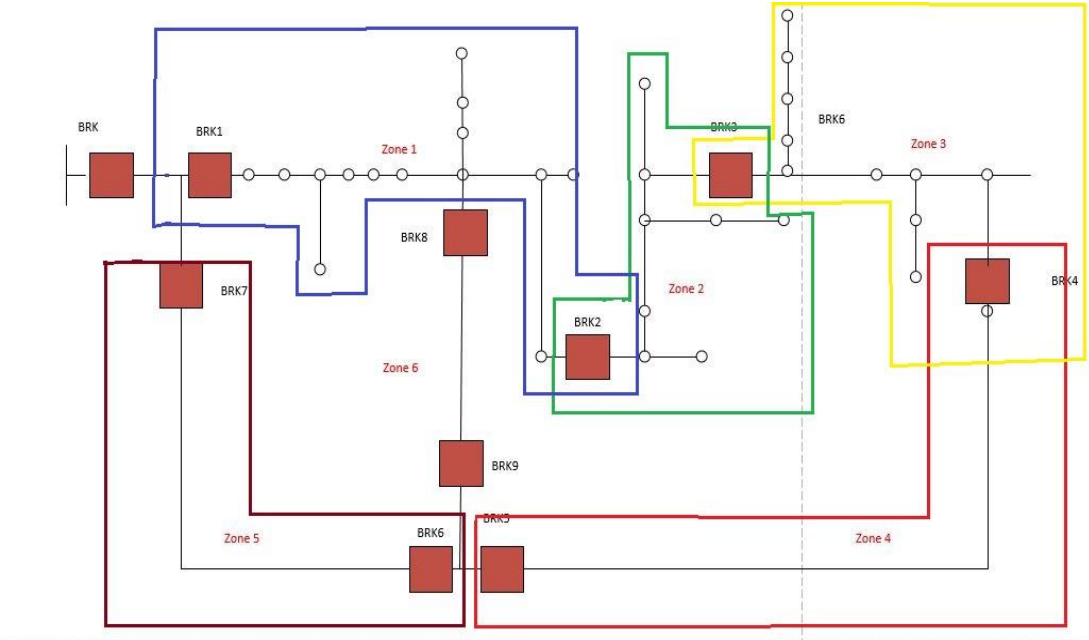

Figure 6.2: Zones of Protection for the Pilot Protection of LSSS System

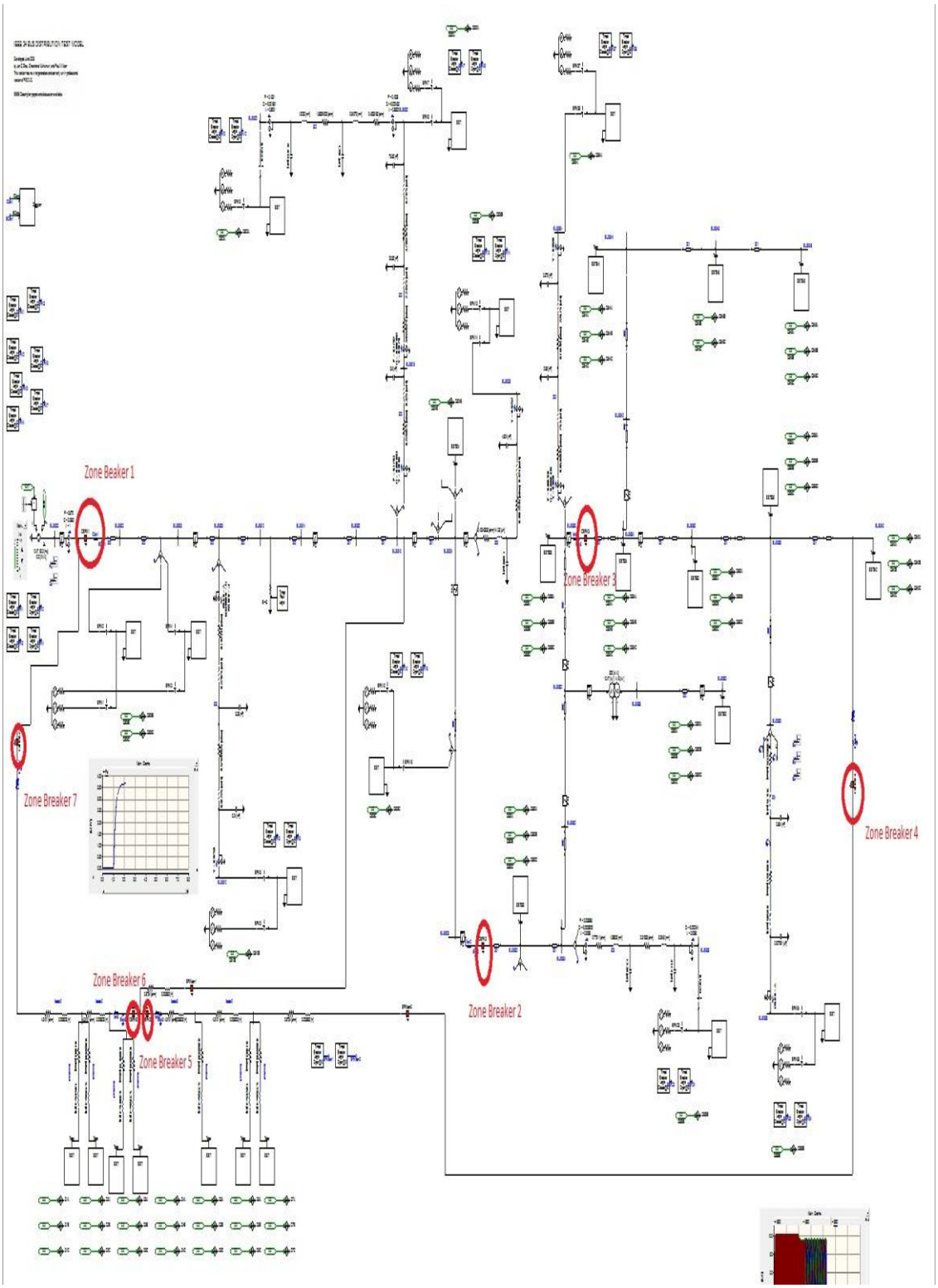

Figure 6.3: Zones of Protection in PSCAD (Red circles shows the location of circuit breakers)

Each zone of the system is protected independently in the pilot protection system. A total of ten current and voltage measuring modules are required for the protection. A fault in any zone will open the circuit breakers of the respective zone. For instance, a fault in zone 3 will open circuit breaker BRK3 and BRK4. Each directional and over current relay at the zone boundary controls the respective zone circuit breaker. The two relays in each zone will communicate with each other about the direction of fault current. The relay will only transmit one bit of information to the neighboring relays. Hence, this reduces the use of high cost and high bandwidth communication channel, and this information is used by relays to decide the tripping of boundary circuit breaker.

The following assumptions are made in this report:

1. Relays can control all circuit breakers.
2. Each zone boundary relay has both a receiving and a transmitting port for communication.
3. A reliable and secure wireless communication has been established in all the relays
4. An instantaneous overcurrent relay is used to reduce the trip time.
5. The negative sequence elements have an upper hand in making the trip decision for unsymmetrical faults.

6.2 Relay flow logic

The directional protection has the capability to detect both negative and positive sequence directional elements. The pilot directional protection scheme uses negative sequence and positive sequence components to detect the direction of the fault. This protection will only commence when there is an over current in that particular zone.

Hence, the combined decision of directional scheme and overcurrent scheme is used to open the circuit breakers of the faulted zone.

The Negative sequence directional element calculates the negative sequence impedance to determine the fault location. The calculated scalar quantity Z_2 is compared with two threshold values to determine whether the fault is in forward or reverse direction to a relay [20]**.**

$$Z_2 = \frac{Re[V_2.(I_2.1\angle\theta)^*]}{{I_2}^2} \tag{6.1}$$

$$V_2 = Negative\ sequence\ voltage$$

$$I_2 = Negative\ Sequence\ current$$

$$Z_2 = Negative\ Sequence\ Impedance$$

$$if\ Z_2 < Z_{2F}, fault\ is\ in\ forward\ direction$$

$$if\ Z_2 > Z_{2R}, fault\ is\ in\ reverse\ direction$$

$$if\ Z_{2F} < Z_2 < Z_{2R}, there\ is\ no\ fault$$

$$Z_{2F} = Forward\ threshold\ impedance$$

$$Z_{2R} = Reverse\ threshold\ impedance$$

During the normal operation, negative sequence quantities do not exist in the system. The calculated negative sequence impedance lies within the forward threshold and reverse threshold value. But during a faulted operation, sequential components come into play and Z_2 could be used to determine the fault location. If the calculated Z_2 is less than forward threshold impedance, then the fault is in a forward direction to a relay. If the calculated Z_2 is greater than reverse threshold impedance, then the fault is in a reverse direction to a relay. The sequence components of currents and voltages are obtained from

the fundamental phase quantities and are given as inputs to the 'Negative sequence directional element 32 Q' available in PSCAD [20] [7].

The SEL 351S relay detect the presence of symmetrical faults by comparing the phase angle difference between the positive sequence current and voltage to a defined range as shown in Figure 6.4 [27] [36] [38].

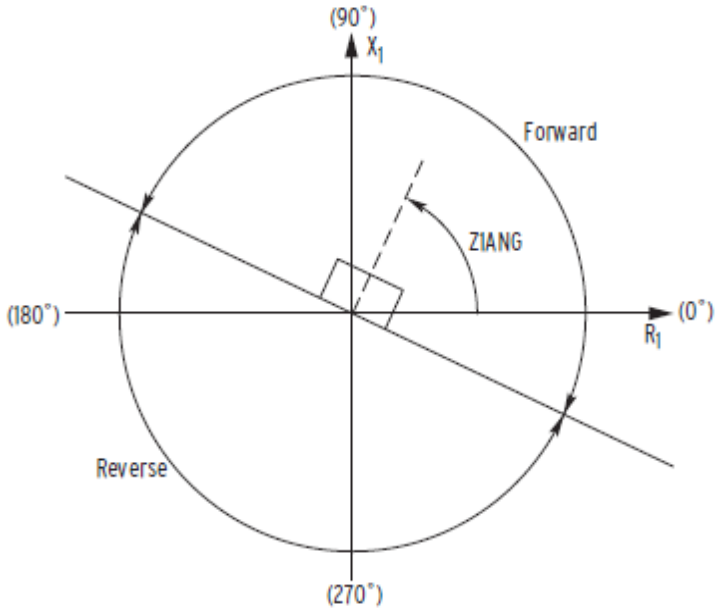

Figure 6.4: Positive Sequence Element Direction [27]

$$90° < \beta - Ø < -90°$$

β =Angle of the positive sequence impedance

Ø =Positive sequence line angle

The logic flow for the complete directional element is shown in Figure 6.5. The sequence current and voltage block will calculate the positive and negative sequence components of the current and voltage.

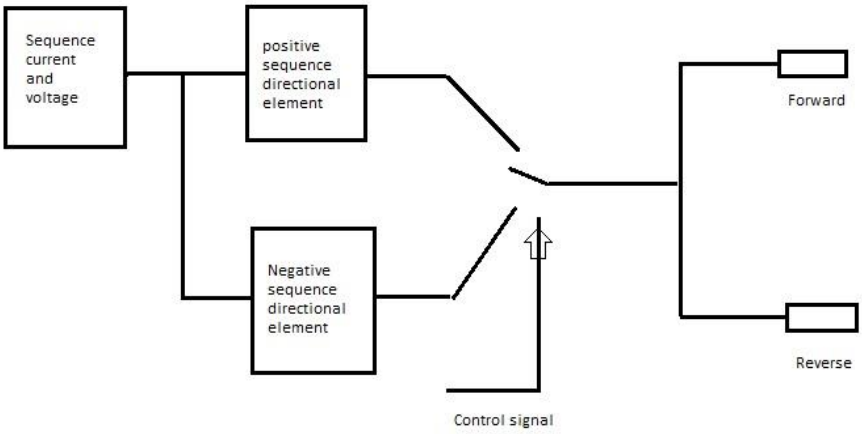

Figure 6.5: Relay Logic Flow

The calculated values will flow to positive and negative sequence block diagram where the fault direction will be determined. The control signal will decide which value to pass on for decision making. A control signal is typically a ratio of I_2/I_1. For unsymmetrical faults, this ratio would be high but it is low for symmetrical faults. Hence, the priority of decision will be made by the control signal. This choice is used to prevent the positive sequence directional element from making the erroneous decision for magnitudes of faults currents comparable to the load current.

Once the fault has been detected by both directional element and overcurrent element, a detection of faulted zone has to be made. A trip signal from the relay is compared with an adjacent relay to detect a fault in that section. Each relay can communicate with other relays using wireless communication. Figure 6.6 shows the

connection of the binary state signal with various zonal boundary elements. This communication is necessary because, for some faults, the corresponding zonal boundary element might not be able to detect the fault. Hence, the sharing of information among boundary elements will add reliability to the protection scheme [35].

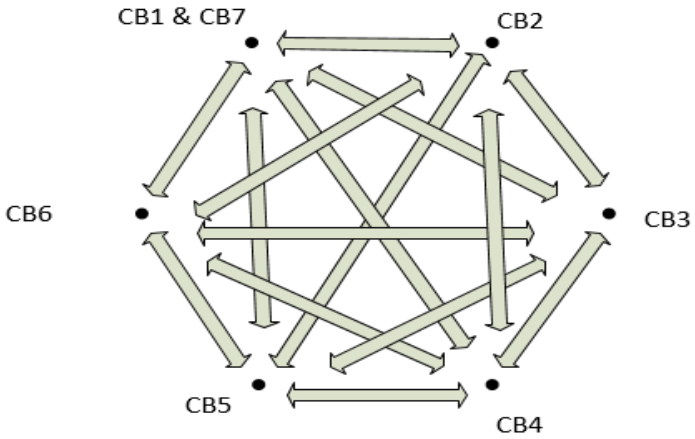

Figure 6.6: Communication among Various Relays

The trip signal to a circuit breaker is generated based on the information received from the directional element and overcurrent element. The direction element detects fault based on negative and positive sequence elements of current and voltage as shown in Figure 6.7.

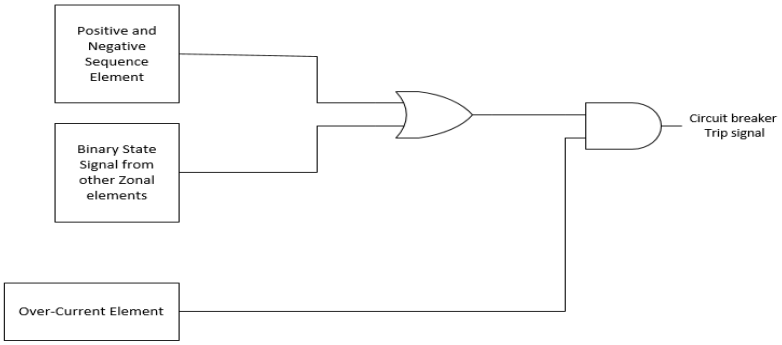

Figure 6.7: Protection Block Diagram

In case a directional element for a relay is not able to detect the fault, any high trip signal from the adjacent boundary element will be used for the decision making provided its over current element is high.

6.3 Implementation in PSCAD

The sequence components of currents and voltages are obtained from the fundamental phase quantities and are given as inputs to the 'Negative sequence directional element 32 Q' available in PSCAD. The negative sequence directional element stays idle during the normal operation and generates +1 or -1 depending on the fault location. It uses negative sequence impedance as the deciding factor to determine the fault location.

For a phase to ground fault and line-line fault, it uses the voltage of un-faulted phases for the relay to be operational. Figure 6.8 shows the implementation of the directional element (E32 Q element) in PSCAD [7] [20].

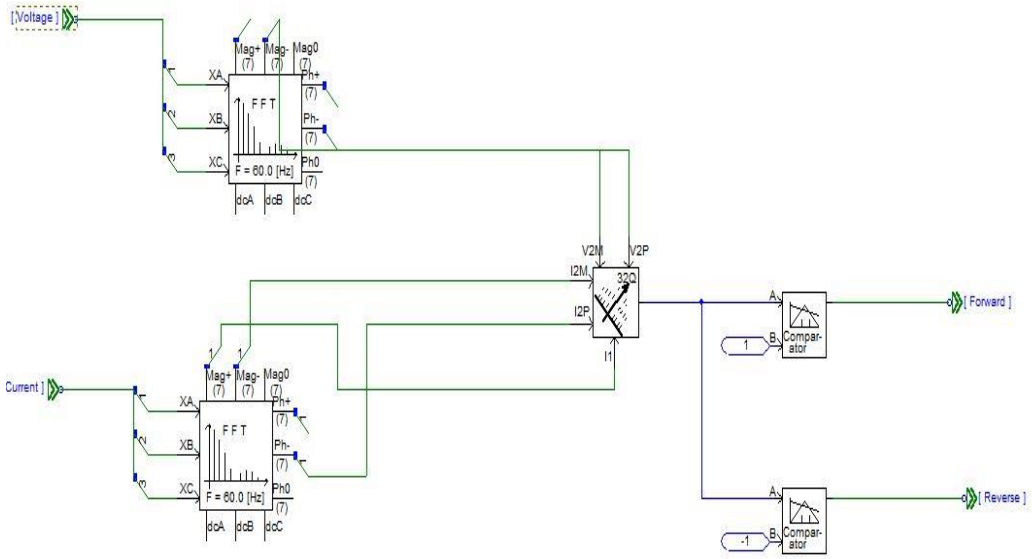

Figure 6.8: Negative Sequence Element in PSCAD

The voltage and current are passed through the positive sequence element to detect the presence of the symmetrical fault in the system as shown in Figure 6.9. The positive sequence directional element script is written in FORTRAN (Appendix B). The priority signal is obtained which is the ratio of negative sequence current to positive sequence current. This signal is used to detect whether the fault is symmetrical or unsymmetrical.

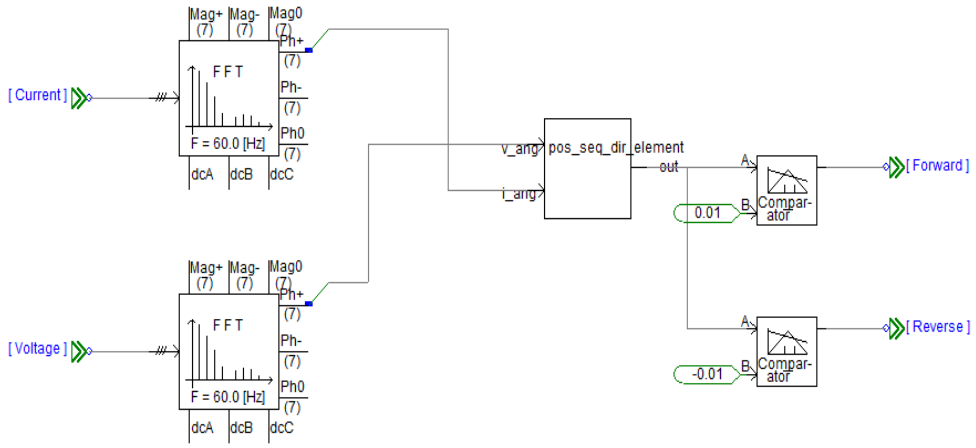

Figure 6.9: Positive Sequence Element in PSCAD

The overcurrent protection in the PSCAD is shown in Figure 6.10. An instantaneous time-based characteristic of the relay is chosen to have minimum tripping time. In this block, the phase current is compared with a fixed value of current which is approx. 1.5 times the full load current. A high signal is generated for any abnormality in the phase current. The overcurrent detector in PSCAD (50) is used to detect the fault.

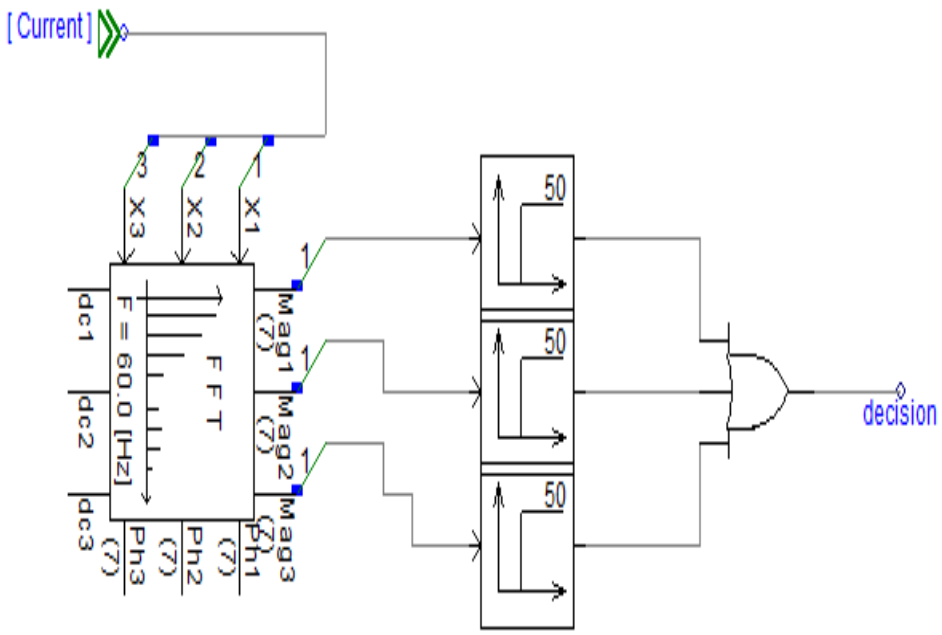

Figure 6.10: Overcurrent Element in PSCAD

The combination of negative sequence element and positive sequence element determines the direction of the fault in forward or reverse direction. This directional element together with over-current logic from each relay is used to determine the direction of fault as shown in Figure 6.11. The priority signal from positive sequence directional element is used to determine whether the fault is symmetrical or unsymmetrical. If priority signal is binary high that means the fault is symmetrical. Therefore, both two-input selector switch will be connected to point B. If priority signal is binary low, than negative sequence directional element will be used to determine the direction of the fault. The Figure 6.11 flow logic can be combined to make one unique component. This component can be used directly as an independent relay element. Hence, this eliminates the need for developing same logic for the different relays.

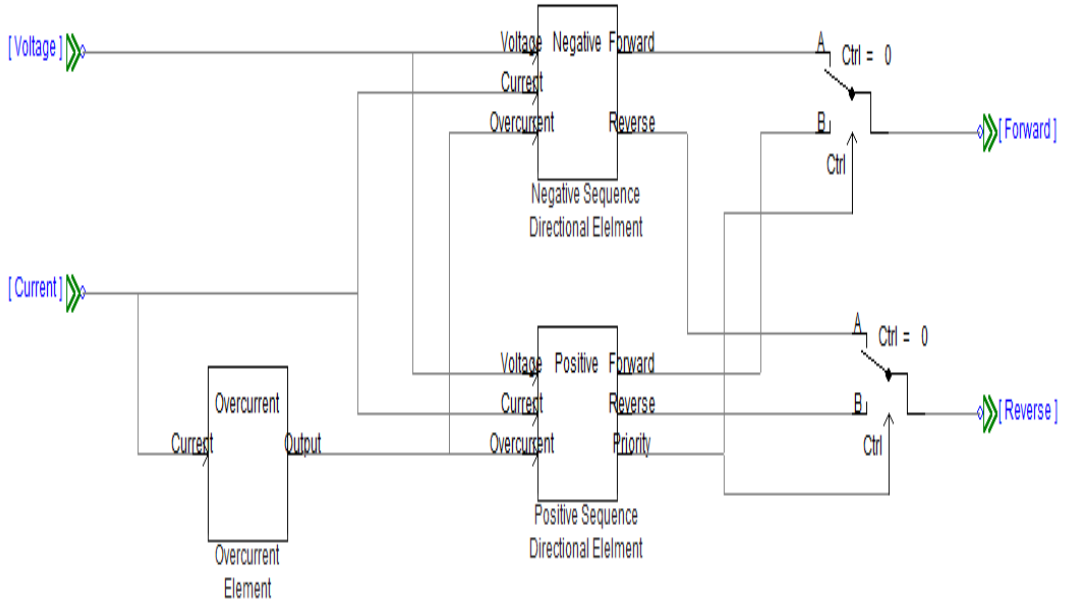

Figure 6.11: Implementing Directional Element in PSCAD

Once the logic for detecting the fault direction has been developed, the next step will be to combine trip signals from relays to detect a fault in zones. The forward signal from the relay is compared with the reverse signal of the adjacent relay. For instance, the forward signal of CB1 is compared with the reverse signal of CB2 as shown in Figure 6.12. If both the signals are high, that means the fault is located in zone 1.

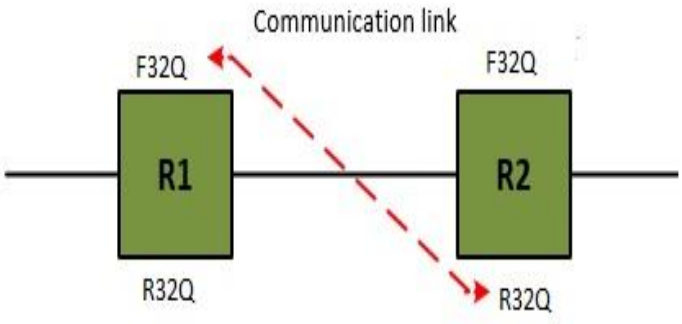

Figure 6.12: Comparison of Forward and Reverse Signal of Relay R1 &R2

Figure 6.13 shows the use of a forward signal from Relay 1 and the reverse signal from Relay 2 for decision making in Zone 1. The trip signal will be generated, if both Forward 1 and Reverse 2 are high. A signal from Relay 3 is also used for the decision making. This signal adds reliability to the scheme if Relay 2 fails to detect the fault.

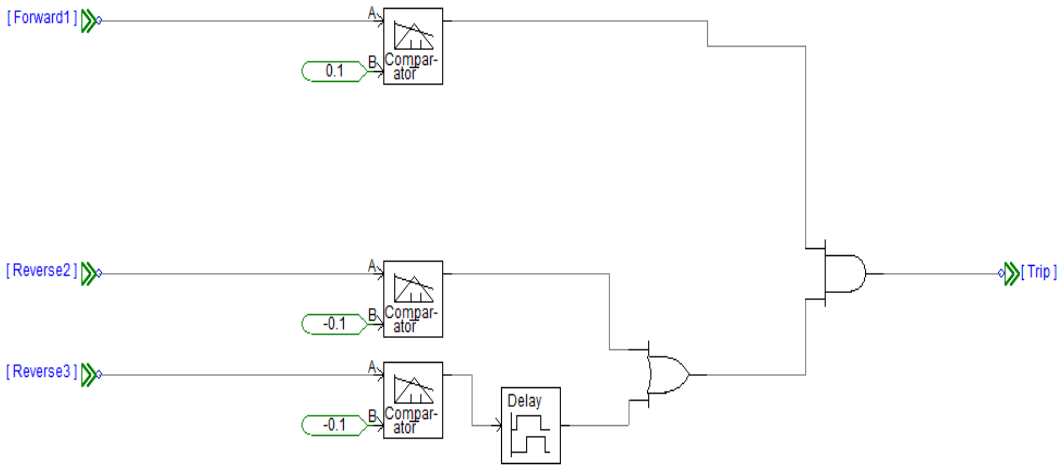

Figure 6.13: Trip Logic for Zone 1 Protection

Trip signals from all the zones are obtained as per the procedure mentioned above. These signals are fed into a decision-making module in PSCAD. Consider a case when there is a fault in Zone 2, Zone 2 protection block will generate a trip signal, but at the same time as per the logic diagram of Figure 6.13, a trip signal will be generated by Zone 1 protection block also. A time domain simulation of the system in PSCAD showed that Zone 1 trip signal lags Zone 2 trip signal by few milliseconds. Therefore, a decision-making block has to be made which can detect the first occurrence of the trip signal with respect to other trip signals. Figure 6.14 shows the block diagram of decision making in PSCAD.

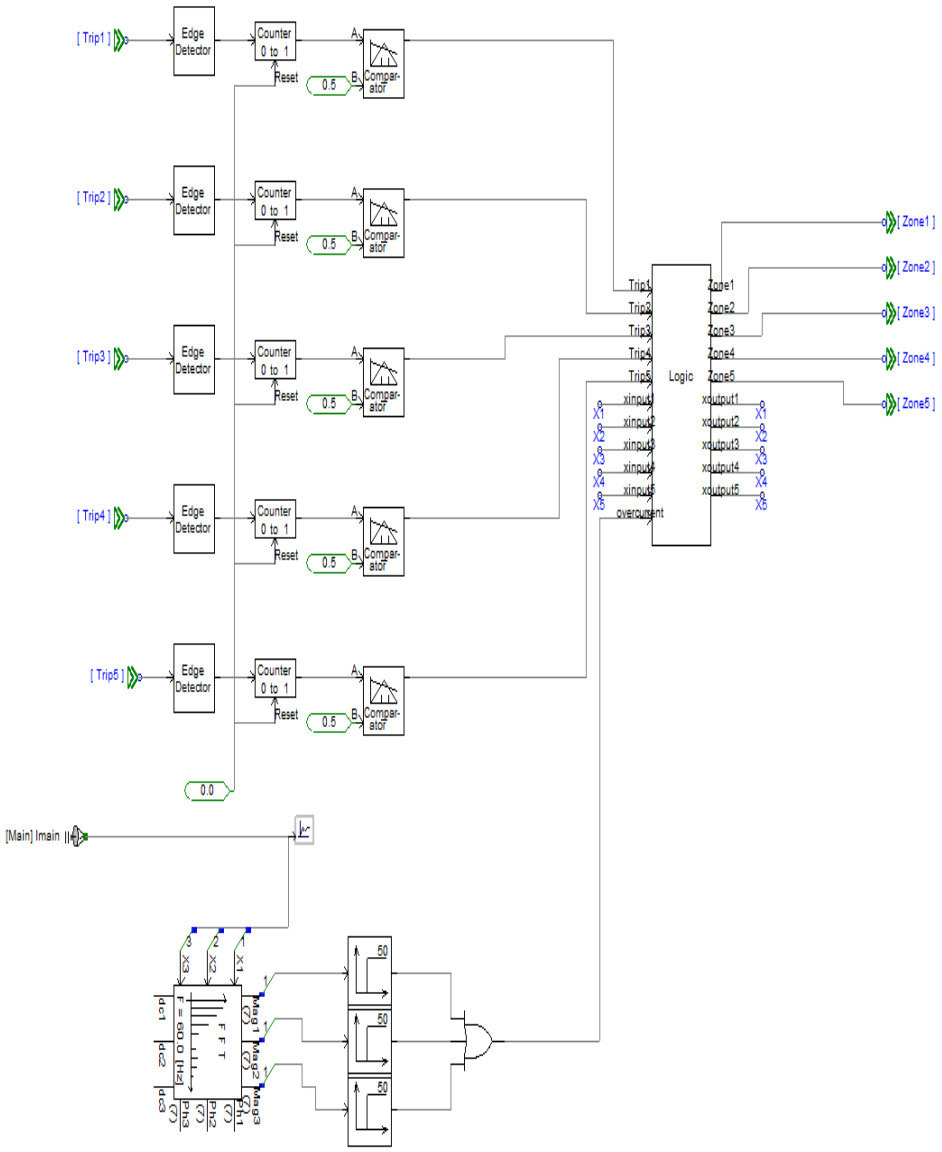

Figure 6.14: Decision-Making Block in PSCAD

The edge detector will detect the transition of the trip signal from a low state to high state. This component compares its present input to its input from the previous time step. The output is dependent on whether the present input is greater than, the same as or lower than the previous input. If there is a positive transition from low to the high then output of edge detector will be one, and when there is a transition from high to low and

no transition, then the output will be zero. A counter stores the value of this change. The counter component will alter its state to the next 'higher' state when it receives a positive value at its input. When it receives a negative value, it will change its state to the next 'lower' state. This increases or decreases the output by one. Here, the COUNTER counts the no of shots from 0 to 1. These signals are fed into a logic block that is written in FORTRAN script [39]. The FORTRAN text can be found in Appendix C. The trip signals from this block are the final trip signal. These signals are used to trip the respective circuit breakers of the faulted zone as shown in Figure 6.15.

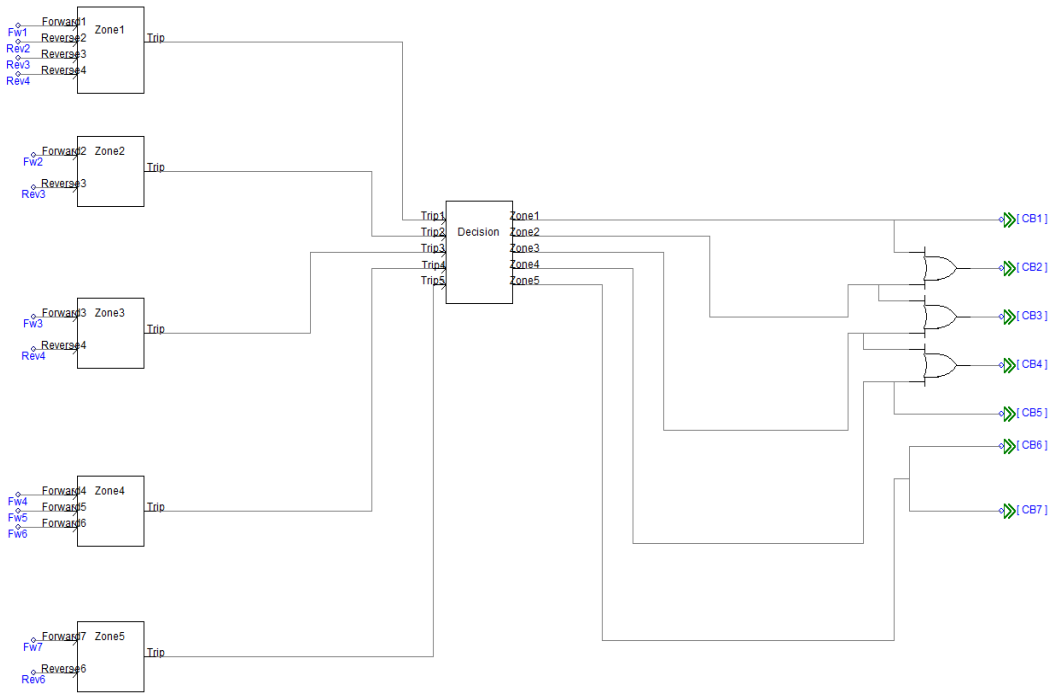

Figure 6.15: Complete Block Diagram for Decision Making in PSCAD

6.4 Relay Settings

This section describes the short circuit analysis of the LSSS system. A short circuit study has been conducted to determine the relay configuration. An instantaneous

overcurrent relay has been used to have minimum trip time. Table 6.1 shows the load current and voltage seen by the relays.

The CT ratio of the relay is 1000:1

As per the protection standard, the relay pick-up current is taken approx half of minimum fault current and greater than 1.5 times the full load current [37].

$$1.5 * IFL \leq I \leq 0.5*Ifmin \quad (6.2)$$

IFL= Full load current seen by relay

Ifmin= minimum fault current seen by relay

I= relay pick up current

Table 6.1 Current and Voltage Measured by Relays without a Fault in the System

Relay	**Current (pk value in kA)**	**Positive sequence current (kA)**	**Negative sequence current (kA)**	**Positive sequence voltage (kV)**	**Positive sequence voltage (kV)**
CB1	0.144	0.99∠-94.5	0.0024∠-27.0	7.198∠-91	$2.51*10^{-5}$∠-86
CB2	0.110	0.072∠-93.8	0.0031∠103.0	6.58∠-94.8	0.027∠58.6
CB3	0.064	0.042∠-89.2	0.003∠83.0	6.24∠-96	0.039∠25.1
CB4	0.0163	0.009∠56.0	0.0016∠-46.9	6.22∠-96.2	0.040∠23.4
CB5	0.0669	0.044∠79.2	0.0017∠-42.8	6.6∠-94	0.023∠56.3
CB6	0.050	0.032∠81.1	0.0020∠18.69	6.6∠ − 94.3	0.023∠56.5
CB7	0.113	0.076∠84.0	0.0020∠20.09	7.198∠-91	$3.87*10^{-5}$∠-12.21

A step by step procedure was used to determine the relay settings for overcurrent and directional protection scheme. Various faults were applied to the different section of buses in each zone and based on that relay settings were calculated.

(a)Setting for Relay CB1

A short circuit study has been conducted for determining the Relay 1 setting.

A CT ratio of 1000:1 is assumed

Table 6.2 shows the fault current in the Zone 1 for various faults

Table 6.2: Fault in Zone 1

Fault location	**Fault type**	**Current in BRK1 (kA)**
802-806	A-G	0.44
802-806	ABC-G	0.56
808-810	B-G	0.34
818-820	C-G	0.34
850-816	ABC-G	0.50
824-828	ABC-G	0.52
828-830	A-G	0.34
828-830	ABC-G	0.41

The maximum fault current measured by Relay 1 is 0.56 kA for three-phase fault in section 802-806, and the minimum fault current is 0.34kA for a single line to ground fault in section 818-820 of zone 1.

$$1.5 * IFL \leq I \leq 0.5*Ifmin$$

I= 220 A was selected for Zone 1 overcurrent protection

The procedure for settings of negative sequence directional element can be found in [18]. The scalar quantity Z_2 is compared with two threshold values to determine whether the fault is in forward or reverse direction to a relay [18]**.**

For practical application, Z_2F can be set for half of positive-sequence impedance of the line and Z_2R can be adjusted equal to $Z_2F+0.1$, as in [20].

The positive sequence impedance of line is $0.22 \angle 72° \ \Omega$/mile

$Z_2F= 0.11$

$Z_2R=0.21$

I_1 restraining factor= 0.2

The line angle is 72°

Positive sequence directional component setting= -18° < β <162°

Where β is the angle difference between positive sequence voltage and current

(b) Setting for Relay CB2

A short circuit study has been conducted for determining the Relay 2 setting.

A CT ratio of 1000:1 is assumed

Table 6.3 shows the fault current in the Zone 2 for various faults

Table 6.3: Fault in Zone 2

Fault location	**Fault type**	**Current in BRK2 (kA)**
830-854	A-G	0.29
830-854	ABC-G	0.34
854-856	B-G	0.24
852-832	AB	0.30
832-890	ABC-G	0.32
832-890	AB	0.28
858-864	A-G	0.29
832-858	ABC-G	0.32
832-858	B-G	0.27

The maximum fault current measured by a relay is 0.34 kA for three-phase fault in section 830-854, and the minimum fault current is 0.27 kA for a single line to ground fault in section 832-858.

I= 160 A was selected for Zone 2 overcurrent protection

For practical application, Z_2F can be set for half of positive-sequence impedance of the line and Z_2R can be adjusted equal to Z_2F+0.1

Positive sequence impedance for zone 2 is 0.24 ∠ 70° Ω/mile

Z_2F= 0.12

Z_2R=0.13

I_1 restraining factor=0.3

Line angle= 70 °

Positive sequence directional component setting= -20° < β < 160°

Where β is angle difference between positive sequence voltage and current

(c) Setting for Relay CB3

A short circuit study has been conducted for determining the Relay 3 setting.

A CT ratio of 1000:1 is assumed

Table 6.4 shows the fault current in the Zone 3 for various faults

Table 6.4 Fault in Zone 3

Fault location	**Fault type**	**Current in BRK3 (kA)**
858-834	A-G	0.13
858-834	ABC-G	0.24
842-844	B-G	0.12
846-848	ABC-G	0.20
834-860	BC	0.19
860-836	AB	0.18
862-838	B-G	0.17
836-840	ABC-G	0.22
836-840	C-G	0.19

The maximum fault current measured by a relay is 0.24 kA for three-phase fault in section 858-834, and the minimum fault current is 0.12 kA for a single line to ground fault in section 842-844.

I= 100 A was selected for Zone 3 overcurrent protection

For practical application, Z_2F can be set for half of positive-sequence impedance of the line and Z_2R can be set equal to $Z_2F+0.1$

Positive sequence impedance= $0.25 \angle 70° \Omega$/mile

$Z_2F= 0.125$

$Z_2R=0.135$

I1 restraining factor= 0.2

Line angle=70 °

Positive sequence directional component setting = $-20° < \beta < 160°$

Where β is angle difference between positive sequence voltage and current

(d) Setting for Relay CB4

A short circuit study has been conducted for determining the Relay 4 setting.

A CT ratio of 1000:1 is assumed

Table 6.5 shows the fault current in the Zone 4 for various faults

Table 6.5 Fault in Zone 4

Fault location	**Fault type**	**Current in BRK4 (kA)**
Feeder 1	A-G	0.039
Feeder 2	ABC-G	0.045
Feeder 2	BC-G	0.031
Feeder 3	B-G	0.033
Feeder 3	C-G	0.029
Feeder 4	ABC-G	0.031

The maximum fault current measured by a relay is 0.045 kA for three phase fault in section Feeder 2, and the minimum fault current is 0.029 kA for a single line to ground fault in section Feeder 3.

I= 20 A was selected for Zone 4 overcurrent protection

For practical application, Z_2F can be set for half of positive-sequence impedance of the line and Z_2R can be set equal to $Z_2F+0.1$

Positive sequence impedance = 0.21 ∠70° Ω/mile

Z_2F= 0.10

Z_2R=0.11

I_1 restraining factor= 0.2

Positive sequence directional component setting = -20° < β < 160°

Where β is angle difference between positive sequence voltage and current

(e) Setting for Relay CB6

A short circuit study has been conducted for determining the Relay 6 setting.

A CT ratio of 1000:1 is assumed

Table 6.6 shows the fault current in the Zone 5 for various faults

Table 6.6 Fault in Zone 5

Fault location	**Fault type**	**Current in BRK6 (kA)**
Feeder 1	A-G	0.23
Feeder 2	ABC-G	0.32
Feeder 2	BC-G	0.27
Feeder 3	B-G	0.26
Feeder 3	C-G	0.29
Feeder 4	ABC-G	0.29

The maximum fault current measured by a relay is 0.32 kA for 3 phase fault in section Feeder 2, and the minimum fault current is 0.26 kA for a single line to ground fault in section Feeder 3.

I= 160 A was selected for Zone 5 overcurrent protection

For practical application, Z_2F can be set for half of positive-sequence impedance of the line and Z_2R can be set equal to $Z_2F+0.1$

Positive sequence impedance= 0.22 ∠71° Ω/mile

Z_2F= 0.11

Z_2R=0.21

I_1 restraining factor= 0.15

Positive sequence directional component setting= $-19° < \beta < 161°$

Where β is angle difference between positive sequence voltage and current

The complete settings for the negative and positive sequence directional component are shown in Table 6.7. CT ratio of 1000:1 and PT ratio of 1000:1 are assumed. Z2 is negative sequence impedance of the protected line. Z2F is forward impedance threshold, and Z2R is reverse impedance threshold.

Table 6.7: Settings of Negative Sequence Directional Element

Parameter	**CB1**	**CB2**	**CB3**	**CB4**	**CB5**	**CB6**	**CB7**
Overcurrent setting (kA)	0.22	0.16	0.10	0.02	0.10	0.10	0.16
Z2 (Ω)	0.22	0.24	0.25	0.21	0.21	0.22	0.22
Z2F (Ω)	0.11	0.12	0.125	0.10	0.10	0.11	0.11
Z2R (Ω)	0.21	0.13	0.135	0.11	0.11	0.21	0.21
I_1 restraint	0.2	0.3	0.2	0.2	0.2	0.15	0.15
Line angle (degrees)	72	70	70	70	70	71	71

6.5 Simulation Cases for Proposed Directional Protection Scheme

The proposed protection scheme was simulated for both symmetrical and unsymmetrical faults. The trip delay times were recorded for the faults in various sections

of zones. At the start of the simulation, the SSTs were not connected to the system. They were independently supplied power by a voltage source. At one second, the SSTs were connected to the main system. The system reached the rated power at 60 Hz at about 2 s. Different cases were studied to look at the performance of the proposed directional scheme.

Case 1.1: A-G fault in Section 814-850 of Zone 1

An A-G fault is applied in section 814-850 of Zone 1. The fault is applied at 2s. An A- G is an unsymmetrical fault hence; negative sequence directional element has been used to detect the direction of the fault. Figure 6.16 (a) and (b) shows the fault current measured by Relay 1 and Relay 2.

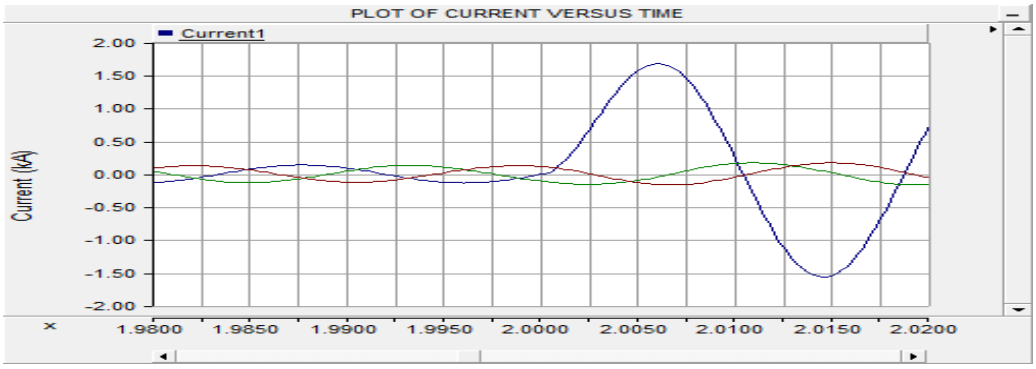

Figure 6.16 (a): Fault Current as seen by Relay 1

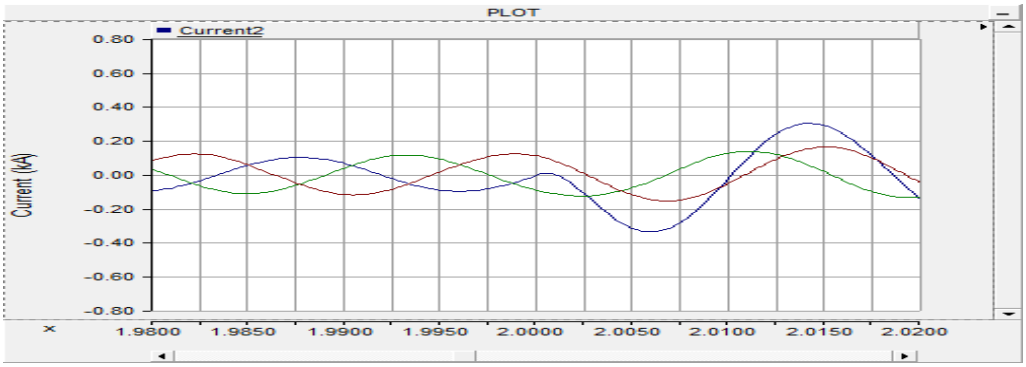

Figure 6.16 (b): Fault Current as seen by Relay 2

Figure 6.17 shows the direction of the fault showed by element CB1, CB2, and CB3. The CB1 shows the fault in the forward direction while CB2 and CB3 show the fault in the reverse direction. This determined the location of the fault in Zone 1.

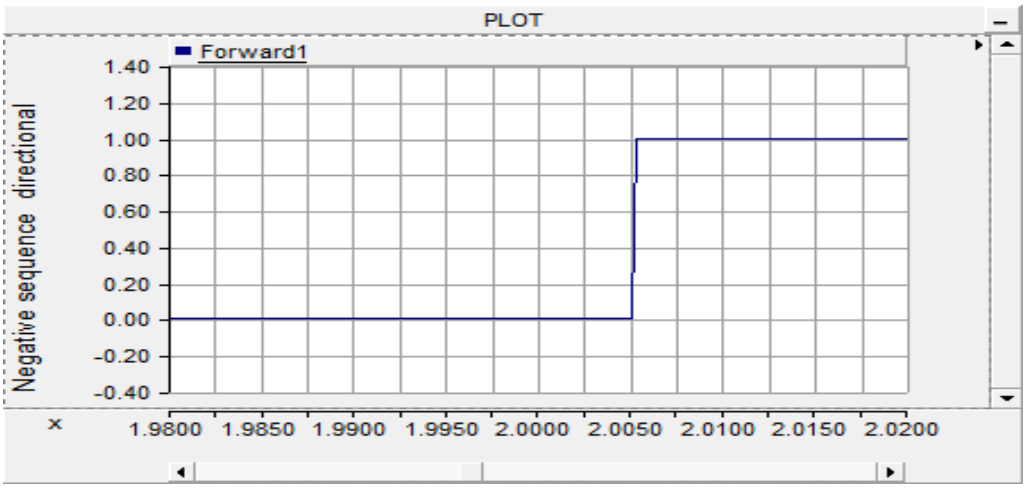

Figure 6.17 (a): Status of Negative Sequence Directional Element for Relay 1

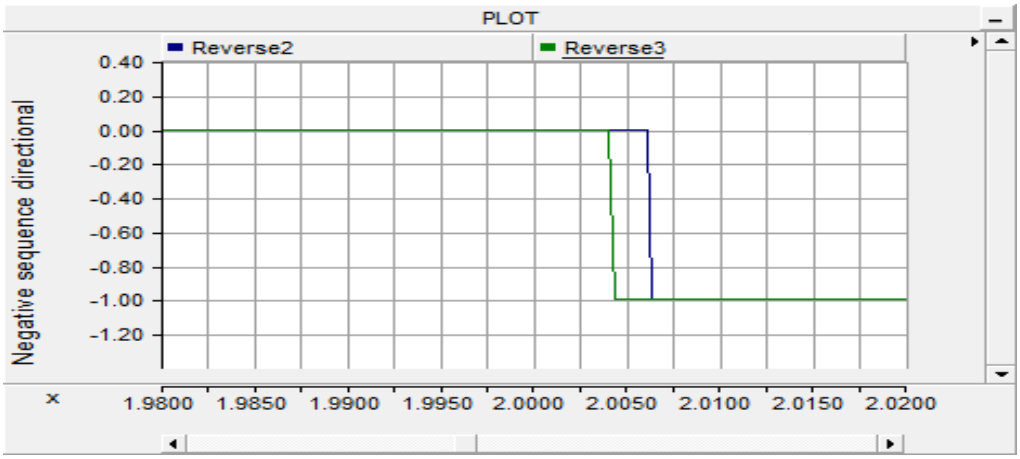

Figure 6.17 (b): Status of Negative Sequence Directional Element for Relay 2

Figure 6.18 shows the trip signal obtained from all the relays. Since, the fault has been detected in Zone 1, only CB1 and CB2 will be tripped. The trip signals for other circuit breakers are zero.

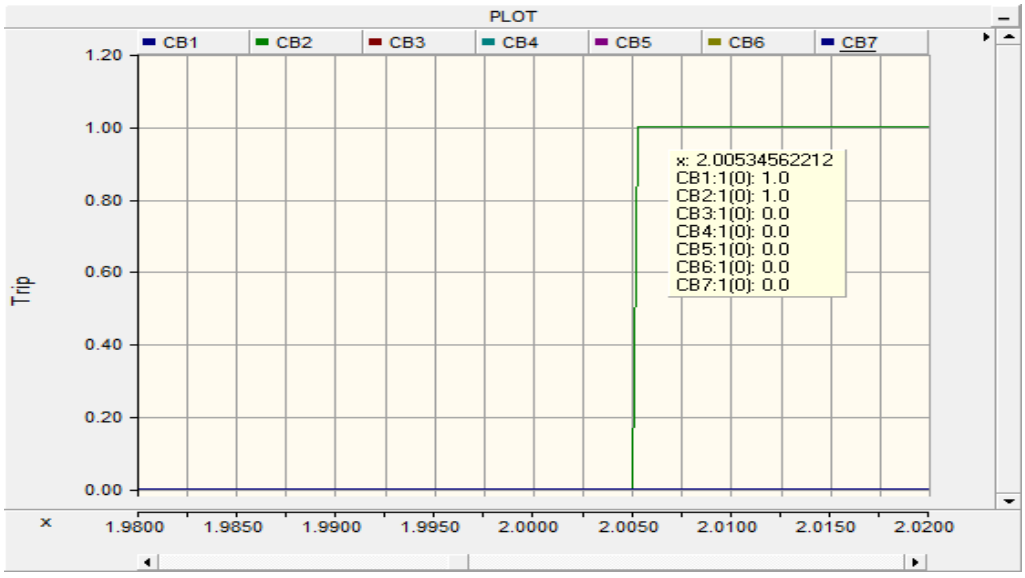

Figure 6.18: Status of Trip Signals for the Circuit Breakers

The trip delay time was found to be 5.34 milliseconds. The waveforms of current after opening the circuit breakers CB1 and CB2 of Zone 1 is shown in Figure 6.19.

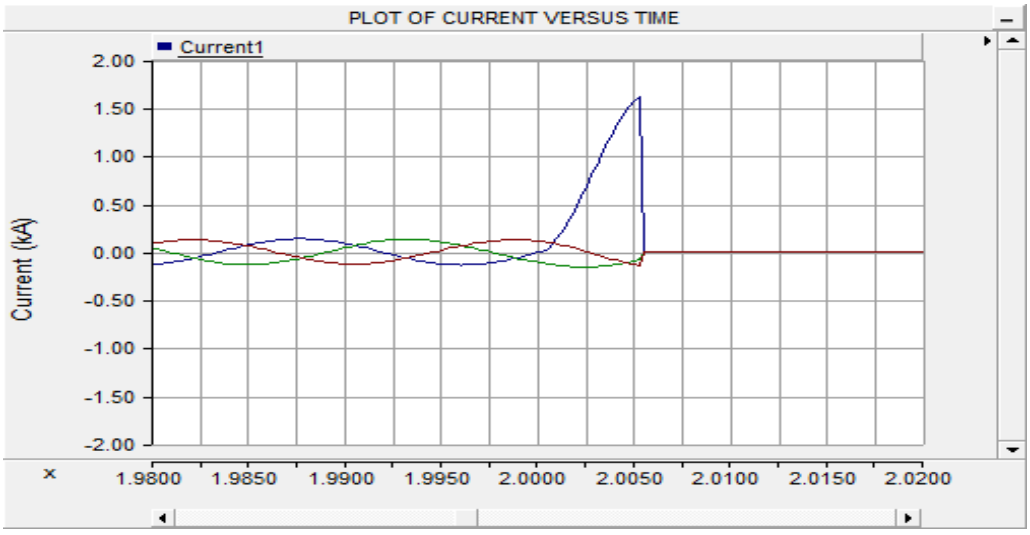

Figure 6.19 (a): Current Interruption by CB1

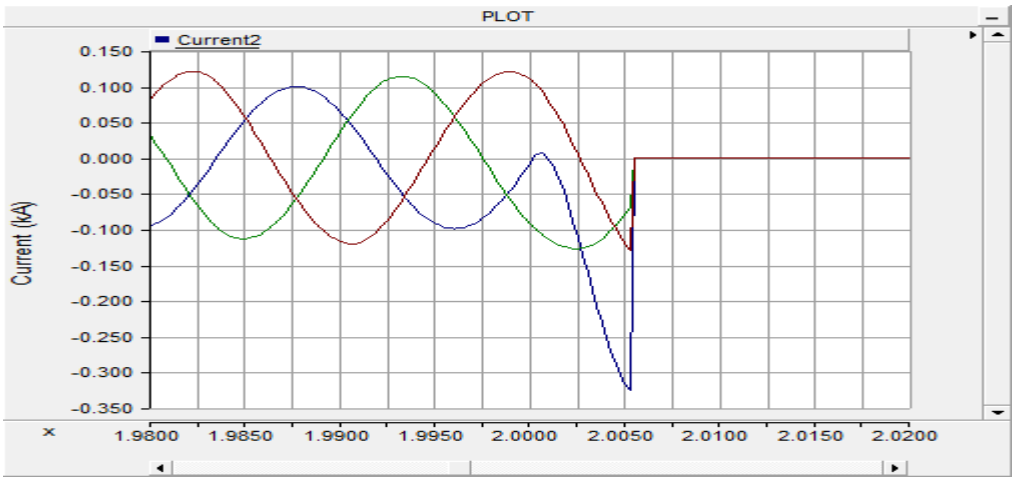

Figure 6.19(b): Current Interruption by CB2

This confirmed that the fault was located in Zone 1.

Case 1.2: AC-G Fault in Section 852-832 of Zone 2

A double line to ground fault was simulated in this case in Zone 2. An LL-G is an unsymmetrical fault hence negative sequence directional element should detect the presence of a fault. Figure 6.20 (a) and (b) shows the fault current seen by the two relays, Relay 1, and Relay 2.

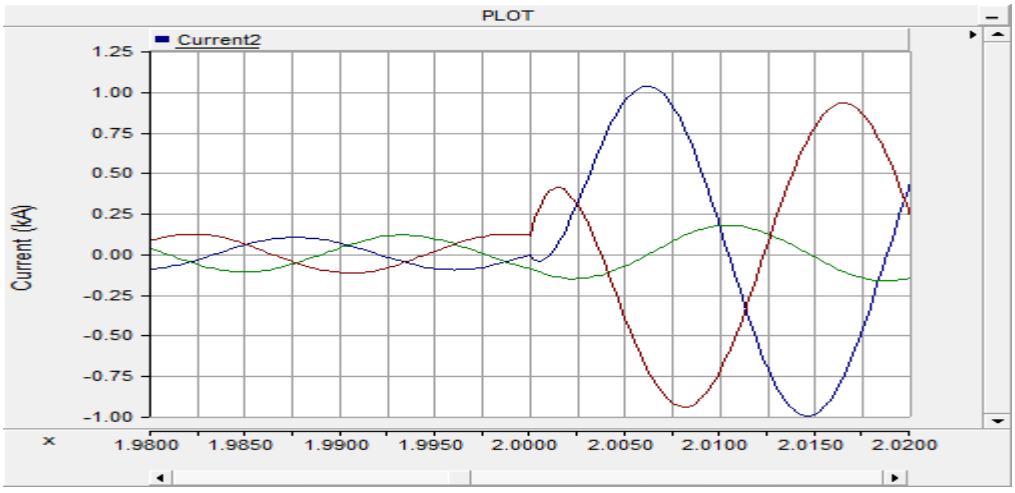

Figure 6.20 (a): Fault Current as seen by Relay 2

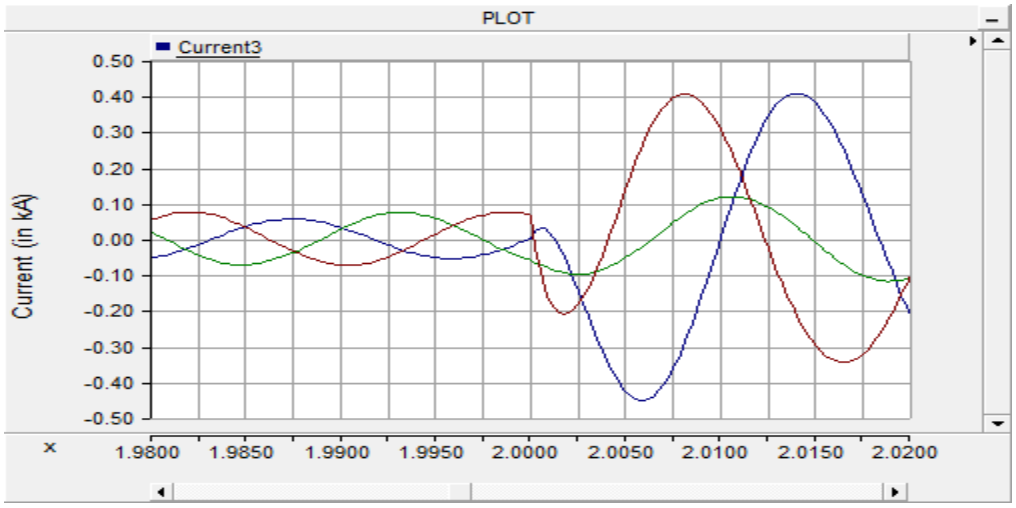

Figure 6.20 (b): Fault Current as seen by Relay 3

Figure 6.21 (a) and (b) shows the response of negative sequence directional element. For Relay 2, a forward fault has been detected as shown in Figure 6.21 (a) whereas for the Relay 3, a reverse fault has been detected as shown in Figure 6.21(b).

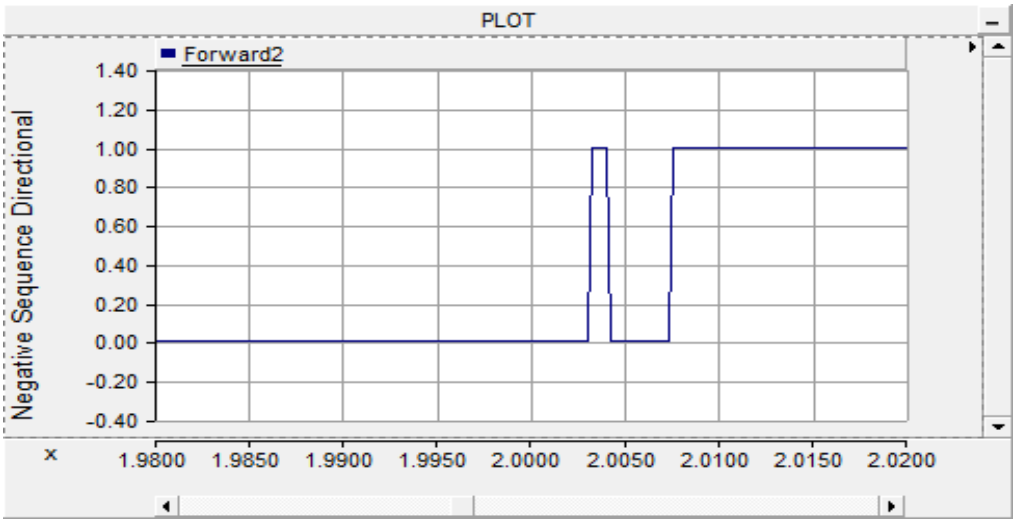

Figure 6.21 (a): Status of Negative Sequence Directional Element for Relay 2

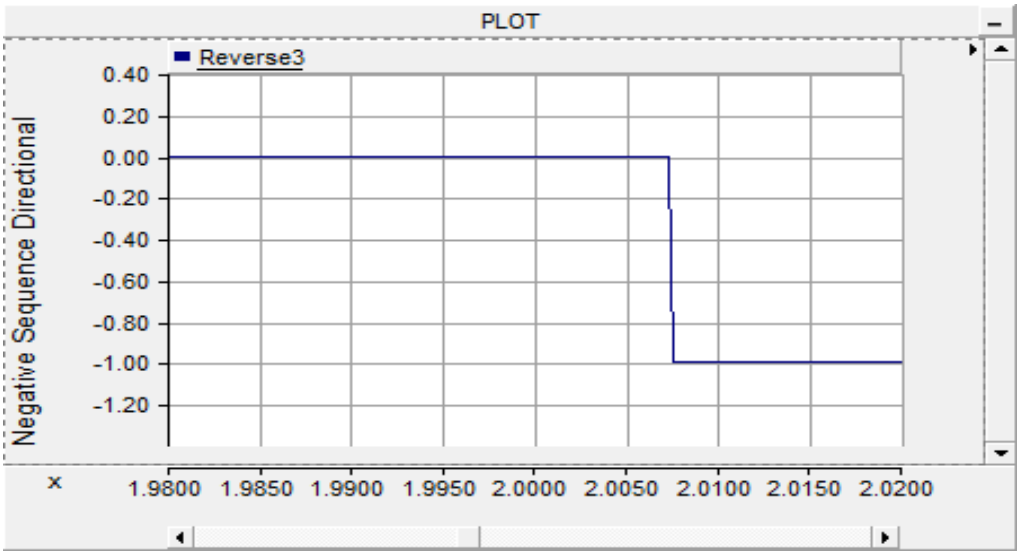

Figure 6.21 (b): Status of Negative Sequence Directional Element for Relay 3

Based on the negative sequence directional element status for Relay 2 and Relay 3, the fault has been located in Zone 2. The trip signal states as shown in Figure 6.22 corroborated the location of the fault in Zone 2.

Figure 6.22: Status of Trip Signals for Circuit Breakers

The trip signal delay time was found to be 8.66 milliseconds that is approx half of one cycle. The Figure 6.23 (a) and (b) shows the interruption of fault current by CB2 and CB3 after receiving a trip signal from Relay 2 and Relay 3.

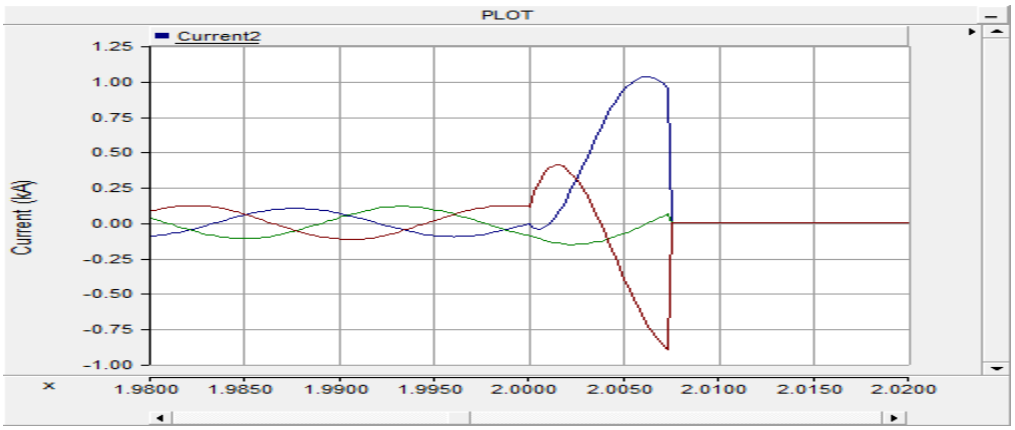

Figure 6.23 (a): Current Interruption by CB2

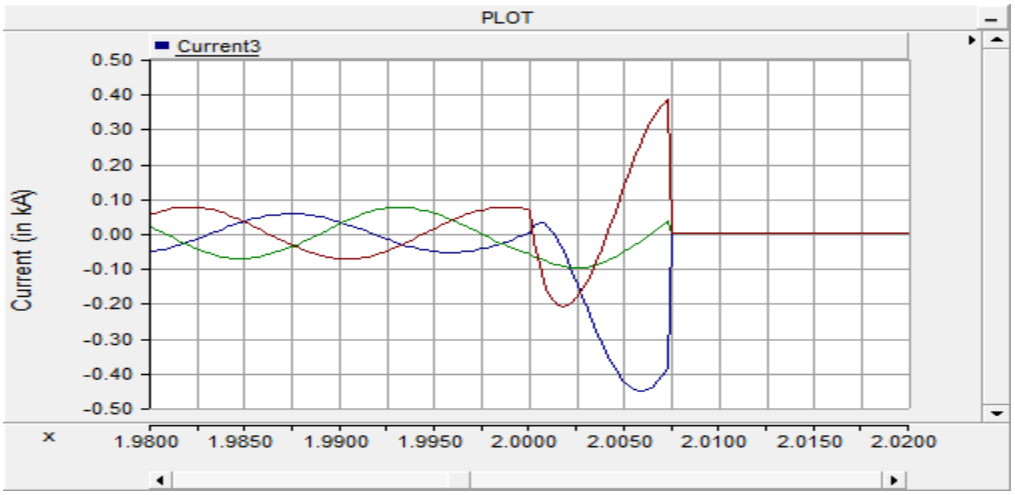

Figure 6.23 (a): Current Interruption by CB3

Case 1.3: ABC-G Fault in section 860- 836 of Zone 3

This case simulated a three-phase balanced fault in section 860-836 of Zone 3. A three-phase balanced fault is also termed as a symmetrical fault. The voltage and current quantities remain balanced even after the application of fault. This is the most severe type

of fault in the power system as it gives rise to a high amount of balanced fault current. Figure 6.24 (a) and (b) shows the fault current in the system as seen by two relays i.e. Relay 3 and Relay 4.

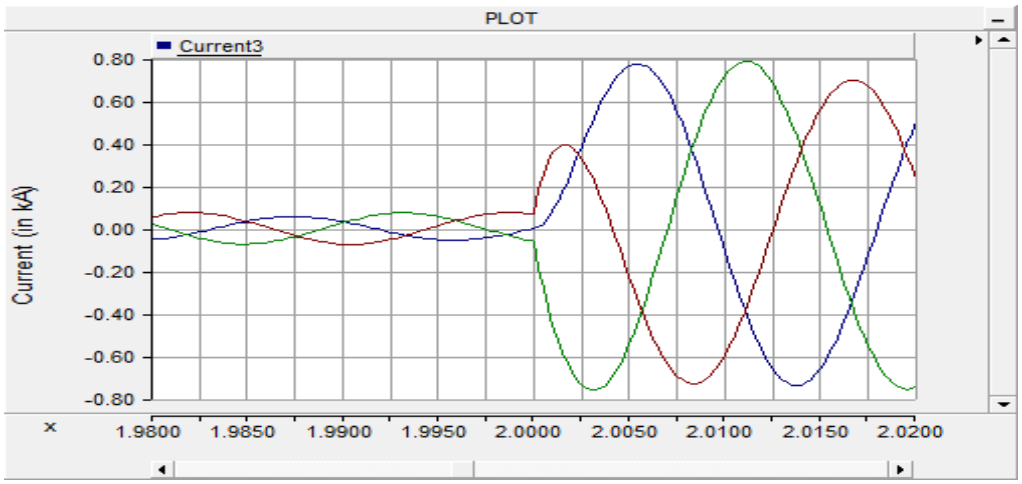

Figure 6.24 (a): Fault Current as seen by Relay 3

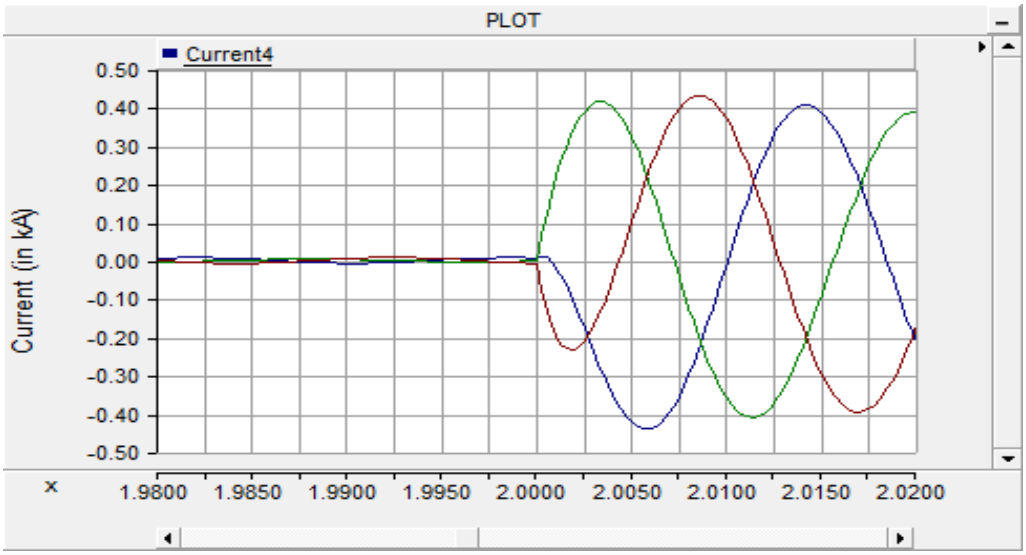

Figure 6.24 (b): Fault Current as seen by Relay 4

The priority signal that is the ratio of I_2 to I_1 is shown in Figure 6.25. This confirms that the fault is the symmetrical type. Hence, positive sequence directional element has the upper hand in decision making.

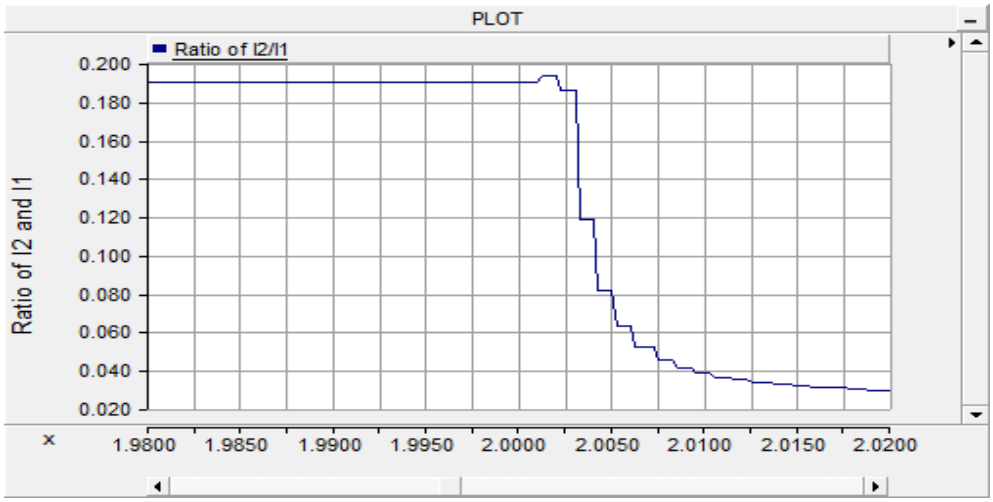

Figure 6.25: Ratio of Negative Sequence Current (I_2) to Positive Sequence Current (I_1)

The positive sequence directional element responded to detect the direction of the symmetrical fault. The angle detected by the directional element of the relay is shown in Figure 6.26 (a) and (b).

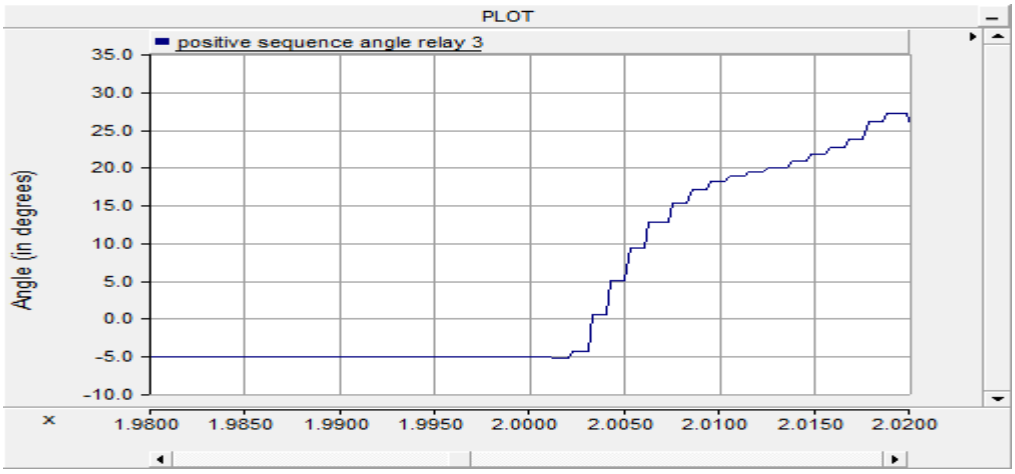

Figure 6.26 (a): The Difference in Positive Sequence Voltage and Current Phase Angle for Relay 3

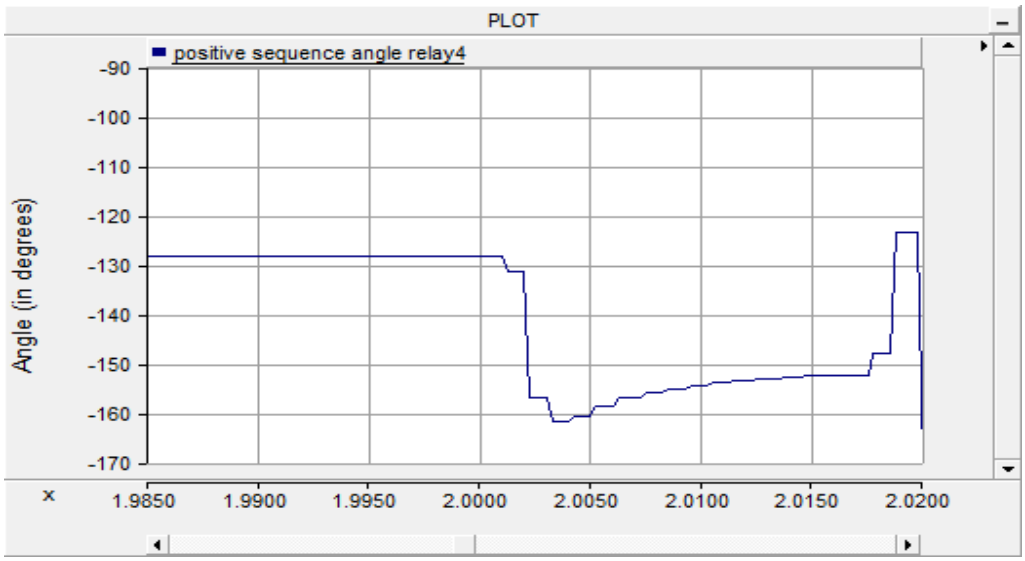

Figure 6.26 (b): The Difference in Positive Sequence Voltage and Current Phase Angle for Relay 4

It can be noticed that angle detected by Relay 3 falls within the forward region while Relay 4 angle falls within the reverse region. Figure 6.27 shows the response of the positive sequence directional element for both Relay 3 and Relay 4.

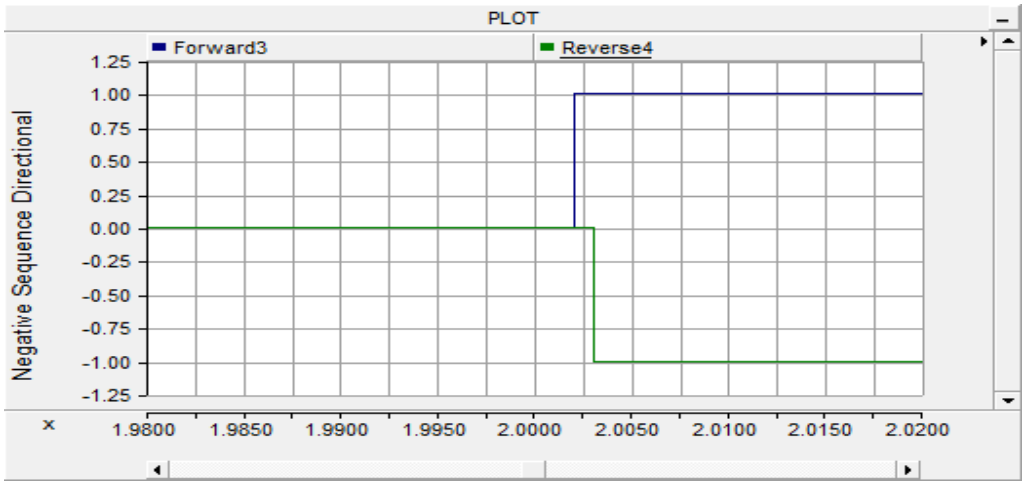

Figure 6.27: Positive Sequence Directional Element States for both Relay 3 and Relay 4

This indicates that the fault has been detected in Zone 3. The trip status from the relays is shown in Figure 6.28. This further confirms the symmetrical fault in Zone 3.

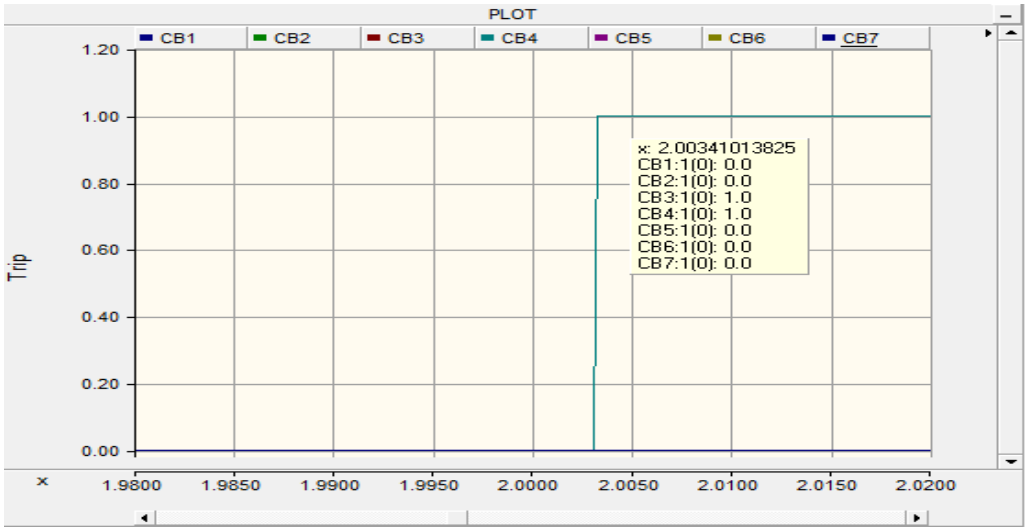

Figure 6.28: Status of Trip Signals for Circuit Breakers

The trip signal delay was found to be 3.2 milliseconds. Figure 6.29 (a) and (b) shows the interruption of fault current by CB2 and CB3 after receiving a trip signal from Relay 3 and Relay 4.

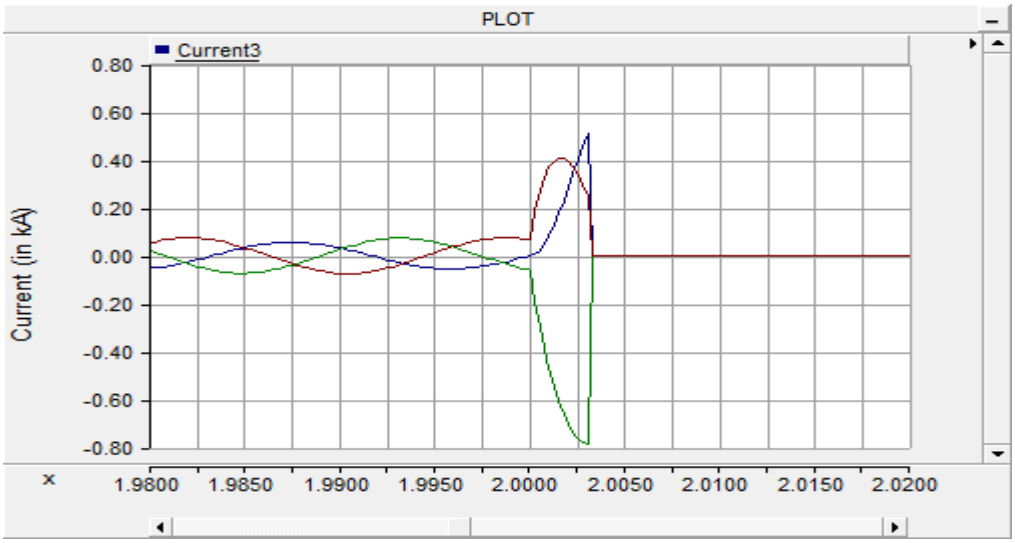

Figure 6.29 (a): Current Interruption by CB3

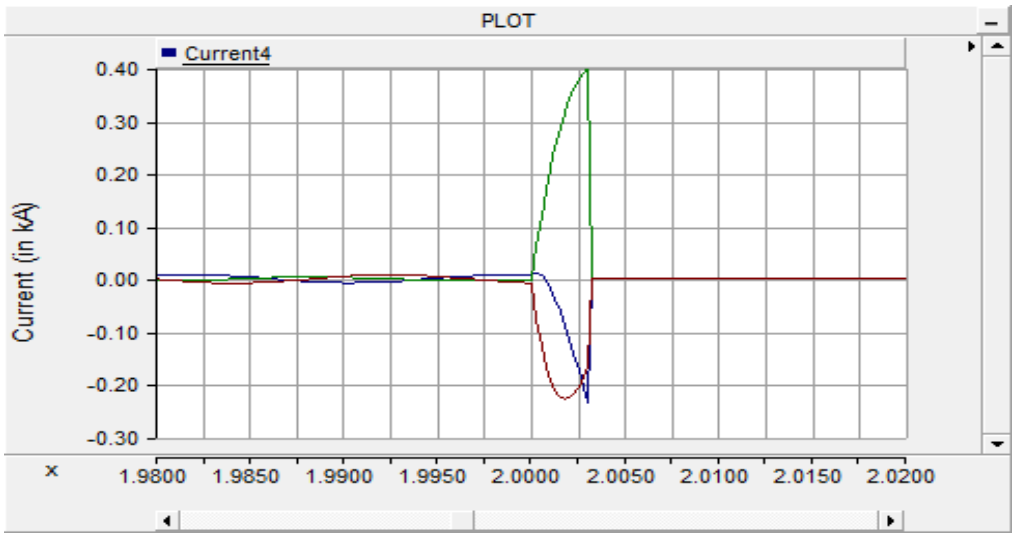

Figure 6.29 (b): Current Interruption by CB4

Case 1.4: AB-G Fault in Feeder 2 of Zone 4

An AB-G fault was applied in Feeder 2 of Zone 4. The fault was simulated at 2s. An AB-G is an unsymmetrical fault hence; negative sequence directional element has been used to detect the direction of the fault. Figure 6.30(a) and (b) shows the fault current measured by Relay 4 and Relay 5.

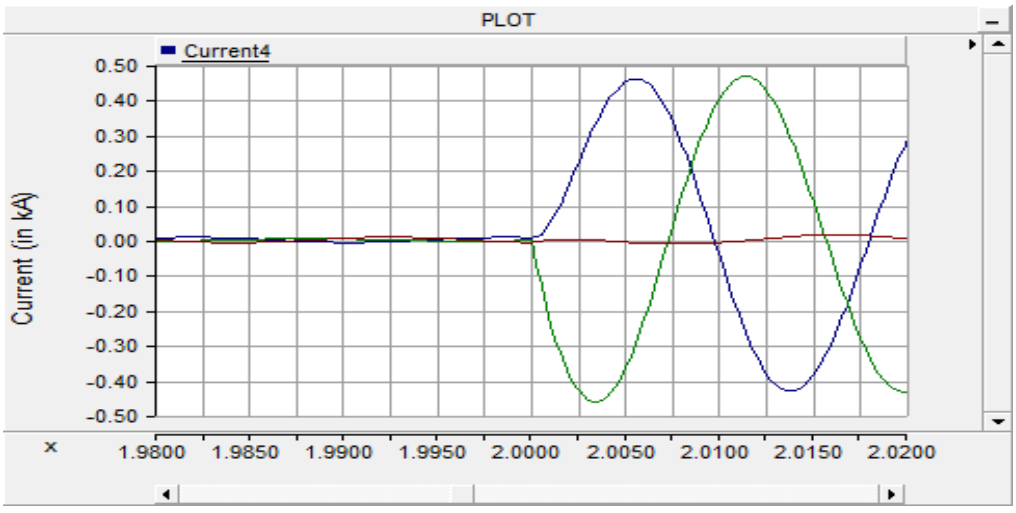

Figure 6.30 (a): Fault Current as seen by Relay 4

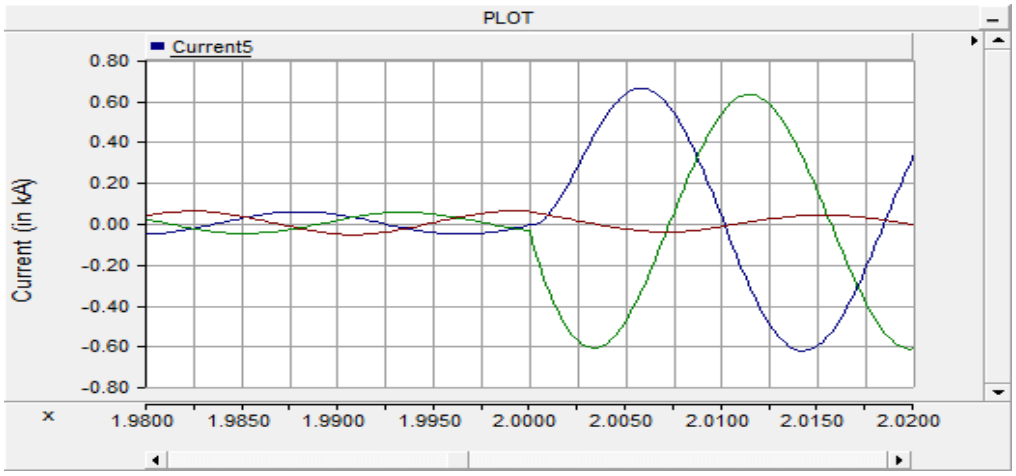

Figure 6.30 (b): Fault Current seen by Relay 5

Figure 6.31(a), (b) shows the direction of the fault showed by element forward 4 and forward 5. The forward 4 and forward 5 have detected the fault in Zone 4. This determined the location of the fault in Zone 4.

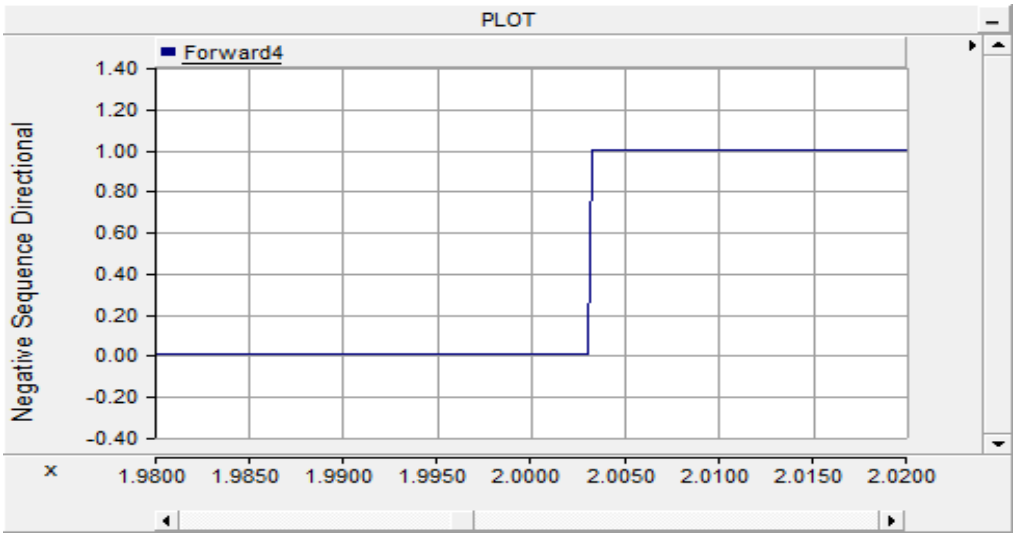

Figure 6.31 (a) Status of Negative Sequence Directional Element for Relay 4

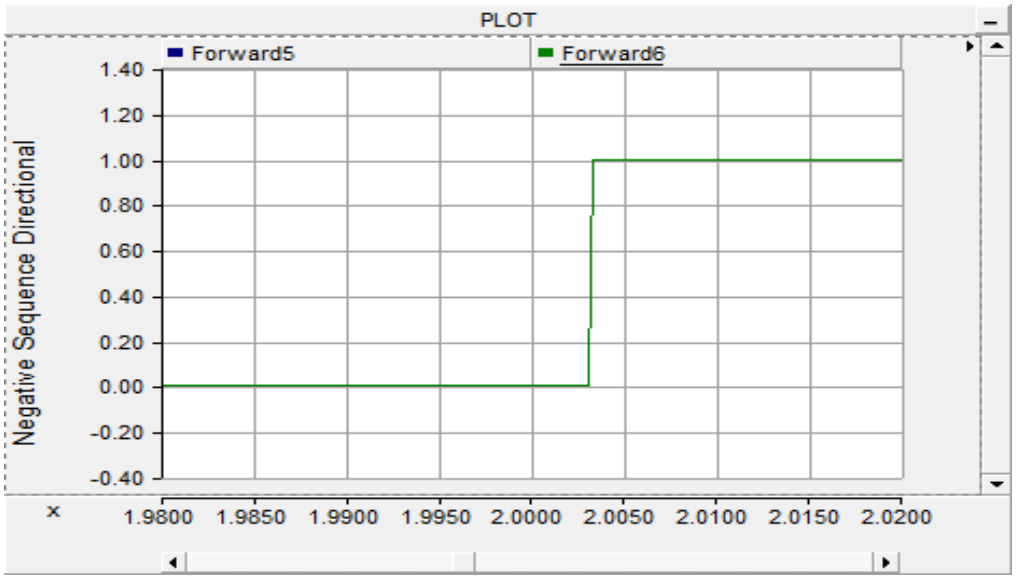

Figure 6.31 (b): Status of Negative Sequence Directional Element for Relay 5

Figure 6.32 shows the trip signal obtained from all the relays. Since, the fault has been detected in Zone 4, only CB4 and CB5 was tripped. The trip signals for other circuit breakers are zero.

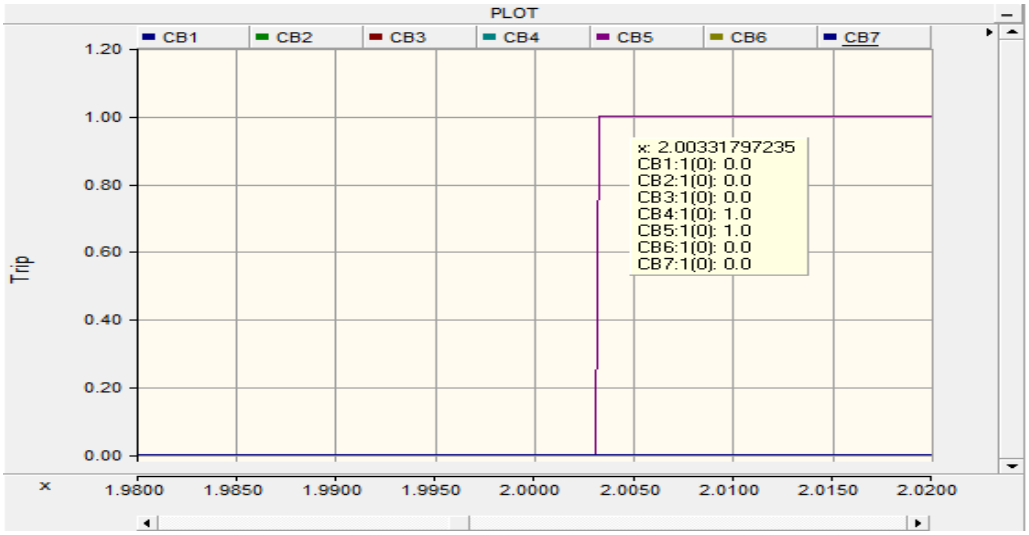

Figure 6.32: Status of Trip Signals for Circuit Breakers

The trip delay time was found to be 3.31 milliseconds. The waveforms of current after opening the circuit breakers CB4 and CB5 of Zone1 is shown in Figure 6.33 (a), (b).

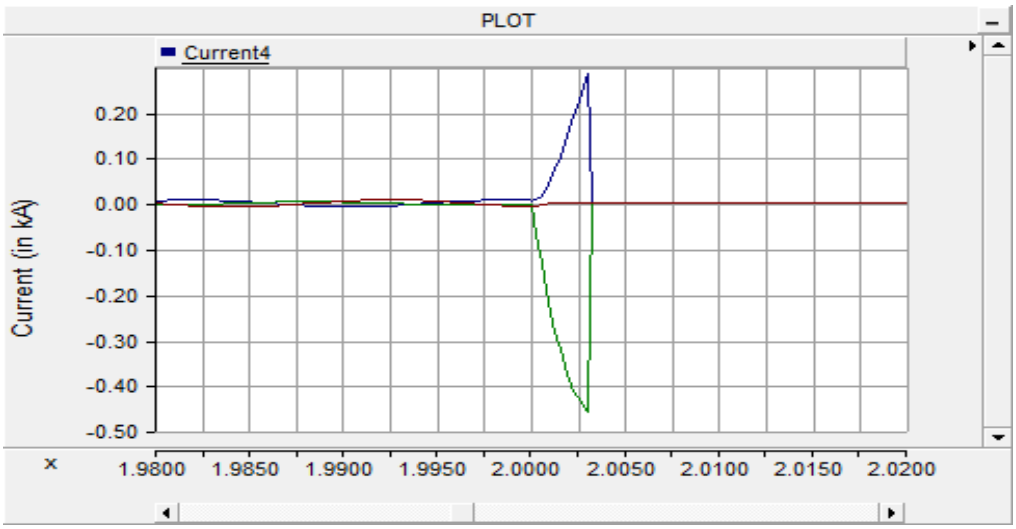

Figure 6.33 (a): Current Interruption by CB4

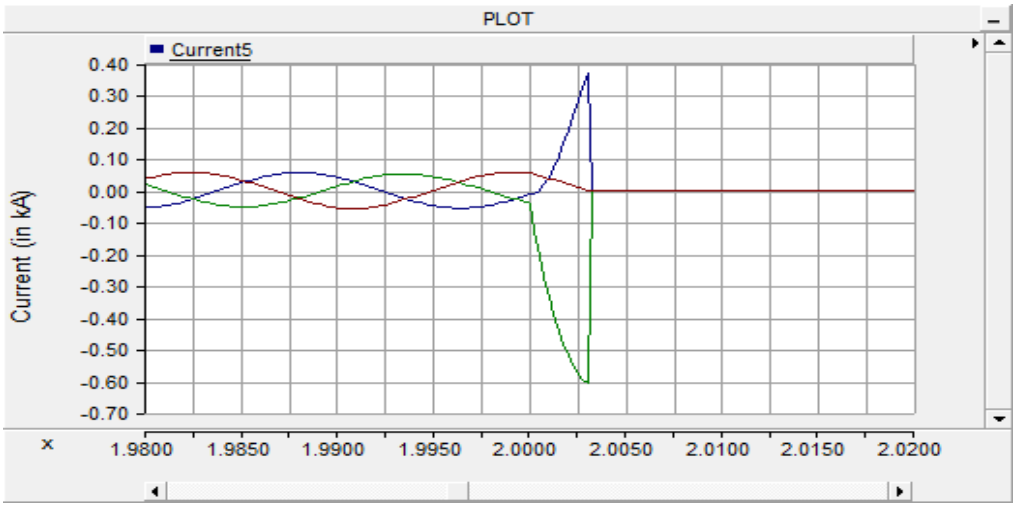

Figure 6.33(b): Current Interruption by CB5

Case 1.5: ABC-G Fault in Feeder 1 of Zone 5

This case simulated a three-phase balanced fault in Feeder 1 of Zone 5. A three-phase balanced fault is also termed as a symmetrical fault. The voltage and current quantities remain balanced even after the application of fault. Figure 6.34 (a) and (b) shows the fault current in the system as seen by two relays i.e. Relay 6 and Relay 7.

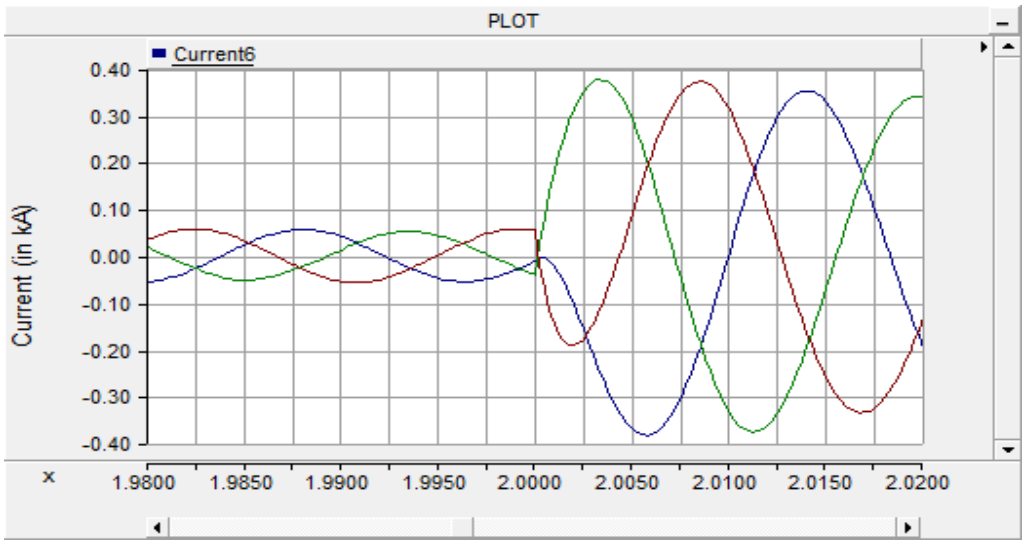

Figure 6.34 (a): Fault Current as seen by Relay 6

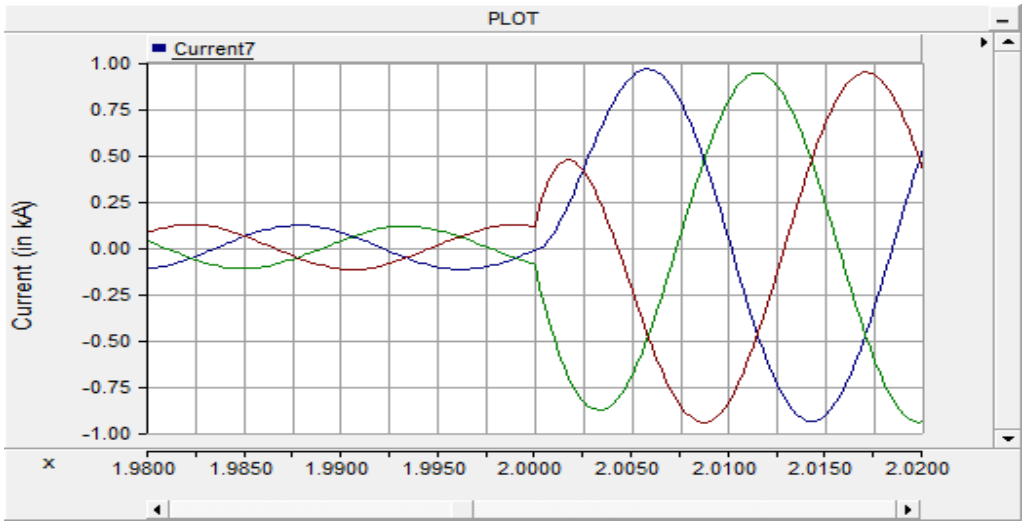

Figure 6.34 (b): Fault Current as seen by Relay 7

The priority signal that is the ratio of I_2 to I_1 confirms that the fault is a symmetrical type. Hence, positive sequence directional element has the upper hand in decision making. The positive sequence directional element responded to detect the direction of the symmetrical fault. The angle detected by the directional element of the relay is shown in Figure 6.35.

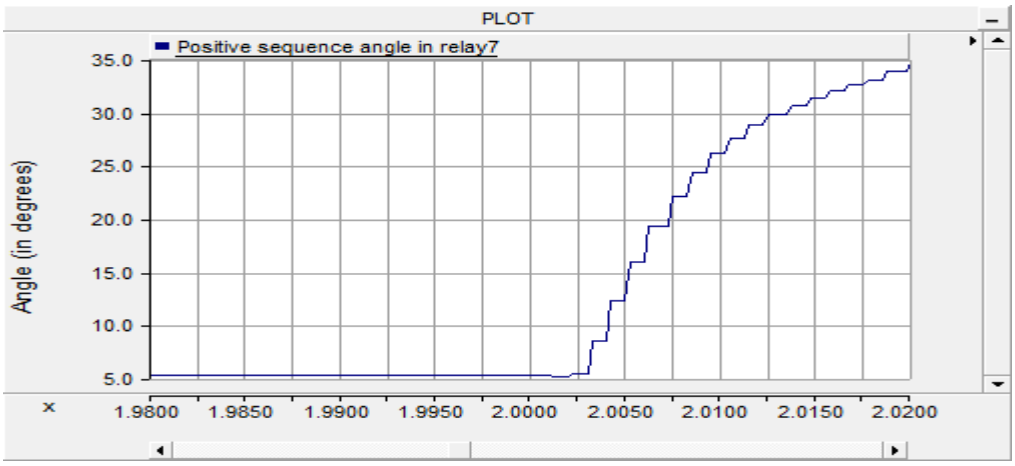

Figure 6.35: Difference of Positive Sequence Voltage and Current Phase Angle for Relay 7

It was noticed that angle detected by Relay 6 falls within the reverse region while Relay 7 angle falls within the forward region. This shows that the fault was in Zone 5. The trip status from the relays is illustrated in Figure 6.36. This further confirms the symmetrical fault in Zone 5.

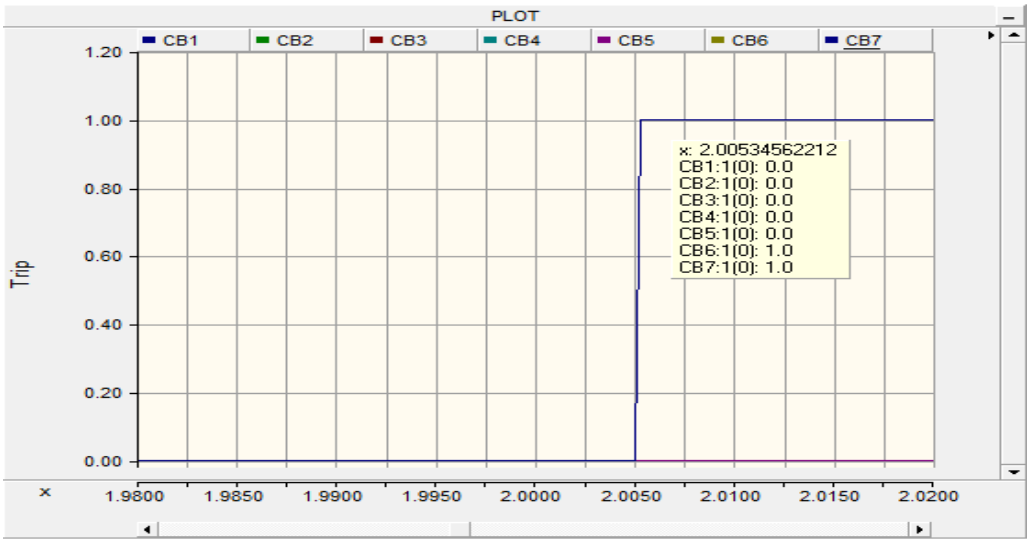

Figure 6.36: Status of Trip Signals for Circuit Breakers

The trip signal delay was found to be 5.4 milliseconds. The figure 6.37 (a) and (b) shows the interruption of fault current by CB6 and CB7 after receiving a trip signal from Relay 6 and Relay 7.

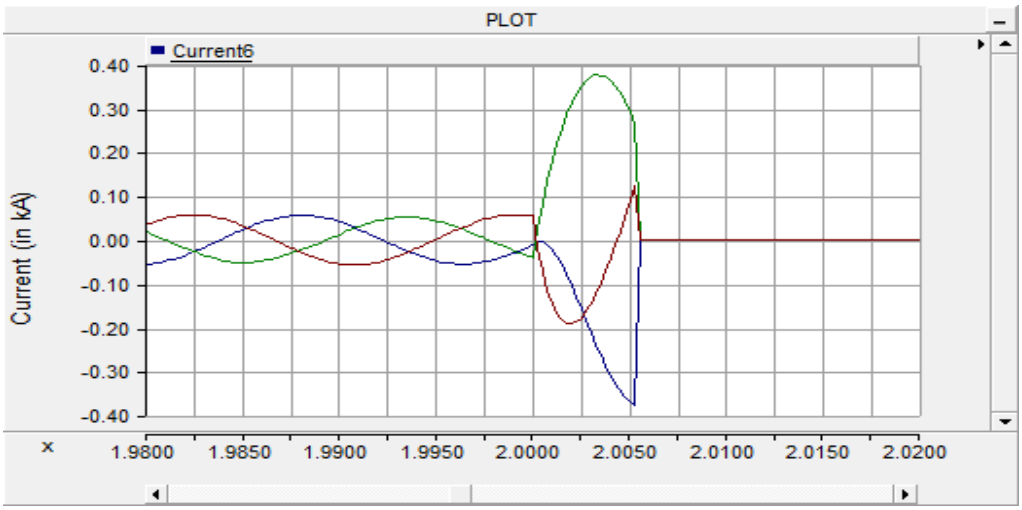

Figure 6.37 (a): Current Interruption by CB6

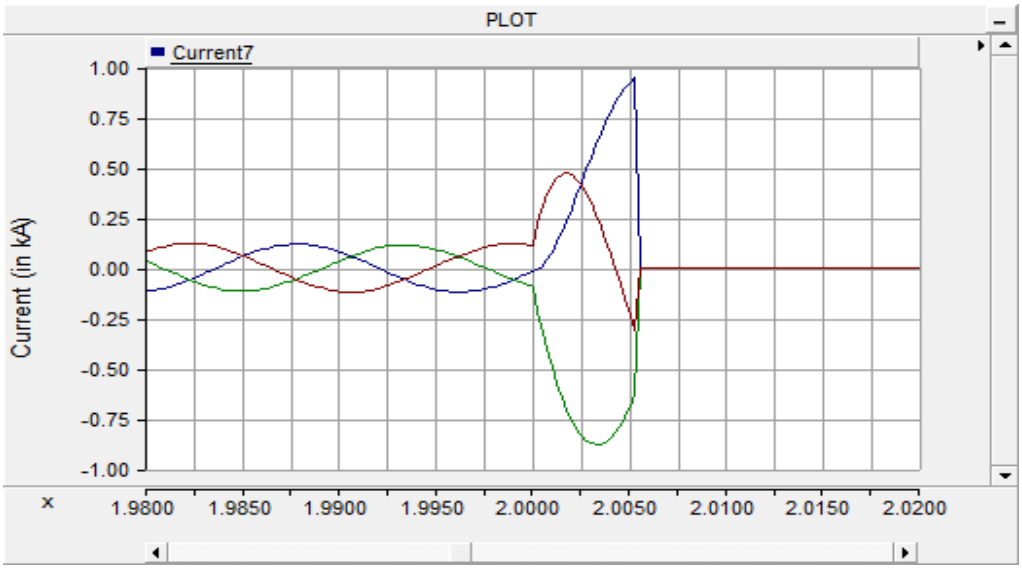

Figure 6.37 (b): Current Interruption by CB7

6.6 Exhaustive Simulation of Proposed Protection Scheme

Exhaustive tests have been conducted for the different type of faults at various locations in large-scale distribution mesh system. All the possible fault locations have been tested to determine the trip time delay. The results of tripped circuit breakers and trip signal delays are summarized in tables below. The column 1 of the table shows the location of the fault. The location in the bold indicates the presence of single phase section. Column 2 displays the type of fault. Column 3 displays the circuit breakers that are opened to isolate the fault. Column 4 presents the trip time delay.

Table 6.7: Trip Time Delay for the Faults in Zone 1

Fault Location	**Fault type**	**Breaker Tripped**	**Trip Time (milliseconds)**
802-806	A-G	CB1 and CB2	4.2
	C-G	CB1 and CB2	4.3
	CA-G	CB1 and CB2	4.4
	AB-G	CB1 and CB2	3.2
	ABC-G	CB1 and CB2	3.5
806-808	B-G	CB1 and CB2	4.5
	C-G	CB1 and CB2	5.6
	AB-G	CB1 and CB2	4.8
	BC-G	CB1 and CB2	5.0
	CA-G	CB1 and CB2	6.1
	ABC-G	CB1 and CB2	4.7
808-810	**B-G**	**CB1 and CB2**	**4.4**
808-812	A-G	CB1 and CB2	4.2
	B-G	CB1 and CB2	4.7
	C-G	CB1 and CB2	4.6
	AC-G	CB1 and CB2	4.8
	BC-G	CB1 and CB2	4.0
	ABC-G	CB1 and CB2	5.1

Table 6.7 Continued

Fault Location	Fault type	Breaker Tripped	Trip Time (milliseconds)
814-850	A-G	CB1 and CB2	3.2
	C-G	CB1 and CB2	4.3
	AB-G	CB1 and CB2	4.1
	BC-G	CB1 and CB2	3.9
	ABC-G	CB1 and CB2	4.0
850-816	B-G	CB1 and CB2	3.8
	AB-G	CB1 and CB2	4.9
	BC-G	CB1 and CB2	4.8
	ABC-G	CB1 and CB2	4.8
816-818	**C-G**	**CB1 and CB2**	**4.7**
818-820	**C-G**	**CB1 and CB2**	**4.1**
820-822	**C-G**	**CB1 and CB2**	**4.4**
816-824	A-G	CB1 and CB2	4.4
	C-G	CB1 and CB2	4.6
	AB-G	CB1 and CB2	4.2
	BC-G	CB1 and CB2	4.6
	AC-G	CB1 and CB2	4.8
	B-G	CB1 and CB2	4.4
	ABC-G	CB1 and CB2	4.3
824-826	**B-G**	**CB1 and CB2**	**4.5**
824-828	A-G	CB1 and CB2	4.6
	C-G	CB1 and CB2	4.7
	AB-G	CB1 and CB2	4.0
	AC-G	CB1 and CB2	4.1
	BC-G	CB1 and CB2	4.2
	ABC-G	CB1 and CB2	4.8

Table 6.8 shows the response of Zone 2 faults. For the unsymmetrical fault, the negative directional element was used to detect the fault. Note that Section 888-890 has largest average trip delay time as compared to other sections of Zone 2. This is due to presence of HV transformer in this section which has essentially reduced the total fault current at zonal boundary elements.

Table 6.8: Trip Time Delay for the Various Faults in Zone 2

Fault Location	Fault Type	Breaker Tripped	Trip Time (milliseconds)
830-854	A-G	CB2 and CB3	5.6
	B-G	CB2 and CB3	5.4
	AB-G	CB2 and CB3	5.5
	BC-G	CB2 and CB3	6.1
	CA-G	CB2 and CB3	7.3
	ABC-G	CB2 and CB3	8.3
854-856	**B-G**	**CB2 and CB3**	**7.3**
854-852	A-G	CB2 and CB3	8.4
	C-G	CB2 and CB3	8.5
	AB-G	CB2 and CB3	7.3
	CA-G	CB2 and CB3	6.4
	ABC-G	CB2 and CB3	5.3
852-832	B-G	CB2 and CB3	4.3
	C-G	CB2 and CB3	4.4
	AB-G	CB2 and CB3	6.1
	BC-G	CB2 and CB3	7.3
	ABC-G	CB2 and CB3	6.9
832-888	A-G	CB2 and CB3	8.0
	B-G	CB2 and CB3	5.1
	AB-G	CB2 and CB3	5.5
	CA-G	CB2 and CB3	5.7
	ABC-G	CB2 and CB3	5.9
888-890	A-G	CB2 and CB3	7.1
	B-G	CB2 and CB3	7.2
	BC-G	CB2 and CB3	7.3
	ABC-G	CB2 and CB3	7.5
832-858	A-G	CB2 and CB3	6.9
	AB-G	CB2 and CB3	6.9
	CA-G	CB2 and CB3	7.1
	ABC-G	CB2 and CB3	4.3
858-864	**A-G**	**CB2 and CB3**	**4.0**

Table 6.9 shows the trip signal delay for various faults in Zone 3. The trip delay signal for Zone 3 was found to be 5.9 milliseconds.

Table 6.9: Trip Signal Delay Time in Zone 3

Fault Location	Fault Type	Breaker Tripped	Trip Time (milliseconds)
858-834	A-G	CB3 and CB4	4.1
	C-G	CB3 and CB4	4.2
	AB-G	CB3 and CB4	4.7
	CA-G	CB3 and CB4	4.4
	ABC-G	CB3 and CB4	4.7
834-842	A-G	CB3 and CB4	4.6
	B-G	CB3 and CB4	4.6
	BC-G	CB3 and CB4	4.7
	CA-G	CB3 and CB4	4.8
	ABC-G	CB3 and CB4	4.9
842-844	B-G	CB3 and CB4	5.0
	AB-G	CB3 and CB4	4.1
	CA-G	CB3 and CB4	4.5
	BC-G	CB3 and CB4	4.4
	ABC-G	CB3 and CB4	4.3
844-846	B-G	CB3 and CB4	4.2
	AB-G	CB3 and CB4	4.7
	CA-G	CB3 and CB4	4.8
	BC-G	CB3 and CB4	4.9
	ABC-G	CB3 and CB4	4.6
846-848	A-G	CB3 and CB4	4.5
	AB-G	CB3 and CB4	4.4
	BC-G	CB3 and CB4	4.8
	CA-G	CB3 and CB4	4.7
	ABC-G	CB3 and CB4	4.7
834-860	A-G	CB3 and CB4	5.1
	AB-G	CB3 and CB4	5.2
	BC-G	CB3 and CB4	5.3
	CA-G	CB3 and CB4	4.3
	ABC-G	CB3 and CB4	4.1
860-836	B-G	CB3 and CB4	4.1
	AB-G	CB3 and CB4	3.9
	BC-G	CB3 and CB4	4.3
	CA-G	CB3 and CB4	4.4
	ABC-G	CB3 and CB4	4.5

Table 6.9 Continued

Fault Location	Fault Type	Breaker Tripped	Trip Time (milliseconds)
836-840	B-G	CB3 and CB4	4.1
	AB-G	CB3 and CB4	4.2
	BC-G	CB3 and CB4	4.3
	CA-G	CB3 and CB4	4.8
	ABC-G	CB3 and CB4	4.9
836-862	B-G	CB3 and CB4	4.0
	AB-G	CB3 and CB4	4.9
	BC-G	CB3 and CB4	4.6
	CA-G	CB3 and CB4	4.4
	ABC-G	CB3 and CB4	4.5
862-838	**B-G**	**CB3 and CB4**	**4.1**

Table 6.10 shows the trip signal delay time for various faults in Zone 4. Zone 4 doesn't have a single phase section. Also, four three-phase SSTs have been connected to this zone. The fault was confirmed when both Relay 4 and Relay 5 showed forward fault in Zone 4.

Table 6.10: Trip Signal Delay in Zone 4

Fault Location	Fault Type	Breaker Tripped	Trip Time (milliseconds)
FEEDER-1	A-G	CB4 and CB5	4.1
	C-G	CB4 and CB5	4.4
	AB-G	CB4 and CB5	4.5
	CA-G	CB4 and CB5	4.7
	ABC-G	CB4 and CB5	4.5
FEEDER-2	A-G	CB4 and CB5	4.9
	B-G	CB4 and CB5	4.6
	BC-G	CB4 and CB5	4.3
	CA-G	CB4 and CB5	4.9
	ABC-G	CB4 and CB5	4.6
FEEDER-3	B-G	CB4 and CB5	4.3
	AB-G	CB4 and CB5	4.4
	CA-G	CB4 and CB5	4.9
	ABC-G	CB4 and CB5	4.6

Fault Location	Fault Type	Breaker Tripped	Trip Time (milliseconds)
FEEDER-4	B-G	CB4 and CB5	4.3
	AB-G	CB4 and CB5	4.4
	CA-G	CB4 and CB5	4.9
	BC-G	CB4 and CB5	4.1
	ABC-G	CB4 and CB5	4.9

Table 6.11 shows the trip signal delay time for various faults in Zone 5. Zone 5 doesn't have any single phase section. Also, three three-phase SSTs have been connected to this zone. The fault was confirmed when both Relay 6 showed reverse direction while Relay 7 showed the forward direction in Zone 5.

Table 6.11: Trip Signal Delay in Zone 5

Fault Location	Fault Type	Breaker Tripped	Trip Time (milliseconds)
FEEDER-1	A-G	CB6 and CB7	4.5
	C-G	CB6 and CB7	4.4
	AB-G	CB6 and CB7	4.3
	CA-G	CB6 and CB7	4.0
	ABC-G	CB6 and CB7	4.9
FEEDER-2	A-G	CB6 and CB7	4.8
	B-G	CB6 and CB7	4.4
	BC-G	CB6 and CB7	4.4
	CA-G	CB6 and CB7	4.3
	ABC-G	CB6 and CB7	4.3
FEEDER-3	B-G	CB6 and CB7	4.2
	AB-G	CB6 and CB7	4.5
	CA-G	CB6 and CB7	4.7
	BC-G	CB6 and CB7	4.8
	ABC-G	CB6 and CB7	4.9
FEEDER-4	B-G	CB6 and CB7	4.7
	AB-G	CB6 and CB7	4.6
	CA-G	CB6 and CB7	4.8
	BC-G	CB6 and CB7	4.4
	ABC-G	CB6 and CB7	4.2

6.7 Summary of Results

A complete approach has been shown in PSCAD for protecting large mesh distribution system against all possible type of faults. The modeling of negative sequence directional element and positive sequence directional has been presented in this chapter. The negative sequence directional element was used to detect the unsymmetrical or unbalanced faults. While, positive sequence directional element was used to detect symmetrical or balanced faults. The large distribution system has been divided into five total zones. Each zone has two circuit breakers at the boundary and two relays to measure the current and voltage at the zonal boundary. These relays are communicating each other via a radio link. A strategy has been developed that involved information sharing among relays to detect a fault in the zone. Various sample cases were studied by simulating a fault in different zones. Exhaustive summary for all possible type of faults has been shown which confirmed the working of protection methodology. The average trip delay time is found to be 4.89 milliseconds which is about quarter of a cycle.

CHAPTER 7: CONCLUSIONS AND FUTURE WORK

7.1 Conclusions

This research work was aimed at the design and validation of the protection system for the large scale meshed distribution system. The large scale system simulation (LSSS) is a system level PSCAD model which is used to validate component models for different time-scale platforms, to provide a virtual testing platform for the Future Renewable Electric Energy Delivery and Management (FREEDM) system and to validate cases of protection, renewable energy profile, and load profiles. A new protection scheme with a wireless scheme was discussed in this thesis. The method of wireless communication was extended to protect the large scale meshed distributed generation from any fault. The trip signal generated by the pilot protection system will be used to trigger the FID (fault isolation device) which is an electronic circuit breaker operation (switched off/opening the FIDs).

A pilot directional protection scheme using wireless communication has been developed that quickly and accurately detects the direction of the faults. The commercial available SEL-3031 radio link and SEL-351S were used to validate the pilot directional algorithm at the ASU power laboratory. Following are the conclusions drawn by this research work:

- A protection system with wireless communication scheme has been developed in this thesis. Directional overcurrent based relays were used to detect and sectionalize the faulty section from the healthy system. The wireless communication was found to have comparable speed and selectivity. A

hardware prototype was developed at ASU power lab using commercial SEL-351S and SEL-3031 radio links.

- The reconfiguration of the system after the successful switching off the faulty section was presented. The reconfiguration effort requires an update of the system architecture with reclosing and automatic sectionalizing link type switches.
- Directional Pilot Protection was incorporated in the LSSS system (Large Scale System Simulation Sub thrust) which is a computer simulation of the IEEE developed distribution network model. This is an accurate and exact representation of the protection system by a computer program, which uses commercial digital relays. The scheme was able to detect the faults within a quarter of a cycle.

The proper operation of the protection system installed in the LSSS system is tested for all possible faults. This testing has validated the correct functioning of the proposed protection system. The effect of transients on the LSSS system is discussed in this section. Figure 7.1 shows the fault current waveform when the fault incident angle is 90 °. The presence of DC offset requires more filtering to obtain sequence components. Therefore, the trip time signal delay is maximum for this incident angle.

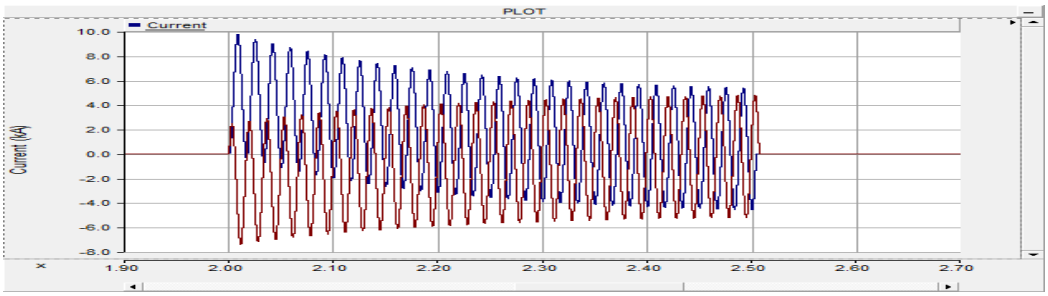

Figure 7.1: Fault Current with Fault Incident Angle of 90°

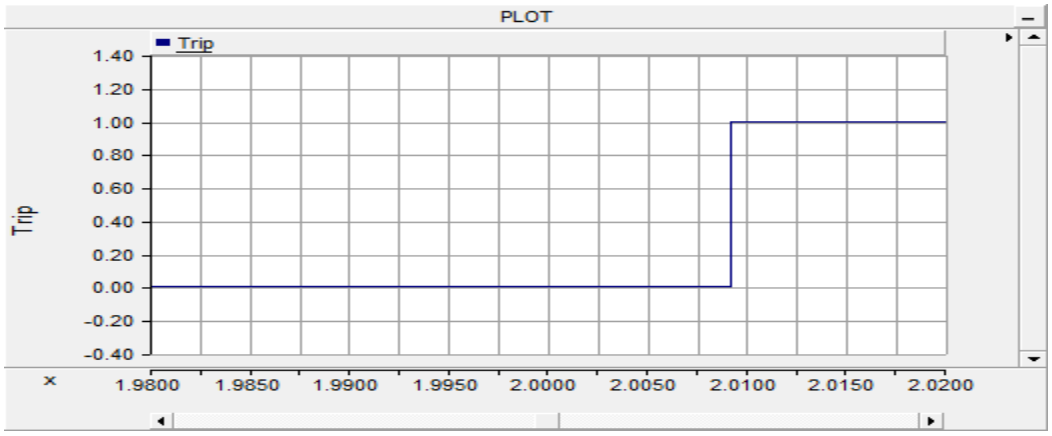

Figure 7.2: Trip Signal Delay for Fault Incident Angle of 90°

It can be seen that the fault current rises suddenly, and the first peak following the fault is 980 A. The trip signal delay for the various fault incident angles in Zone 1 of LSSS is shown in Table 7.1. Also, the peak value of the current will vary with the instant of the occurrence of the fault. However, the peak value of the current is nearly five times the pre-fault current value in this case.

Table 7.1: Trip Time for Various Fault Incident Angles

Fault Incident Angle (degrees)	**Trip Time (ms)**
0	7.1
30	7.3
45	7.4
60	7.7
90	8.9
120	8.8
135	8.1
150	7.7
180	7.0
210	7.2
240	8.1
270	9.2
300	7.9
330	7.5
360	7.2

The trip signal delay time is maximum for the fault incident angle of 90° and 270°.

The substation SST and FCL limit the fault current to 2.0 pu in the FREEDM system. Hence, this could introduce a problem in the fast tripping scheme as developed in Chapter 6. The effect of chopping the peak value of fault current has been studied in this section. The relay settings are same as described in Section 6.4. Tables 7.2, 7.3 and 7.4 show the observations made from the fault current chopping.

1. The fault currents were chopped to 50% of its peak value. The protection scheme has successfully worked in this case without any error as shown in Table 7.2.

Table 7.2: Fault Currents Chopped to 50% of Peak Values

Fault	**Zone 1 Trip Time (ms)**	**Zone 2 Trip Time (ms)**	**Zone 3 Trip Time (ms)**	**Zone 4 Trip Time (ms)**	**Zone 5 Trip Time (ms)**
814-850	5.1	XX	XX	XX	XX
888-890	XX	8.1	XX	XX	XX
860-836	XX	XX	5.2	XX	XX
Feeder2	XX	XX	XX	5.7	XX
Feeder1	XX	XX	XX	XX	4.9

2. The fault currents were chopped to 33% of its peak value. The protection scheme was successful in detecting the fault in the system. Table 7.3 show the observations for the different faults.

Table 7.3: Fault Currents Chopped to 33% of Peak Values

Fault	**Zone1 Trip Time (ms)**	**Zone2 Trip Time (ms)**	**Zone3 Trip Time (ms)**	**Zone4 Trip Time (ms)**	**Zone5 Trip Time (ms)**
814-850	5.9	XX	XX	XX	XX
888-890	XX	8.8	XX	XX	XX
860-836	XX	XX	5.4	XX	XX
Feeder2	XX	XX	XX	5.9	XX
Feeder1	XX	XX	XX	XX	5.3

3. The fault currents were chopped to 16% of its peak value. The protection scheme was successful in detecting the fault except in section 888-890. This is due to the presence of transformer in this section that has further reduced the fault current.

Table 7.4: Fault Currents Chopped to 16% of Peak Values

Fault	Zone1 Trip Time (ms)	Zone2 Trip Time (ms)	Zone3 Trip Time (ms)	Zone4 Trip Time (ms)	Zone5 Trip Time (ms)
814-850	6.3	XX	XX	XX	XX
888-890	XX	Fails	XX	XX	XX
860-836	XX	XX	6.3	XX	XX
Feeder2	XX	XX	XX	6.6	XX
Feeder1	XX	XX	XX	XX	6.9

4. The fault currents were chopped to 10% of its peak value. The protection failed to detect the fault in the system. To improve the trip time, the new settings should be calculated for the corresponding chopped fault current.

Table 7.5: Fault Currents Chopped to 10% of Peak Values

Fault	Zone1 Trip Time (ms)	Zone2 Trip Time (ms)	Zone3 Trip Time (ms)	Zone4 Trip Time (ms)	Zone5 Trip Time (ms)
814-850	Fails	XX	XX	XX	XX
852-832	XX	Fails	XX	XX	XX
860-836	XX	XX	Fails	XX	XX
Feeder2	XX	XX	XX	Fails	XX
Feeder1	XX	XX	XX	XX	Fails

7.2 Future Work

The followings aspects could be added to the research work:

- The time delay losses via the radio link can be modeled in PSCAD to study the impact on trip signal delay.

- The integration of Solid State Transformer- disconnection and reconnection during and after the clearance of fault in the PSCAD model.
- The protection model extension of functionality to islanded operation and distributed generation.
- The development of PMU based secondary protection for the large mesh distribution system.
- The reclosing model is still not modeled for the large mesh distribution system; this can be implemented once the issue of connection and de-connection of the SSTs with the grid on reconnection is solved.
- The Optimal location of PMU placement for back up protection in the large mesh distribution system.

REFERENCES

[1] P. Yilmaz, M. H. Hocaoglu, A. Er. S. Konukman, "A pre-feasibility case study on integrated resource planning including renewables," Energy Policy, v. 36, No. 3, March 2008, pp. 1223-1232.

[2] W. Schroppel, "Seamless integration of renewable energies into the electrical supply system," IEEE Conference on Power Electronics and Applications, 2005, pp. 1 – 5.

[3] Huang, A.,' FREEDM system - a vision for the future grid', 2010 IEEE Power and Energy Society General Meeting, 25-29 July 2010, p.p 1 – 4.

[4] Jianhua Zhang; Wenye Wang; Bhattacharya, S. "Architecture of solid state transformer-based energy router and models of energy traffic", Innovative Smart Grid Technologies (ISGT), 2012 IEEE PES, p.p 1 – 8.

[5] G. Karady, P. Mandava and V. Iyengar"FREEDM Loop description" FREEDM, Arizona State University, Tempe, AZ, 2012.

[6] Xing Liu, Arvind Thirumalai, George G. Karady, "Design and Development of an Ultra-Fast Pilot Protection," Power Systems Conference and Exposition (PSCE), 2011 IEEE/PES.

[7] Pavanchandra Mandava "Design and Development of protection schemes for the FREEDM smart grid systems " M.S. dissertation, Dept. of Electrical Computer and Energy Engineering., Arizona State University, Tempe, 2014.

[8] J. Lewis Blackburn, Thomas J. Domin, "Protective Relaying: Principles and Applications," Third Edition, CRC Press, Dec. 21, 2006.

[9] B. Fleming, "Negative-Sequence Impedance Directional Element," 10th Annual ProTest user group meeting, Feb. 24-26, Pasadena, CA.

[10] Gu, Bin, Jiancheng Tan, and Hua Wei. "High speed directional relaying algorithm based on the fundamental frequency positive sequence superimposed components." IET Generation, Transmission & Distribution 8, no. 7 (2014): 1211-1220.

[11] N.Zhang, X.Z.Dong, Z.Q.Bo, S.Richards, A. Klimek, "Universal Pilot Wire Differential Protection for Distribution System," IET 9th International Conference on Developments in Power System Protection, pp.224-228, 2008.

[12] Karady, G.G. , Xing Liu' Fault management and protection of FREEDM systems', 2010 IEEE, Power and Energy Society General Meeting, 25-29 July 2010, pp. 1 – 4.

[13] Xing Liu, Arvind Thirumalai, George G. Karady, "Design and Development of an Ultra-Fast Pilot Protection," Power Systems Conference and Exposition (PSCE), 2011 IEEE/PES

[14] D. Costello, M. Moon, and G. Bow, "Use of Directional Elements at the Utility-Industrial Interface," proceedings of the 5th Annual Power Systems Conference, Clemson, SC, March 2006.

[15] B. Li, X. Yu, Z. Bo, and S. Member, "Protection schemes for closed loop distribution network with distributed generator," in 1st International Conference on Sustainable Power Generation and Supply, 2009, no. 8, pp. 1-6, Apr. 2009.

[16] M. Vitins, "A fundamental concept for high speed relaying", IEEE Trans.Power Apparatus and Systems, vol. 100, pp.163-173, 1981.

[17] A.F. Elneweihi, E.O. Schweitzer III, M.W. Feltis, "Negative-Sequence Overcurrent Element Application and Coordination in Distribution Protection," IEEE /PES Summer Meeting, Seattle, WA, July 1992.

[18] E. O. Schweitzer, III, Jeff Roberts, "Distance relay element design," Sixth annual conference for protective relay engineers Texas A&M University college station, Texas April 12- 14, 1993.

[19] Rintamaki, Olli; Distrib. Autom. Ylinen, J,' Communicating line differential protection for urban distribution networks' Electricity Distribution, 2008. CICED 2008. China International Conference on, pp. 1 - 5

[20] Edmund O. Schweitzer, Jeffrey B. Roberts," Negative Sequence Directional Element for a Relay Useful in Power Transmission Lines," U.S. Patent CA 2108443 C, Apr. 11, 2000.

[21] P. G. McLaren, E. Dirks, R. P. Jayasinghe, I. Fernado, G. W. Swift, and Z. Zhang, "A positive sequence directional element for numerical distance relays," in Proc. Conf. Developments in Power System Protection, 1997, pp. 239–242.

[22] A. K. Pradhan, A. Routray, and G. S. Madhan, "Fault direction estimation in a radial distribution system using phase change in sequence current," IEEE Trans. Power Del., vol. 22, no. 4, pp. 2065–2071, Oct. 2007.

[23] S.M. Brahma and A.A. Girgis, "Microprocessor-based reclosing to coordinate fuse and recloser in a system with high penetration of distributed generation", Power Engineering Society Winter Meeting, vol.1, IEEE, pp. 453-458, 2002.

[24] Hunt, R.; Adamiak, M.; King, A.; McCreery, S. "Pilot Protection," IEEE Industry Applications Magazine, Vol. 15, pp 51-60, Sep. 2009.

[25] R. Hunt, M. Adamiak, A. King, and S. McCreery, "Application of Digital Radio for Distribution Pilot Protection and Other Applications, " proceedings of the 34th Annual Western Protective Relay Conference, Spokane, WA, October 2007.

[26] “Instruction manual of SEL 3031-serial radio transceiver,” available at: https://www.selinc.com/SEL-3031.

[27] “Instruction manual of SEL 351S-7,” available at: https://www.selinc.com/SEL-351.

[28] “Instruction manual of SEL 5030 AcSELerator quickset,” available at: https://www.selinc.com/SEL-351.

[29] Ken Behrendt, Ken Fodero, “Implementing MIRRORED BITS Technology over Various Communications Media,” available at: https://www.selinc.com/literature/ApplicationGuides/ document number: AG2001-12.

[30] “Information about the FREEDM system,” available at: http://www.freedm.ncsu.edu

[31] O. Vadhyako, M. Steurer, D. Neumayr, C.S Edrington, G. Karady, S. Bhattacharya ”Solid state fault isolation device : application to future power electronics based distribution systems”IET Electric Power Applications, vol.5 ,issue 6,pp. 521-528, July 2011.

[32] Chris Widener, Mischa Steurer, ‘Fault Isolation in Power Electronic Based Distribution Systems without Circuit Breakers’, FREEDM Industry meeting conference 2013.

[33] V.Ramachandran , A.Kuvar, U. Singh , S. Bhattacharya, “A system level study employing improved solid state transformer average models with renewable energy integration” IEEE PES General Meeting Conference & Exposition, pp. 1-5, July 27-31 2014.

[34] B.Baddipadiga, “Substation SST and Load/Distribution SST Protection Summary”, LSSS-2015 meeting.

[35] K. Okuyama, T. Kato, Y. Suzuoki, and T. Funabashi, "Protection relay system using information network for distribution system with DGs," Electrical Engineering in Japan (English translation of Denki Gakkai Ronbunshi), vol. 155, pp. 30-35, Jun. 2006.

[36] H. Gao and P. A. Crossley, “Design and evaluation of a directional algorithm for transmission-line protection based on positive sequence fault components,” Proc. Inst. Elect. Eng., Gen., Transm. Distrib. vol. 153, no. 6, pp. 711–718, 2006.

[37] J. Horak, “Directional overcurrent relaying (67) concepts,” in Proc. IEEE 59th Annu. Protect. Relay Eng. Conf., 2006, p. 13.

[38] Suonan, J.L., Xu, Q.Q., Song, G.B., Wu, Y.: `A reliable directional relay based on positive sequence compensated voltage and current components', Int. Conf. Developments in Power System Protection, IEE Conf. Pub. 500, 2004, p. 104–107.

[39] "EMTP/PSCAD X4," Manitoba HVDC Research Centre Inc, Jan. 11, 2011. [Online]. Available: https://pscad.com/products/pscad/past_present_and_future/

[40] “Fortran 90 Programming Manual”, by Tanja Van Mourik University College London.

[41] Mwakabuta, N., Sekar, A.’ Comparative Study of the IEEE 34 Node Test Feeder under Practical Simplifications’ Power Symposium, 2007. NAPS '07. 39th North American.pp.484-491

[42] V. Iyengar, G. Karady, D. Crow, D. shah ‘Implementation of pilot protection system for IEEE 34 load system with SST Loads’, FREEDM Indutry meeting conference 2014.

APPENDIX: A

NEGATIVE AND POSITIVE SEQUENCE DIRECTIONAL ELEMENT

Negative Sequence Directional Relay [18]

The negative sequence directional element uses negative sequence components to calculate the direction of fault. Consider a radial system, as shown in Figure A.1, subjected to an unsymmetrical fault.

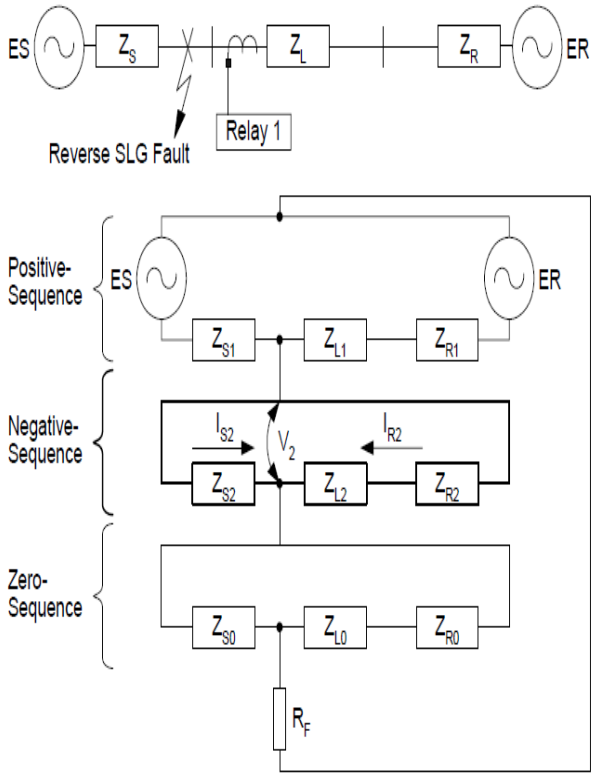

Figure A.1: Three-phase Radial System [18]

A sequence network for a ground fault at the relay bus is shown in Figure A.1. The relay measures I_{S2} for forward faults, and $-I_{R2}$ for reverse faults.

The negative sequence impedance for the above figure can be calculated.

For a forward single line to ground faults

$$\text{Negative sequence impedance, } Z_2 = \frac{-V_2}{I_{S2}} = -Z_{s2} \qquad (1)$$

For a reverse single line to ground faults

Negative sequence impedance, $Z_2 = \frac{-V_2}{-I_{R2}} = Z_{L2} + Z_{R2}$ (2)

The above calculation shows that the negative sequence impedance for the forward fault is always negative while it is positive for the reverse fault.

In R-X plane the impedance can be shown as shown in Figure A.2

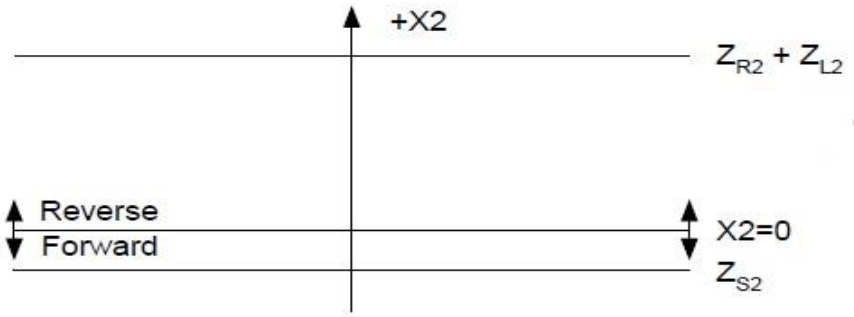

Figure A.2: Location of Negative Sequence Impedance in R-X Plane [18]

Hence, this method can be used to detect the direction of fault for the unsymmetrical faults.

Positive Sequence Directional Element [36]

The absence of negative sequence components during symmetrical faults require the use of positive directional element to detect the fault direction. Figure A.3 shows a three-phase radial system subjected to both forward and reverse fault.

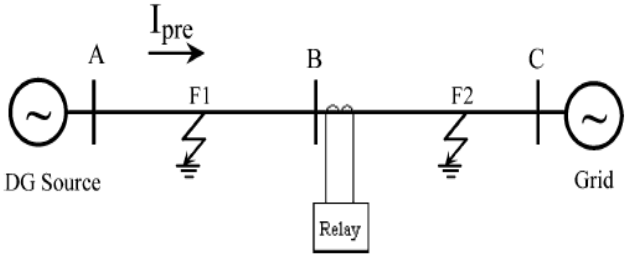

Figure A.3: Three-phase Radial System [36]

The prefault current in the line can be expressed as:

$$I_{pre} = \frac{E_A - E_c}{Z} \quad (3)$$

Where E_A and E_C are the bus voltages and Z is the total line impedance.

For a reverse fault, the positive sequence network diagram is shown in Figure A.4

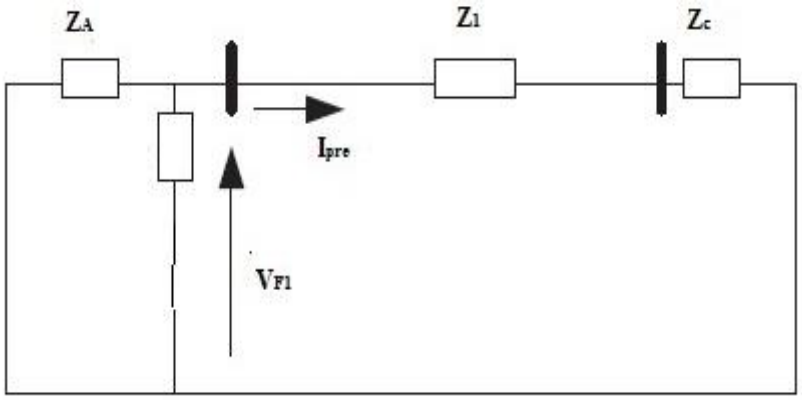

Figure A.4: Positive Sequence Network Diagram [36]

The positive sequence fault voltage measured by relay is

$$V_{F1} = -(I_1 + I_{pre}) * Z_1 \quad (4)$$

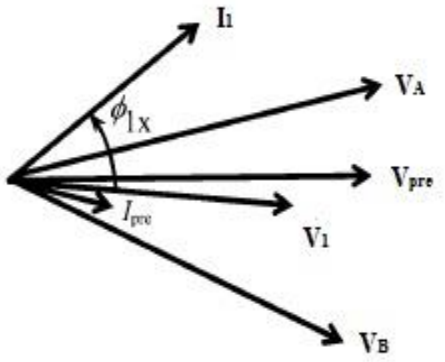

Figure A.5: Phasor Diagram for Reverse Fault [22]

For a forward fault, the positive sequence network diagram is shown in Figure A.6

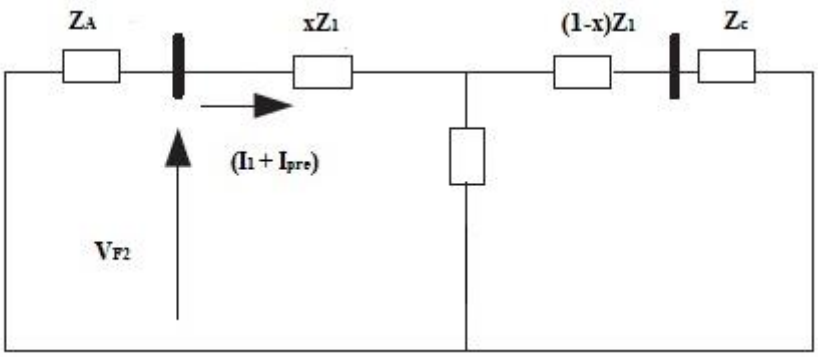

Figure A.6: Positive Sequence Network Diagram [36]

The positive sequence fault voltage measured by relay is

$$V_{F2} = \left(I_1 + I_{pre} \right) * \left(Z_A + xZ_1 \right) \tag{5}$$

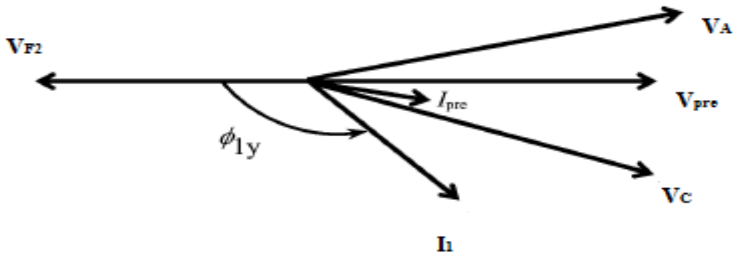

Figure A.7: Phasor Diagram for Forward Fault [22]

Since, the positive-sequence impedances are predominantly reactive, the phase relationships between voltage and current at the relay location is

$$\arg\frac{V_1}{I_1} - \theta = \begin{cases} between -90° \; and \; 90° \; than \; forward \; fault \\ otherwise \; reverse \; fault \end{cases}$$

Where θ = line angle in degrees

Hence, the directional criterion for a forward fault is

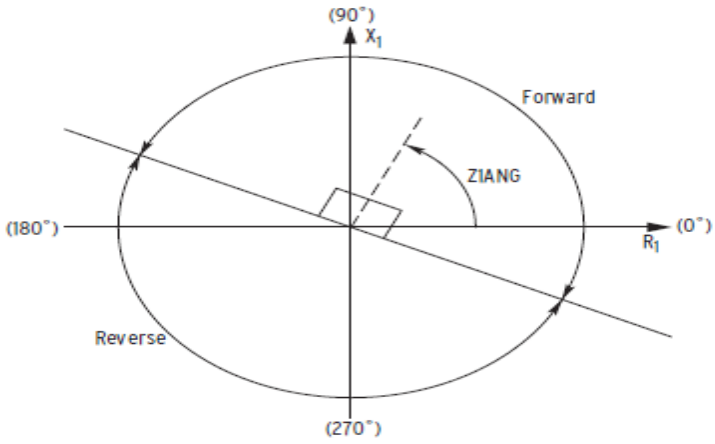

Figure A.8: Positive Sequence Element Direction [27]

$90° < \beta - \emptyset < -90°$

β =Angle of the positive sequence impedance

Ø =Positive sequence line angle

APPENDIX: B

LINE DATA OF LSSS DISTRIBUTION SYSTEM

The listings of the line data for each phase are provided in the tables below. This feeder uses some of the data from the IEEE 34 node radial test feeder. Column one shows the name of the bus and corresponding to it the length and line data are given.

Table B.1: Line Data of all the Phases for the LSSS System

From	To	Length (mi.)	Configuration	Z Matrix (R+jX) in Ohms per mile						B in micro Siemens per mile		
				R	X	R	X	R	X			
800	802	0.48864	300	0.334	0.334	0.053	0.145	0.053	0.1254	21.34	-6.1252	-3.9772
				0.053	0.145	0.331	0.339	0.052	0.1148	-6.1252	20.3916	-2.4848
				0.053	0.125	0.052	0.115	0.332	0.3368	-3.9772	-2.4848	19.552
802	806	0.32765	300	0.334	0.334	0.053	0.145	0.053	0.1254	21.34	-6.1252	-3.9772
				0.053	0.145	0.331	0.339	0.052	0.1148	-6.1252	20.3916	-2.4848
				0.053	0.125	0.052	0.115	0.332	0.3368	-3.9772	-2.4848	19.552
806	808	6.10417	300	0.334	0.334	0.053	0.145	0.053	0.1254	21.34	-6.1252	-3.9772
				0.053	0.145	0.331	0.339	0.052	0.1148	-6.1252	20.3916	-2.4848
				0.053	0.125	0.052	0.115	0.332	0.3368	-3.9772	-2.4848	19.552
808	810	1.09924	303	0	0	0	0	0	0	0	0	0
				0	0	0.7	0.371	0	0	0	16.9004	0
				0	0	0	0	0	0	0	0	0
808	812	7.10227	300	0.334	0.334	0.053	0.145	0.053	0.1254	21.34	-6.1252	-3.9772
				0.053	0.145	0.331	0.339	0.052	0.1148	-6.1252	20.3916	-2.4848
				0.053	0.125	0.052	0.115	0.332	0.3368	-3.9772	-2.4848	19.552
812	814	5.63068	300	0.334	0.334	0.053	0.145	0.053	0.1254	21.34	-6.1252	-3.9772
				0.053	0.145	0.331	0.339	0.052	0.1148	-6.1252	20.3916	-2.4848
				0.053	0.125	0.052	0.115	0.332	0.3368	-3.9772	-2.4848	19.552
814	850	0.00189	301	0.483	0.353	0.058	0.161	0.059	0.1423	20.4828	-5.7456	-3.7608
				0.058	0.161	0.479	0.357	0.057	0.131	-5.7456	19.622	-2.3804
				0.059	0.142	0.057	0.131	0.481	0.3552	-3.7608	-2.3804	18.8616
816	818	0.32386	302	0.7	0.371	0	0	0	0	16.9004	0	0

From	To	Length (mi.)	Configuration	Z Matrix (R+jX) in Ohms per mile						B in micro Siemens per mile		
				0	0	0	0	0	0	0	0	0
				0	0	0	0	0	0	0	0	0
816	824	1.93371	301	0.483	0.353	0.058	0.161	0.059	0.1423	20.4828	-5.7456	-3.7608
				0.058	0.161	0.479	0.357	0.057	0.131	-5.7456	19.622	-2.3804
				0.059	0.142	0.057	0.131	0.481	0.3552	-3.7608	-2.3804	18.8616
818	820	9.11932	302	0.7	0.371	0	0	0	0	16.9004	0	0
				0	0	0	0	0	0	0	0	0
				0	0	0	0	0	0	0	0	0
820	822	2.60227	302	0.7	0.371	0	0	0	0	16.9004	0	0
				0	0	0	0	0	0	0	0	0
				0	0	0	0	0	0	0	0	0
824	826	0.57386	303	0	0	0	0	0	0	0	0	0
				0	0	0.7	0.371	0	0	0	16.9004	0
				0	0	0	0	0	0	0	0	0
824	828	0.15909	301	0.483	0.353	0.058	0.161	0.059	0.1423	20.4828	-5.7456	-3.7608
				0.058	0.161	0.479	0.357	0.057	0.131	-5.7456	19.622	-2.3804
				0.059	0.142	0.057	0.131	0.481	0.3552	-3.7608	-2.3804	18.8616
828	830	3.87121	301	0.483	0.353	0.058	0.161	0.059	0.1423	20.4828	-5.7456	-3.7608
				0.058	0.161	0.479	0.357	0.057	0.131	-5.7456	19.622	-2.3804
				0.059	0.142	0.057	0.131	0.481	0.3552	-3.7608	-2.3804	18.8616
830	854	0.09848	301	0.483	0.353	0.058	0.161	0.059	0.1423	20.4828	-5.7456	-3.7608
				0.058	0.161	0.479	0.357	0.057	0.131	-5.7456	19.622	-2.3804
				0.059	0.142	0.057	0.131	0.481	0.3552	-3.7608	-2.3804	18.8616
832	858	0.92803	301	0.483	0.353	0.058	0.161	0.059	0.1423	20.4828	-5.7456	-3.7608
				0.058	0.161	0.479	0.357	0.057	0.131	-5.7456	19.622	-2.3804
				0.059	0.142	0.057	0.131	0.481	0.3552	-3.7608	-2.3804	18.8616
832	888	0	XFM-1									

From	To	Length (mi.)	Configuration	Z Matrix (R+jX) in Ohms per mile						B in micro Siemens per mile		
834	860	0.38258	301	0.483	0.353	0.058	0.161	0.059	0.1423	20.4828	-5.7456	-3.7608
				0.058	0.161	0.479	0.357	0.057	0.131	-5.7456	19.622	-2.3804
				0.059	0.142	0.057	0.131	0.481	0.3552	-3.7608	-2.3804	18.8616
834	842	0.05303	301	0.483	0.353	0.058	0.161	0.059	0.1423	20.4828	-5.7456	-3.7608
				0.058	0.161	0.479	0.357	0.057	0.131	-5.7456	19.622	-2.3804
				0.059	0.142	0.057	0.131	0.481	0.3552	-3.7608	-2.3804	18.8616
836	840	0.16288	301	0.483	0.353	0.058	0.161	0.059	0.1423	20.4828	-5.7456	-3.7608
				0.058	0.161	0.479	0.357	0.057	0.131	-5.7456	19.622	-2.3804
				0.059	0.142	0.057	0.131	0.481	0.3552	-3.7608	-2.3804	18.8616
836	862	0.05303	301	0.483	0.353	0.058	0.161	0.059	0.1423	20.4828	-5.7456	-3.7608
				0.058	0.161	0.479	0.357	0.057	0.131	-5.7456	19.622	-2.3804
				0.059	0.142	0.057	0.131	0.481	0.3552	-3.7608	-2.3804	18.8616
842	844	0.25568	301	0.483	0.353	0.058	0.161	0.059	0.1423	20.4828	-5.7456	-3.7608
				0.058	0.161	0.479	0.357	0.057	0.131	-5.7456	19.622	-2.3804
				0.059	0.142	0.057	0.131	0.481	0.3552	-3.7608	-2.3804	18.8616
844	846	0.68939	301	0.483	0.353	0.058	0.161	0.059	0.1423	20.4828	-5.7456	-3.7608
				0.058	0.161	0.479	0.357	0.057	0.131	-5.7456	19.622	-2.3804
				0.059	0.142	0.057	0.131	0.481	0.3552	-3.7608	-2.3804	18.8616
846	848	0.10038	301	0.483	0.353	0.058	0.161	0.059	0.1423	20.4828	-5.7456	-3.7608
				0.058	0.161	0.479	0.357	0.057	0.131	-5.7456	19.622	-2.3804
				0.059	0.142	0.057	0.131	0.481	0.3552	-3.7608	-2.3804	18.8616
850	816	0.05871	301	0.483	0.353	0.058	0.161	0.059	0.1423	20.4828	-5.7456	-3.7608
				0.058	0.161	0.479	0.357	0.057	0.131	-5.7456	19.622	-2.3804
				0.059	0.142	0.057	0.131	0.481	0.3552	-3.7608	-2.3804	18.8616
852	832	0.00189	301	0.483	0.353	0.058	0.161	0.059	0.1423	20.4828	-5.7456	-3.7608
				0.058	0.161	0.479	0.357	0.057	0.131	-5.7456	19.622	-2.3804
				0.059	0.142	0.057	0.131	0.481	0.3552	-3.7608	-2.3804	18.8616

From	To	Length (mi.)	Configuration	Z Matrix (R+jX) in Ohms per mile						B in micro Siemens per mile		
854	856	4.41856	303	0	0	0	0	0	0	0	0	0
				0	0	0.7	0.371	0	0	0	16.9004	0
				0	0	0	0	0	0	0	0	0
854	852	6.97538	301	0.483	0.353	0.058	0.161	0.059	0.1423	20.4828	-5.7456	-3.7608
				0.058	0.161	0.479	0.357	0.057	0.131	-5.7456	19.622	-2.3804
				0.059	0.142	0.057	0.131	0.481	0.3552	-3.7608	-2.3804	18.8616
858	864	0.30682	302	0.7	0.371	0	0	0	0	16.9004	0	0
				0	0	0	0	0	0	0	0	0
				0	0	0	0	0	0	0	0	0
858	834	1.10417	301	0.483	0.353	0.058	0.161	0.059	0.1423	20.4828	-5.7456	-3.7608
				0.058	0.161	0.479	0.357	0.057	0.131	-5.7456	19.622	-2.3804
				0.059	0.142	0.057	0.131	0.481	0.3552	-3.7608	-2.3804	18.8616
860	836	0.50758	301	0.483	0.353	0.058	0.161	0.059	0.1423	20.4828	-5.7456	-3.7608
				0.058	0.161	0.479	0.357	0.057	0.131	-5.7456	19.622	-2.3804
				0.059	0.142	0.057	0.131	0.481	0.3552	-3.7608	-2.3804	18.8616
862	838	0.92045	304	0	0	0	0	0	0	0	0	0
				0	0	0.48	0.355	0	0	0	17.4548	0
				0	0	0	0	0	0	0	0	0
888	890	2	300	0.334	0.334	0.053	0.145	0.053	0.1254	21.34	-6.1252	-3.9772
				0.053	0.145	0.331	0.339	0.052	0.1148	-6.1252	20.3916	-2.4848
				0.053	0.125	0.052	0.115	0.332	0.3368	-3.9772	-2.4848	19.552
800	866	9		0.479	0.357	0	0	0	0	0	0	0
				0	0	0.479	0.357	0	0	0	0	0
				0	0	0	0	0.479	0.357	0	0	0
866	868	9		0.479	0.357	0	0	0	0	0	0	0
				0	0	0.479	0.357	0	0	0	0	0
				0	0	0	0	0.479	0.357	0	0	0

From	To	Length (mi.)	Configuration	Z Matrix (R+jX) in Ohms per mile						B in micro Siemens per mile		
868	870	9		0.479	0.357	0	0	0	0	0	0	0
				0	0	0.479	0.357	0	0	0	0	0
				0	0	0	0	0.479	0.357	0	0	0
870	872	9		0.479	0.357	0	0	0	0	0	0	0
				0	0	0.479	0.357	0	0	0	0	0
				0	0	0	0	0.479	0.357	0	0	0
868	816	6		0.479	0.357	0	0	0	0	0	0	0
				0	0	0.479	0.357	0	0	0	0	0
				0	0	0	0	0.479	0.357	0	0	0
872	840	6		0.479	0.357	0	0	0	0	0	0	0
				0	0	0.479	0.357	0	0	0	0	0
				0	0	0	0	0.479	0.357	0	0	0

APPENDIX: C

FORTRAN CODE FOR POSITIVE SEQUENCE DIRECTIONAL ELEMENT IN PSCAD

FORTRAN CODE for positive sequence directional element in PSCAD [40]

```
#IF Dim==1

PHI=$V_ANG-$I_ANG

    IF (((PHI-$Z).GE.-90).AND.((PHI-$Z).LE.90)) THEN
    $OUT=1
    ELSE
    $OUT=-1

    ENDIF

#ENDIF

!
```

Block in PSCAD is shown in Figure C.1

The inputs to this block are:

v_ang that is positive sequence voltage phase angle

i_ang that is positive sequence current phase angle

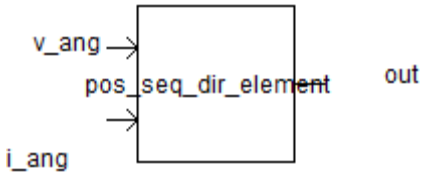

Figure C.1: Positive Sequence Directional Block

The output (out) of this block is either +1 or -1 depending on the forward or reverse direction of the symmetrical fault.

APPENDIX: D

FORTRAN CODE FOR DECISION MAKING IN PSCAD

FORTRAN code for decision making in PSCAD [40]

```
 threshold =0

     IF
(($Trip1.GT.threshold.OR.$xinput1.GT.threshold).AND.($overcurrent.GT.threshold).AN
D.($xoutput2.NE.1.AND.$xoutput3.NE.1.AND.$xoutput4.NE.1.AND.$xoutput5.NE.1))
THEN
     $Zone1=1
     $xoutput1=1
     GO TO 45

     ELSEIF
(($Trip2.GT.threshold.OR.$xinput2.GT.threshold).AND.($overcurrent.GT.threshold).AN
D.($xoutput1.NE.1.AND.$xoutput3.NE.1.AND.$xoutput4.NE.1.AND.$xoutput5.NE.1))
THEN
     $Zone2=1
     $xoutput2=1
     GO TO 45

     ELSEIF
(($Trip3.GT.threshold.OR.$xinput3.GT.threshold).AND.($overcurrent.GT.threshold).AN
D.($xoutput1.NE.1.AND.$xoutput2.NE.1.AND.$xoutput4.NE.1.AND.$xoutput5.NE.1))
THEN
     $Zone3=1
     $xoutput3=1
     GO TO 45

     ELSEIF
(($Trip4.GT.threshold.OR.$xinput4.GT.threshold).AND.($overcurrent.GT.threshold).AN
D.($xoutput1.NE.1.AND.$xoutput2.NE.1.AND.$xoutput3.NE.1.AND.$xoutput5.NE.1))
THEN
     $Zone4=1
     $xoutput4=1
     GO TO 45

     ELSEIF
(($Trip5.GT.threshold.OR.$xinput5.GT.threshold).AND.($overcurrent.GT.threshold).AN
D.($xoutput1.NE.1.AND.$xoutput2.NE.1.AND.$xoutput3.NE.1.AND.$xoutput4.NE.1))
THEN
     $Zone5=1
     $xoutput5=1
     GO TO 45
```

```
ELSE

$xoutput1=0
$xoutput2=0
$xoutput3=0
$xoutput4=0
$xoutput5=0
$Zone1=0
$Zone2=0
$Zone3=0
$Zone4=0
$Zone5=0

45 ENDIF
```

The block in PSCAD is shown in Figure D.1.

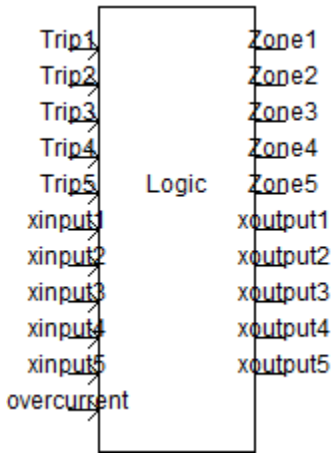

Figure D.1: Decision Making Block in PSCAD

The inputs to this block are trip signals from negative and sequence directional element from each zone. The xinput1…5 and xoutput1…5 are the internal variables used for the decision making.